

**Induction of Alzheimer's disease-related tau pathology by heparan sulphates and
its regulation via TGF- β**

**Inaugural Dissertation
submitted to the
Faculty of Veterinary Medicine
in partial fulfillment of the requirements
for the PhD-Degree
of the Faculties of Veterinary Medicine and Medicine
of the Justus Liebig University Giessen**

**by
Castillo Negrete Rafael**

**of
Puebla, Mexico**

Giessen 2023

**From the Versuchstierkunde und Tierschutz & 3R-Zentrum
Director: Prof. Stephanie Krämer
of the Faculty of Veterinary Medicine or Medicine of the Justus Liebig University
Giessen**

First reviewer and supervisor: Peter Jedlicka

Second reviewer: Dulce Papy-Garcia

Vice-chair: Martin Diener

Chair: Klaus-Dieter Schlüter

Date of Doctoral Defense: 7 of December 2023

Table of Contents

1. ABSTRACT	7
2. ZUSAMMENFASSUNG	8
3. INTRODUCTION	10
3.1. ALZHEIMER'S DISEASE	10
3.2. ALZHEIMER'S DISEASE PHYSIOPATHOLOGY	11
3.3. SENILE PLAQUES	14
3.4. TAU PROTEIN	16
3.5. TAU PHOSPHORYLATION	18
3.6. NEUROFIBRILLARY TANGLES	20
3.7. HEPARAN SULPHATE IN THE GLYCOSAMINOGLYCAN FAMILY OF COMPLEX POLYSACCHARIDES	22
3.9. 3-O-SULPHATED HEPARAN SULPHATES IN ALZHEIMER'S DISEASE	27
3.10. REGULATION OF HEPARAN SULPHATE 3-O-SULPHOTRANSFERASES GENE EXPRESSION	28
3.11. GENE REGULATION IN ALZHEIMER'S DISEASE	30
3.12. THE TGF- β SIGNALLING PATHWAY IN ALZHEIMER'S DISEASE	31
4. RATIONALE AND AIMS	34
5. OBJECTIVES OF THE WORK	36
5.1. ESTABLISHMENT OF AN <i>IN VITRO</i> MODEL FOR THE STUDY OF AD RELATED TAU PATHOLOGY.	36
5.2. INVESTIGATE THE ROLE OF HEPARAN SULPHATE PROTEOGLYCANS BIOSYNTHESIS IN THE DEVELOPMENT OF TAU PATHOLOGY.	36
5.3. DECIPHER THE GENE REGULATION OF 3-O-SULPHATED HEPARAN SULPHATES IN AD RELATED TAU PATHOLOGY IN RELATION WITH THE TGF- β 1 PATHWAY.	36
5.4. DECIPHER THE SPECIFICITY AND EFFECT OF 3-O-SULPHATED HEPARAN SULPHATES IN AD RELATED TAU PATHOLOGY.	36
6. MATERIAL AND METHODS	37

6.1. EXPERIMENTAL MODEL	37
6.2. GENOTYPING OF RTG4510 MICE	38
6.3. PRIMARY CULTURE OF RAT CORTICAL GLIAL CELLS	39
6.4. PRIMARY CELL CULTURE OF MURINE HIPPOCAMPAL NEURONS	40
6.5. TRANSDUCTION OF PRIMARY HIPPOCAMPAL NEURONS	40
6.6. TREATMENT OF PHN	41
6.7. PROTEIN QUANTIFICATION	42
6.8. ELECTROPHORESIS	42
6.9. IMMUNOBLOTTING OF RIPA-EXTRACTED PROTEINS	43
6.10. IMMUNOBLOTTING OF HIGH SALT SARKOSYL OLIGOMERS	44
6.11. RNA ISOLATION FROM HPN	45
6.12. RNA ISOLATION FROM HIPPOCAMPAL FORMATION, 2 AND 4 MONTHS.	45
6.13. RNA QUANTIFICATION	46
6.14. RNA EXPRESSION ANALYSIS	46
6.15. IMMUNOFLUORESCENCE OF PHN	47
6.16. TRANSCARDIAL PERFUSION, FIXATION AND BRAIN DISSECTION	48
6.17. FIXATION, CRYOPROTECTION AND LONG-TERM STORAGE	49
6.18. BRAIN SLICING	49
6.19. HISTOPATHOLOGICAL ANALYSIS OF MICE BRAIN WITH THE CHROMOGEN DAB	50
6.20. IMMUNOFLUORESCENCE ANALYSIS OF MICE BRAIN	50
6.21. HUMAN POST-MORTEM MATERIAL	51
6.22. IMMUNOFLUORESCENCE OF HUMAN BRAIN	51
6.23. STATISTICAL ANALYSIS	52
6.24. RNA SEQUENCING AND DATA ANALYSIS	52
6.25. MODELLING OF TAU PROTEIN AND 3-O-HEPARAN SULPHATES	53
6.26. STAR METHODS	55
7. RESULTS	59
<hr/>	
7.1. ESTABLISHMENT AND CHARACTERISATION OF TAUOPATHY IN PRIMARY HIPPOCAMPAL NEURONAL CULTURES FROM RTG4510 MICE MODEL.	59

7.1.1.	NEURONS ARE THE PREDOMINANT CELL TYPE IN DISSECTED HIPPOCAMPUS FROM 16 DAYS MOUSE EMBRYOS	59
7.1.2.	PRIMARY HIPPOCAMPAL NEURONS FROM THE RTG4510 MICE MODEL ARE A GOOD MODEL TO STUDY AD-RELATED TAU PATHOLOGY	61
7.1.3.	TAU OLIGOMERISATION EVOLVES DURING TIME IN CULTURED RTG4510 PHN.	63
7.2.	INCREASED LEVELS OF HEPARAN SULFATE PROTEOGLYCANS BIOSYNTHETIC MACHINERY CORRELATE WITH AN INCREASE IN TAU OLIGOMERIZATION	65
7.2.1.	RTG4510 MICE MODEL DEVELOPS TAUOPATHY IN PYRAMIDAL LAYER OF CA1 REGION	65
7.2.2.	TAU OLIGOMERIZATION STARTS AT EARLY STAGES OF TAU PATHOLOGY DEVELOPMENT IN RTG4510 MICE BRAIN.	67
7.2.3.	TRANSCRIPTOMICS ANALYSIS IDENTIFIES AN UPREGULATION OF HEPARAN SULFATE PROTEOGLYCANS BIOSYNTHETIC MACHINERY RELATED GENES AT EARLY STAGES OF TAU PATHOLOGY DEVELOPMENT	68
7.2.4.	PROTEIN MODELLING OF 3-O-SULPHATED HEPARAN SULPHATES DISACCHARIDE UNITS BIND TO TAU RESIDUES SUSCEPTIBLE TO ABNORMAL HYPERPHOSPHORYLATION	71
7.3.	TGF-β1 CONTROLS THE EXPRESSION OF THE HEPARAN SULPHATE 3-O SULPHOTRANSFERASES AND REGULATES TAU ABNORMAL PHOSPHORYLATION	72
7.3.1.	SMAD2 AND SMAD3 PHOSPHORYLATION INCREASES IN AD HUMAN BRAIN HIPPOCAMPAL FORMATION	72
7.3.2.	SMAD2 AND SMAD3 PHOSPHORYLATION INCREASES IN RTG4510 PHN	74
7.3.3.	TGF- β 1 CONTROLS GENE EXPRESSION OF HEPARAN SULPHATE 3-O SULPHOTRANSFERASES	75
7.3.4.	SELECTIVE INHIBITION OF TGF- β 1 SIGNALING DECREASES TAU PATHOLOGY	77
7.4.	3-O-SULPHATED HEPARAN SULPHATES SYNTHETIZED BY Hs3ST2 ARE INVOLVED IN TAU ABNORMAL PHOSPHORYLATION AND OLIGOMERIZATION	79
7.4.1.	Hs3ST2 AND Hs3ST4 ARE INVOLVED IN AD	79
7.4.2.	Hs3ST2 AND NOT Hs3ST4 DECREASES TAU ABNORMAL PHOSPHORYLATION AND AGGREGATION	81
7.5.	Hs3ST2 LOSS OF FUNCTION ENHANCES GLUTAMATE SYNAPSE SIZE AND CONNECTIVITY, COGNITION AND LEARNING OR MEMORY IN ALZHEIMER'S DISEASE RELATED TAUOPATHY	85
7.5.1.	TRANSCRIPTOMIC ANALYSIS OF Hs3ST2 LOF IN RTG4510 PHN REVEALS PATHWAYS INVOLVED IN COGNITION AND LEARNING OF MEMORY	85
7.5.2.	Hs3ST2 LOF ENHANCES SYNAPTIC SIZE AND CONNECTIVITY	87
8.	DISCUSSION	90
9.	CONCLUSION	101

10.	ANNEX	103
10.1.	CONTEXT OF THE RESEARCH	103
10.2.	RNASEQ QUALITY CONTROLS	104
10.3.	PERCENTAGE OF MAPPED READS BY SALMON	105
10.4.	RTG4510 GENOTYPAGE CONFIRMATION	106
10.5.	GLIAL CELL CULTURE FROM P5 RATS	107
11.	DECLARATION	108
12.	REFERENCES	109
13.	ACKNOWLEDGEMENTS	119

1. Abstract

Alzheimer's disease (AD) is the seventh cause of death in the world, and surprisingly one of the only ones without any effective treatment to cure or stop the disease. Several neuropathological studies have shown the correlation of neurofibrillary tangles (NFTs) burden with the degree of cognitive impairment in AD, whereas deposition of amyloid- β (A β) plaques has failed to show this correlation. Despite continued emphasis on drug development targeting A β plaques in various studies, the lack of a clear association between amyloids and cognitive impairments has resulted in limited positive outcomes. NFTs are the result of tau aggregation, a process in which the heparan sulphates have shown a crucial role. *In vitro*, the aggregation of tau is not possible in the absence of heparin, a highly sulphated heparan sulphate carrying a rare 3-O-sulphation. Here, we show that the gene expression of heparan sulphate 3-O-sulphotransferases, producing specific heparan sulphate chains, the 3-O-sulphated heparan sulphates, is under the control of TGF- β signalling pathway. TGF- β 1 is a pleiotropic cytokine upregulated in AD patients and can modulate gene expression through its transcription factor SMAD4. Furthermore, we demonstrate that the neural heparan sulfate-glucosamine 3-sulphotransferase 2 (Hs3st2) is critical for the AD related tau abnormal phosphorylation and oligomerization, and that its loss of function decreases tau pathology, leading to the recovery of synapse density and connectivity, which is known to be correlated with an improvement in cognition and learning or memory. Together, our results position intracellular 3-O-sulphated heparan sulphates produced by Hs3st2 and its TGF- β related regulatory pathway, as key modulators of AD tau pathology, opening a wide area of research with therapeutic potential for AD and other tauopathies.

2. Zusammenfassung

Die Alzheimer-Krankheit (AD) ist weltweit die siebthäufigste Todesursache und stellt überraschenderweise eine der wenigen Erkrankungen dar, für die es weder eine Heilung noch effektive Eindämmung gibt. Mehrere neuropathologische Studien haben gezeigt, dass der Grad der kognitiven Beeinträchtigung bei AD stark mit der Belastung durch neurofibrilläre Tangles (NFTs) korreliert, wohingegen keine Korrelation mit der Ablagerung von β -Amyloid-Plaques festgestellt wurde. Während der Schwerpunkt der Arzneimittelentwicklung weiterhin auf β -Amyloid-Plaques liegt, haben viele klinische Studien aufgrund des fehlenden Zusammenhangs zwischen Amyloiden und kognitiven Beeinträchtigungen nur minimale positive Ergebnisse erzielt.

NFTs entstehen durch die Aggregation von Tau-Proteinen, wobei Heparansulfate eine entscheidende Rolle spielen. In vitro zeigt sich, dass die Aggregation von Tau ohne Heparin, einem stark sulfatierten Heparansulfat mit seltener 3-O-Sulfatierung, nicht erfolgt. In dieser Studie konnten wir zeigen, dass der TGF- β -Signalweg die Genexpression von Heparansulfat-3-O-Sulfotransferasen reguliert. Diese Enzyme sind verantwortlich für die Bildung spezifischer Heparansulfatketten, nämlich der 3-O-sulfatierten Heparansulfate. TGF- β 1, ein multifunktionales Zytokin, das bei AD-Patienten in signifikant erhöhten Konzentrationen vorliegt, vermag unter anderem die Genexpression dieser Proteine über seinen Transkriptionsfaktor SMAD4 zu beeinflussen.

Des Weiteren konnten wir zeigen, dass die neuronale Heparansulfat-Glucosamin-3-sulfotransferase 2 (Hs3st2) von entscheidender Bedeutung für die abnormalen Tau-Phosphorylierungs- und Oligomerisierungsprozesse im Zusammenhang mit AD ist. Ein Funktionsverlust von Hs3st2 reduziert die Tau-Pathologie, was zur Wiederherstellung der Synapsendichte und -vernetzung führt. Dieser Prozess wiederum ist mit einer Verbesserung der kognitiven Fähigkeiten, des Lernens und der Gedächtnisleistung korreliert.

Zusammengefasst positionieren unsere Ergebnisse die intrazellulären 3-O-sulfatierten Heparansulfate, welche von Hs3st2 synthetisiert und dem TGF- β -vermittelten Signalweg reguliert werden, als Schlüsselmodulatoren der Tau-Pathologie bei AD. Dies eröffnet ein vielversprechendes Forschungsfeld mit therapeutischem Potenzial nicht nur für AD, sondern auch für andere Tauopathien.

3. Introduction

3.1. Alzheimer's Disease

Dementia is a general term used to describe a decline in cognitive ability and memory loss that interferes with a person's quality of life¹. It is not a specific disease, but rather a group of symptoms associated with several underlying conditions. The most common cause of dementia is Alzheimer's disease (AD)². Other causes include vascular dementia, Lewy body dementia, frontotemporal dementia, and mixed dementia. In addition to cognitive decline, dementia is characterised by language problems, impaired judgment, behavioural changes, disorientation, and difficulty performing familiar tasks. It affects thinking, reasoning, problem-solving, decision-making, and the ability to plan and organize daily tasks. Language difficulties make it difficult to find words, express thoughts, and understand conversations. Impaired judgment can lead to poor decision-making, while behavioral changes include mood swings, irritability, anxiety, depression, apathy, and agitation. Ultimately, dementia makes it difficult to complete daily tasks, leading to dependency and assistance³.

Alzheimer's disease, which accounts for as much as 80% of dementia cases, is a progressive neurodegenerative disorder affecting mainly the elderly population⁴. According to the World Health Organisation (WHO), there were an estimated 47 million people living with dementia globally in 2015, and this number is projected to triple by 2050. The prevalence of AD increases with age and is more common in women than in men. The age-specific prevalence of AD ranges from 1% in people 60 to 64 years old to 35% in people 85 years or older. The global prevalence of dementia, including AD, was estimated to be 5 % in people aged 60 years or older in 2020. However, the prevalence varies widely by region, with higher rates reported in high-income countries such as North America and Europe than in low- and middle-income countries such as Asia and Africa. To date, in Europe there are 7 million patients diagnosed with AD and are expected to double by 2030⁵. Currently, there is not really effective treatment for AD. However, 172

clinical trials involving 143 potential drugs are running. These agents are classified by the Common Alzheimer's Disease Research Ontology (CADRO) based on their drug targets and mechanism of actions. Most of these agents target amyloid plaques, inflammation/immunity and synaptic plasticity/neuroprotection. From all these 143 agents targeting nucleic acids, peptides, and lipids, only one carbohydrate-based agent is being tested, reflecting the lack of research in the field of carbohydrate based/target molecules⁴.

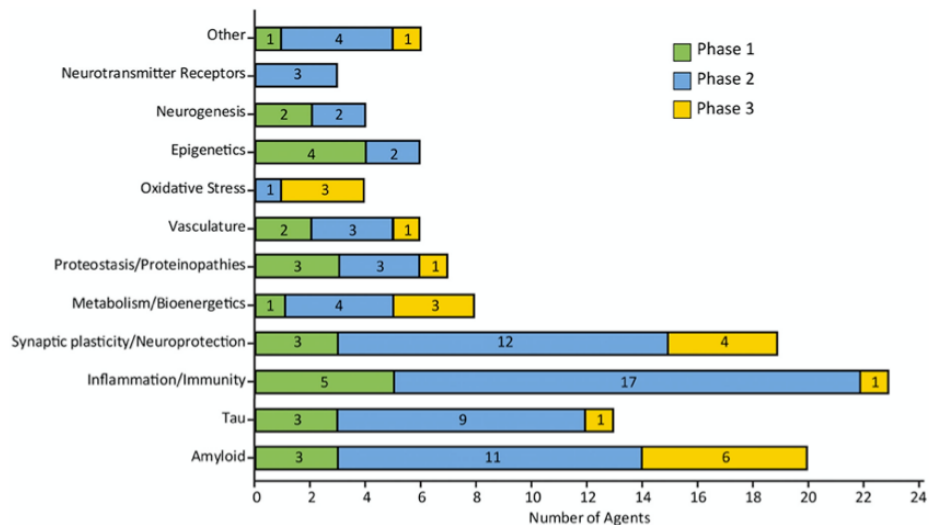


Figure 1. Mechanisms of action of disease modifying agents in all phases of clinical trials. Agents grouped according to the Common Alzheimer's Disease Research Ontology (CADRO) (Figure from © J Cummings; M de la Flor, PhD, Illustrator).

3.2. Alzheimer's disease pathophysiology

The exact aetiology of AD is not yet fully understood, but is believed to be multifactorial, involving genetic, environmental, and lifestyle factors. Genetic factors play an important role, particularly in Early-onset Alzheimer's disease (EOAD) cases, which represent a small proportion of all AD cases with a strong genetic basis⁶. EOAD is linked to mutations in the genes APP, PSEN1, and PSEN, identified as causative factors in EOAD⁷. Mutations in these genes lead to altered processing of amyloid precursor protein (APP) and

overproduction or beta-amyloid peptide, resulting in the accumulation of amyloid plaques, recognized as one as the main hallmarks of AD. On the other hand, Late-onset sporadic Alzheimer's disease (LOAD) is the most common form of the disease, typically occurring after the age of 65⁸. The apolipoprotein E (APOE) gene has been identified as the strongest genetic risk factor for LOAD and its cellular uptake is enhanced by 3-O-sulphated heparan sulphates⁹. The APOE protein encoded by the APOE gene, and it is a strong heparin binding protein. The gene has three major alleles: $\epsilon 2$, $\epsilon 3$, and $\epsilon 4$ among which the $\epsilon 4$ allele is associated with an increased risk and an earlier onset of AD. APOE $\epsilon 4$ carriers have higher levels of amyloid plaques and an increased risk of developing AD compared to non-carriers¹⁰. The APOE $\epsilon 4$ allele has also been shown to increase the risk of developing tau-related neurodegenerative diseases and is associated with more severe tau pathology¹¹. Nonetheless, it's important to note that the APOE $\epsilon 4$ allele is neither necessary nor sufficient to cause the disease, indicating a complex interplay between genetic and environmental factors.

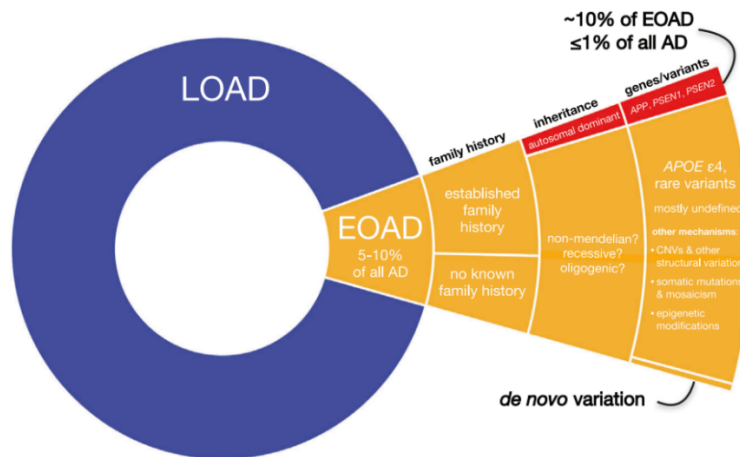


Figure 2. Prevalence and associated genes in early-onset Alzheimer's disease. Hierarchical pie chart illustrates the prevalence of EOAD in relation to LOAD. EOAD is thought to represent ~5–10% of all AD. The major genes implicated in EOAD are APP,

PSEN1, and PSEN2, while the primary risk factor for non-mendelian EOAD is the APOE ϵ 4 allele. Figure modified Sirkis, D., et al. (2022).

Several other genetic risk factors have been identified through genome-wide association studies (GWAS). These include TREM2, CLU, PICALM, ABCA7, BIN1, CR1, EPHA1, among others⁶. These coding genes are membrane-associated proteins involved in various biological processes, such as immune response, lipid metabolism, and endocytosis, suggesting their potential contribution to AD pathogenesis. Interestingly, TREM2 is a membrane protein capable of binding cell-surface proteoglycans, disrupting phospholipid signaling¹². The probability of developing AD may also be increased by environmental factors such as exposure to chemicals, traumatic brain injury, and infections.

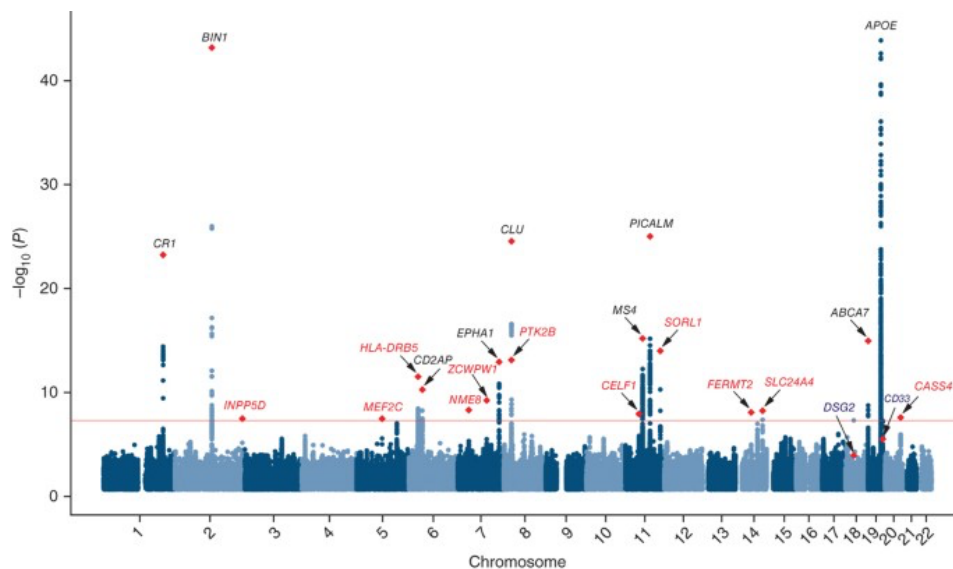


Figure 3. Manhattan plot of genome-wide association with Alzheimer's disease (17,008 cases and 37,154 controls). The threshold for genome-wide significance is indicated by the red line. Genes previously identified by GWAS are shown in black, and newly associated genes are shown in red. From Lambert, JC., et al. (2013).

With respect to pathological anatomy, AD is characterised by the presence of specific brain characteristics, including two main hallmarks: senile plaques (SP) principally made

of the A β peptide (A β) and neurofibrillary tangles (NFT), principally made of abnormally phosphorylated forms of the microtubule associated protein tau (MAPT)¹³. These pathological features are known to play a crucial role in the development and progression of the disease. The relationship between SP and NFT in AD is complex and not entirely understood, but it is believed that they may interact and influence each other¹⁴. A common hallmark for SP and NFT is the presence of heparan sulphates, which are known to interact with APP, APOE, TREM2, PSEN1, PSEN2, EPHA1, and tau, and that have been found to co-deposit in both, NFT and SP¹⁵.

3.3. Senile plaques

Senile plaques, also called amyloid plaques, are abnormal extracellular deposits of A β peptides that accumulate between neurons in the brain. A β is physiologically produced following APP processing by two enzymes: alpha-secretase and gamma-secretase, in a non-amyloidogenic pathway leading to the production of soluble fragments with neuroprotective properties¹⁶. However, in AD, there is an aberrant processing of APP by beta-secretase (also known as BACE-1) and gamma-secretase, leading to the longer and more aggregation-prone A β ₄₂¹⁷. This leads to the accumulation of A β with a tendency to aggregate into insoluble fibrils. The aggregation of A β peptides is associated with conformational changes, beta-sheet formation, and the formation of oligomers and protofibrils, which contribute to the A β toxicity. These fibrils then form small groups, which eventually aggregate to form amyloid plaques in the brain. heparan sulphates play a central role in the amyloidogenic process by their capacity to accelerate fibrillization of specific proteins and peptides¹⁸. The relevance of heparan sulphates in the formation of A β *in vivo* and *in vitro* has been demonstrated in several studies¹⁹. The importance of the APP interaction with heparan sulphates during the amyloidogenic process has been evidenced by the decreased in the number of A β peptides in an *in vivo* transgenic model overexpressing the enzyme heparanase, which activity decreases the heparan sulphates content²⁰. Moreover, a reduction in the amyloid deposition has been observed in a

knockout model in which the expression of the first enzyme involved in heparan sulphates biosynthesis, *Ext1*, was suppressed¹⁹. This has suggested that targeting the axis A β -heparan sulphates could be an effective strategy for AD prevention and treatment (Figure 4).

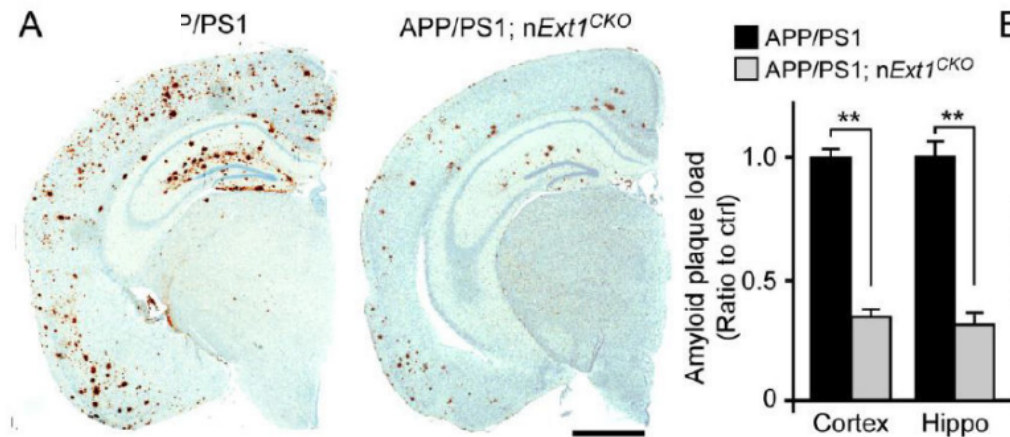


Figure 4. Neuronal heparan sulphates deficiency reduces amyloid deposition. (A) Brain sections from control (APP/PS1) and neuronal heparan sulphate-deficient (APP/PS1; nExt1^{CKO}) at 12 months of age were immunostained with a pan-A β antibody. Scale bar, 1 mm. The percentage of area covered by plaques was quantified, and the plaque load was normalized to that of APP/PS1 mice. Modified from Liu CC., et al. (2016).

Although currently controversial, the production of A β has been for a long time proposed to initiate a cascade of AD pathological events, including inflammation, oxidative stress, and neuronal dysfunction. This has been supported by the A β neurotoxicity and capacity to disrupt the normal functioning of synapses, contributing to the cognitive decline and memory deficits observed in AD²¹. A high buildup of A β peptide in the AD brain has been proposed to be due to insufficient clearance systems with diminished enzymatic activity, impaired microglial function or to other mechanisms altered transit across the blood-brain barrier or altered phagocytosis by microglial cells²². Although most components of the

amyloid cascade have been the target of several therapeutic strategies, their missing or low efficacy on clinical trials has directed the scientific community to focus in the tau cascade leading to formation of NFT²³, and positioning the tau protein as a new promising target for treating AD.

3.4. Tau protein

Tau is a microtubule-binding protein encoded by the MAPT gene. Tau stabilises microtubules within neurons, allowing proper intracellular transport and maintaining the cytoskeleton. The MAPT gene undergoes alternative splicing, resulting in the expression of different tau isoforms in the brain, allowing functional diversity and specialisation in different neuronal populations and developmental stages²⁴. These isoforms differ in the presence or absence of specific repeat domains, such as the 3-repeat (3R) and 4-repeat (4R) domains. The physiological role of MAPT, specifically the tau protein, is associated with maintaining the structural integrity of neurons, facilitating intracellular transport, regulating neuronal morphology, and contributing to neuronal signalling and plasticity. It stabilizes microtubules, promotes their assembly and stability, and facilitates the transport of essential molecules within neurons. Tau also regulates neuronal morphology, influencing axonal growth, branching, and guidance during neuronal development. Additionally, tau is involved in neuronal connectivity, modulating the activity of signalling molecules, receptors, and other proteins. It participates in the regulation of synaptic plasticity, neurotransmitter release, and neuronal excitability. Tau interacts with various proteins, including those involved in tau phosphorylation, cellular transport, cytoskeletal organization, and synaptic function, influencing their activities and localization within neurons²⁵. Tau protein contains two major domains, the projection domain and the microtubule binding domain, together organized in fourth functional domains: 1) the N-terminal domain mainly regulating its subcellular localization and stability. 2) The proline-rich domain (aa 197-244) with interaction sites for DNA-RNA binding, proteins containing Src homology 3 (SH3) domains involved in cellular signaling and cytoskeletal

organization. 3) The microtubule-binding repeat domain (aa 245-369) comprising multiple imperfect repeat sequences rich in positively charged amino acids, these repeats allow tau to interact with microtubules. 4) The C-terminal domain (aa 370-441) is involved in protein-protein interactions, intracellular localisation, and molecular chaperones that regulate its degradation²⁴. A heparin binding region (or heparin binding domain) in tau extends among the major microtubule binding domain, predominantly in the functional microtubule assembly domain, forming a 1:1 complex with heparin, or another polyanions, that triggers the tau abnormal phosphorylation and fibrillization¹⁸ (Figure 5).

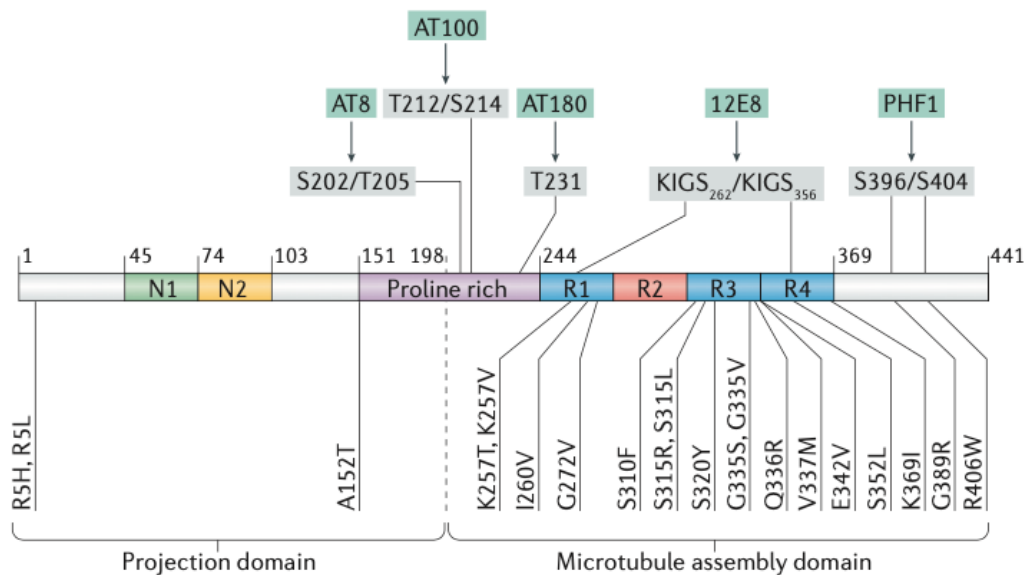


Figure 5. Tau can be subdivided into major domains. The projection domain is the amino-terminal section that projects away from microtubules. The microtubule assembly domain (amino acids 198-441) contains the heparin binding domain (amino acids 244-372) and contains multiple motifs that are targets of kinases such as glycogen synthase kinase 3 β (GSK3 β), cyclin-dependent kinase 5 (CDK5), mitogen-activated protein kinase (MAPK) and JUN N-terminal kinase (JNK). Modified from Wang Y., et al (2016).

3.5. Tau phosphorylation

Phosphorylation is a key post-translational modification that regulates the physiological function of tau. In its normal, non-pathological state, tau undergoes dynamic phosphorylation and dephosphorylation processes that finely tune its function within the cell. The physiological phosphorylation of tau is tightly regulated by the balance between the activities of various kinases and phosphatases. In a physiological context, tau phosphorylation involves the activity of several kinases. Glycogen synthase kinase-3 beta (GSK-3 β) plays a crucial role in the phosphorylation of specific sites in tau, contributing to its normal regulation and function. Moreover, cyclin-dependent kinase 5 (CDK5), in conjunction with its activators p35 and p25, also participates in tau phosphorylation, affecting its function and localization in neurons. The microtubule affinity-regulating kinase (MARK)/PAR-1 family of kinases is involved in the process, phosphorylating tau at specific sites to affect tau-microtubule interactions. Protein kinase A (PKA), another key player, can phosphorylate tau and modulate its activity. Additionally, calcium/calmodulin-dependent protein kinase II (CaMKII) participates in tau phosphorylation in response to changes in intracellular calcium levels. Finally, casein kinase 1 (CK1) and casein kinase 2 (CK2) contribute to tau phosphorylation and normal regulation of tau function²⁶ (Figure 5).

The abnormal hyperphosphorylation of tau disrupts its normal function, leading to its dissociation from microtubules and promoting the aggregation of tau into neurofibrillary tangles, characteristic features of AD and other tauopathies. Tau abnormal hyperphosphorylation is a complex process influenced by a combination of genetic, environmental, and age-related factors. However, the exact reasons for abnormal tau hyperphosphorylation are not fully understood, although several factors have been described. One of the proposed mechanisms suggests that 3-O-sulphated heparan sulphates bind to the heparin binding site of tau in a molecular chaperon-like manner inducing its abnormal phosphorylation, as previously described²⁷ (Figure 6).

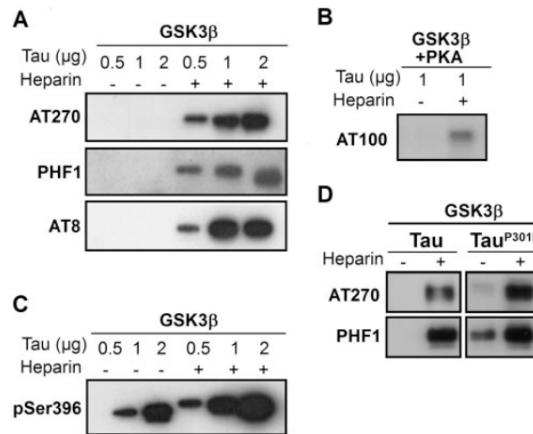


Figure 6. Phosphorylation of tau and tauP301L at pathological phosphorylation sites is induced by heparin *in vitro* and by 3-O-sulphated heparan sulphates *in vitro* and *in cells*. (A–C) GSK3B-mediated abnormal phosphorylation of wild-type tau and tauP301L is dependent on the presence of heparin in the reaction mixture. (D) GSK3B-mediated abnormal phosphorylation of tau and tauP301L at epitopes AT270 and PHF1. Modified from Sepulveda-Diaz JE., et al (2015).

3-O-sulphated heparan sulphates induce a conformational change in tau allowing the access of the different kinases to epitopes that were previously inaccessible for phosphorylation²⁸. The tau protein undergoes abnormal hyperphosphorylation at specific sites, including serine 199, 202 (pS199, pS202), threonine 231, serine 235 (pT231, pS235), serine 396, serine 404 (pS396, pS404), serine 422 (pS422), serine 262, and serine 356 (pS262, pS356)²⁶, most of them occurring at the heparin binding site. Additionally, dysregulation of kinases and phosphatases, responsible for the addition and removal of phosphate groups, respectively, disrupts the delicate balance of tau phosphorylation. Overactivation of certain kinases or reduced phosphatase activity results in tau becoming hyperphosphorylated. Moreover, genetic mutations in the tau gene (MAPT) or other genes involved in tau metabolism can contribute to increased phosphorylation²⁹. Chronic neuroinflammation, which is often observed in neurodegenerative diseases, can trigger signalling pathways that lead to tau

hyperphosphorylation. Similarly, inflammatory molecules and cytokines, such as IL-1 β , IL-6, TNF- α and TGF- β , released in response to brain injury or chronic inflammation, can regulate and activate enzymes that target tau³⁰. Furthermore, alternative splicing of the tau gene produces different tau isoforms, some of which are more susceptible to abnormal hyperphosphorylation and aggregation³¹. The abnormal hyperphosphorylation of tau tends to increase with age and, as individuals age, the regulation of tau phosphorylation may become less efficient. The interplay of these factors contributes to the pathological hyperphosphorylation of tau, leading to the formation of neurofibrillary tangles and neurodegeneration in diseases such as AD.

3.6. Neurofibrillary tangles

The abnormal hyperphosphorylation of tau leads to a series of events that ultimately result in its aggregation. After the tau abnormal phosphorylation weakens its microtubule-binding ability, promoting its detachment from microtubules, the hyperphosphorylated tau misfolds, exposing hydrophobic regions that are normally not accessible within the protein's structure. Misfolded tau acts as a seed or nucleus, initiating aggregation and forming small tau oligomers. These oligomers are further aggregated into insoluble neurofibrillary tangles composed of hyperphosphorylated tau filaments. Several studies have shown that heparan sulphates co-localize with tau in NFT, suggesting that these sulphated polysaccharides might contribute to the aggregation of tau and to the stabilization of tau filaments (Figure 7)²⁸. Indeed, the aggregation of tau *in vitro* is not possible in the absence of heparin or other polyanions. Moreover, heparan sulphates were detected in the intracellular compartment in non-tangle bearing neurons in AD brains, suggesting a possible intracellular accumulation before the NFT formation¹⁵.

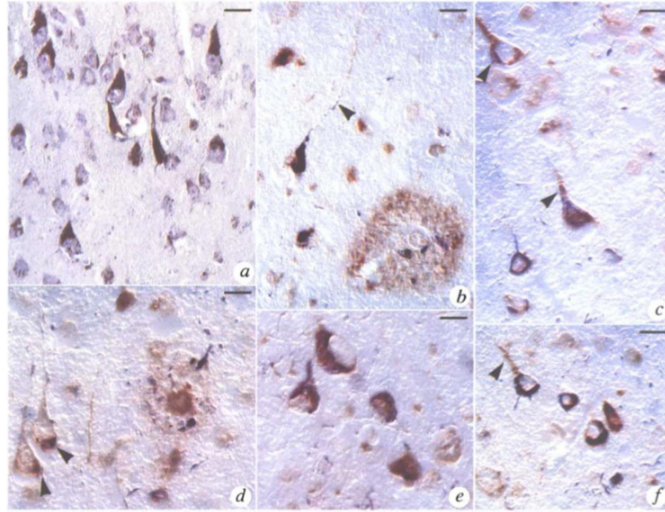


Figure 7. Heparan sulphates co-localize with NFT in AD hippocampal human brain. **a**, the anti-heparan sulphate antibody 10E4 and counterstained with thionine. **b-f**, double staining with 10E4 (brown) and the phosphorylated anti-tau antibody AT8 (blue). From Goedert M., et al (1996).

This NFT accumulation disrupts cellular processes, leading to neuronal dysfunction and eventually cell death. The presence of NFT near synapses interferes with synaptic signaling and communication between neurons, contributing to synaptic dysfunction. Synaptic loss occurs as tau accumulates and leads to cognitive deficits in AD. Additionally, tau oligomers, which are the intermediate forms of tau aggregation, are considered more toxic and can directly interfere with synaptic function, further contributing to synaptic dysfunction, neuronal degeneration, and neuroinflammation³². Interestingly, heparan sulphates also modulate inflammatory responses³³, potentially influencing the chronic neuroinflammation observed in AD.

Heparan sulphate proteoglycans are central players in the development and functions of synapses. These complex heparan sulphates carrying proteins are important components of the synapse-organizing protein complexes and serve as ligands for leucine-rich repeat transmembrane neuronal proteins (LRRTMs)³⁴. LRRTM3 is involved in the development of LOAD by promoting the processing of APP by BACE-1. Several

proteins are involved in synaptic dysfunction³⁵. Among them, synaptic vesicle proteins, such as synapsin and synaptophysin, regulate the release of synaptic vesicles and the release of neurotransmitters at synapses. Postsynaptic density protein-95 (PSD-95) acts as a scaffolding protein critical for organising and stabilising synaptic receptors and signaling molecules in the postsynaptic membrane. N-methyl-D-aspartate (NMDA) receptors, ion channels, play a significant role in synaptic plasticity, learning, and memory processes. Glutamate receptors, including AMPA and kainate receptors, mediate excitatory synaptic transmission. Vesicle fusion proteins, such as synaptobrevin, SNAP-25, and syntaxin, are crucial for neurotransmitter release. Neurotrophic factors, such as the heparin binding brain-derived neurotrophic factor (BDNF) and nerve growth factor (NGF), play a vital role in promoting synaptic growth, maintenance and survival³⁶. Dysfunction of heparan sulphate proteoglycans metabolism and its interaction with synaptic proteins and receptors may disrupt synaptic function and neurotransmission, which might be crucial for cognitive decline in AD.

3.7. Heparan sulphate in the glycosaminoglycan family of complex polysaccharides

Glycosaminoglycans (GAGs) are long, linear polysaccharides composed of repeating disaccharide units, crucial components of the extracellular matrix (ECM) and the cell membrane³⁷. Each disaccharide unit consists of an amino sugar (either N-acetylglucosamine or N-acetylgalactosamine) and a uronic acid or galactose. There are several types of GAGs, including hyaluronic acid (HA), chondroitin sulphates (CS), dermatan sulphates (DS), keratan sulphates (KS), and heparan sulphates. HA, a nonsulphated GAG, provides lubrication and shock absorption in joints and synovial fluid. CS, a sulphated GAG, forms proteoglycans and contributes to the tensile strength of cartilage, tendons, and ligaments. DS, another sulphated GAG, maintains the integrity of the skin, blood vessels, and heart valves and aids in tissue repair. KS, a sulphated GAG, contributes to the structural stability of the cornea, cartilage, and bone³⁸. Lastly, heparan

sulphates, also sulphated, are involved in cell signalling, inflammation, growth factor regulation, and at the cell membrane are central players during synaptic transmission in the brain. Heparan sulphates are the most complex GAGs, they are composed of 50-200 saccharidic units that are present intracellularly (serglycin is the only intracellular HSPG), on the cell surface (glypicans and syndecans), and in the extracellular matrix (perlecan, agrin and collagen XVIII) of various tissues, including the brain. Each heparan sulphate molecule is a linear polysaccharide composed of repeating disaccharides of hexuronic acid and glucosamine (GlcN) that can exhibit immense structural diversity due to substitution with sulfate groups at varying extents and to epimerization of glucuronic acid (GlcA) to iduronic acid (IdoA)¹⁸. Heparan sulphates are structurally related to heparin, which is indeed an the more highly sulfated form of heparan sulphates mainly expressed by mastocytes. Biosynthesis and modification of heparan sulphates chains take place within the endoplasmic reticulum, Golgi apparatus, and trans Golgi network, producing unique heparan sulphates chains that are covalently attached to a range of core proteins to form heparan sulphates-proteoglycans (HSPG)³⁹.

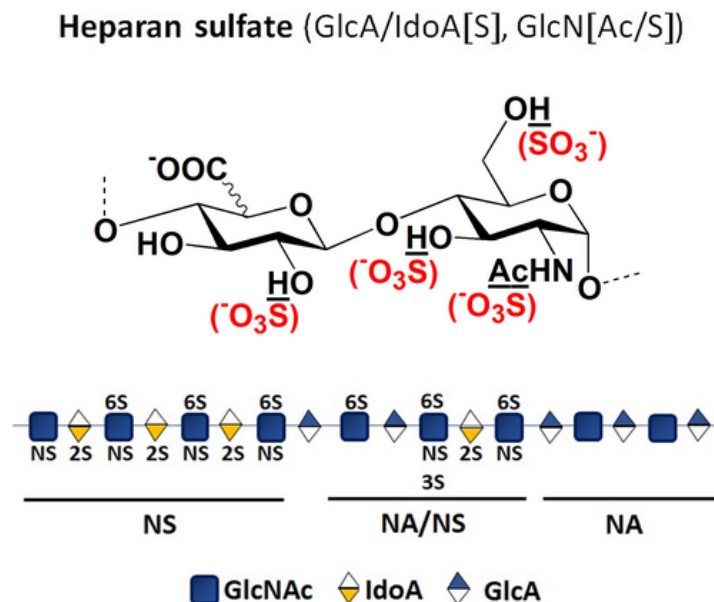


Figure 8. Schematic representation of a heparan sulfate (HS) chain. The different HS domains are represented: NA (unsulfated domains), NA/NS (mixed *N*-sulfated and *N*-

acetylated domains) and NS (rich *N*- and *O*-sulfated domains). The structure of a disaccharide characteristic of HS is represented to note the framed groups susceptible to carry sulfate groups. From Maïza A., et al. (2018).

3.8. Heparan sulphate proteoglycans biosynthesis

Proteoglycans are complex macromolecules principally located in the extracellular matrix (ECM) and in the plasma membrane of cells, although a particular proteoglycan, serglycin, is located in intracellular structures of mastocytes. Proteoglycans are composed of a core protein to which GAG chains are covalently attached⁴⁰. The core protein of a proteoglycan provides the backbone and stability for the molecule, while the attached GAG chains confer unique properties to the proteoglycan. The GAG chains in proteoglycans are highly negatively charged because of the presence of sulphate and carboxyl groups, making them highly hydrophilic.

Proteoglycans exhibit remarkable functional diversity, defined by the identity of the core protein and the structure of the attached glycanic chain. This diversity is evident in the range of diseases and syndromes that result from defects in genes responsible for their biosynthesis. Among proteoglycans, HSPG are the most structurally and functionally complex. This diversity arises primarily from the numerous genes involved in their synthesis, each displaying unique expression patterns. Interestingly, while some of these genes are crucial for normal development and tissue homeostasis, others are not, indicating that certain HSPG play essential biological roles, depending on the specific core protein and associated heparan sulphates chains produced by the HSPG biosynthetic machinery specifically expressed in each individual tissue or cell. Despite their structural diversity, heparan sulphates are often regarded as a single ubiquitous molecule, mainly because of their highly complex and challenging structure⁴¹.

Through a systematic review and analysis, a new classification on HSPG has emerged, providing a deeper understanding of the involvement of each biosynthetic gene in generating heparan sulphates sequences with diverse functions. These heparan sulphates structures can play a role in tissue homeostasis, disease development, behavioral disorders, proper tissue responses to stimuli, and tissue-specific susceptibility to disease. The great structural diversity of heparan sulphates chains in HSPG is defined by its biosynthetic machinery. The core protein biosynthesis occurs at the endoplasmic reticulum-Golgi apparatus interface and the heparan sulphates chain synthesis and maturation occurs in the Golgi apparatus³⁹.

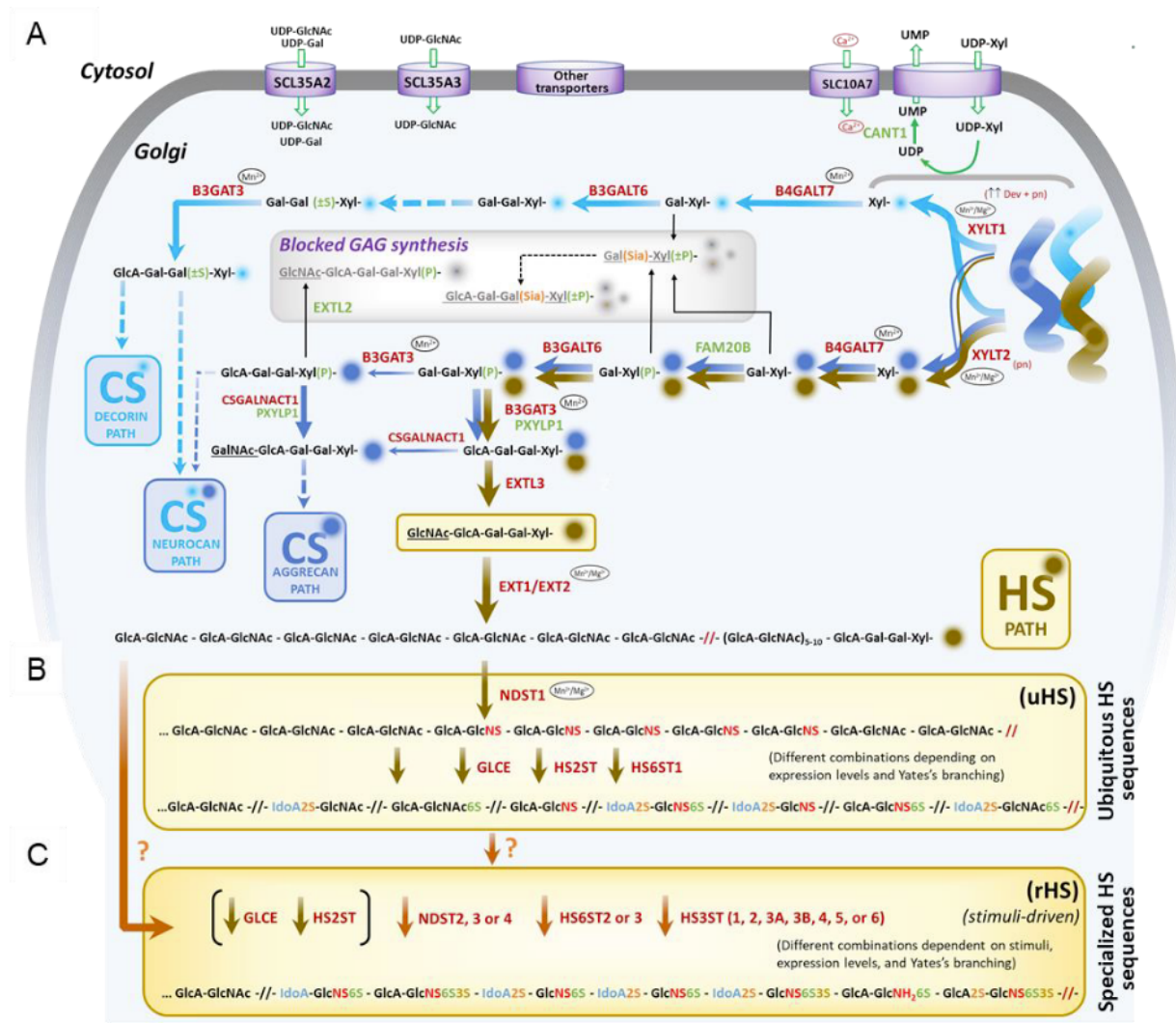


Figure 9. Schematic representation of the HSPG biosynthetic pathway. A) Biosynthesis of the GAG-CP linker tetrasaccharide common to HSPG and CSPG. B) Ubiquitously expressed enzymes drive the synthesis of ubiquitous heparan sulphate sequences (uHS). C) Tissue restricted enzymes form HS sequences (rHS) likely during response to stimuli. rHS might contain high NS domains formed either from uHS or directly from unsulfated chains). From Ouidja MO., et al. (2022).

The biosynthesis starts with the assembly of a GAG-protein linker, which initiates the covalent binding of heparan sulphates to proteoglycan core proteins, followed by the polymerization of the heparan sulphates chain, and lastly, the structural modification of the elongated chain. The first two stages of heparan sulphates biosynthesis involve the sequential transfer of sugar residues to the growing chain and are catalysed by different glycosyltransferases, including XYLT1, XYLT2, B4GALT7, B3GALT6 and B3GAT3, kinases (FAM20B), phosphatases (PXYLP1), nucleosidases (CANT1) with their corresponding transporter (SCL26A2, SLC35A2, and SLC35A3), and ion transporters (SLC10A7). The polymerized chain then undergoes maturation by several heparan sulphate modifying enzymes, including *N*-deacetylase/*N*-Sulphotransferases (NDSTs), D-glucuronyl C5-Epimerase (GLCE) and different *O*-sulphotransferases (2OST, 6OSTs, 3OSTs) (Figure 9). Finally, further modifications of heparan sulphates structure take place post-synthetically, through the action of 6-*O*-endosulfatases Sulf-1 and Sulf-2, and heparanase. In particular, specialized heparan sulphates, such as 3-*O*-sulfated heparan sulphates, are exclusively produced in specific tissues, particularly the brain. The enzymes responsible for producing 3-*O*-sulfated heparan sulphates are called heparan sulphate 3-*O*-sulphotransferases. These enzymes have tissue-specific expression patterns and transfer sulphate groups to specific positions on the glucosamine residues of heparan sulphates chains. The seven heparan sulphate 3-*O*-sulphotransferases enzymes are: HS3ST1, HS3ST2, HS3ST3A, HS3ST3B, HS3ST4, HS3ST5, and HS3ST6.

3.9. 3-O-Sulphated heparan sulphates in Alzheimer's disease

Heparan sulphates are traditionally found at the cell surface and in the extracellular matrix, but their accumulation inside neurons in AD challenges the conventional belief of their extracellular location. Specifically, the rare sulphation at the position 3 in the glucosamine residue results into the intracellular translocation of 3-O-sulfated heparan sulphates in cell models of AD-related tau pathology¹⁸. It has been shown that within cells, 3-O-sulfated heparan sulphates act as molecular chaperones that can interact with tau and promote its abnormal phosphorylation and aggregation, the two main molecular events characteristic of AD-related tau pathology. Whereas 3-O-sulfated heparan sulphates are detected at synapses in developing brains from mice, they are internalized in neurons and in synaptosomes from a transgenic mice model overexpressing a repressible form of human tau containing the P301L mutation (rTg4510)⁴². The importance of 3-O-sulphated heparan sulphates in tau pathology was shown when cultured cells and synaptosomes were treated with heparinase, leading to a decrease in the internalisation of heparan sulphates and preventing the production of pathological tau²⁷. These findings align with the *in vitro* need for polyanions such as heparan sulphates/heparin in the abnormal phosphorylation and aggregation of tau, as they induce specific conformational states allowing kinases to access previously inaccessible tau epitopes, ultimately leading to aggregation. In the brain, 3-O-sulphation is ensured by expression of several neuronal heparan sulphate 3-O-sulphotransferases, including HS3ST1, HS3ST2, HS3ST4 and HS3ST5 (Figure 10A)³⁷. Notably, the heightened expression of HS3ST2 in the AD hippocampus suggested its involvement in the mechanism behind tauopathy, highlighting heparan sulphate 3-O-sulphotransferases as potential new targets for AD. Furthermore, the gain of function of HS3ST2 induces the autonomous aggregation of tau, resembling the intracellular accumulation of heparan sulphates observed in AD neurons and the characteristic tau aggregation in the development and progression of tau pathology (Figure 10B)⁴³. However, how the expression of HS3ST2 is regulated, and whether its transcriptomic regulation can impact tau pathology it is unknown.

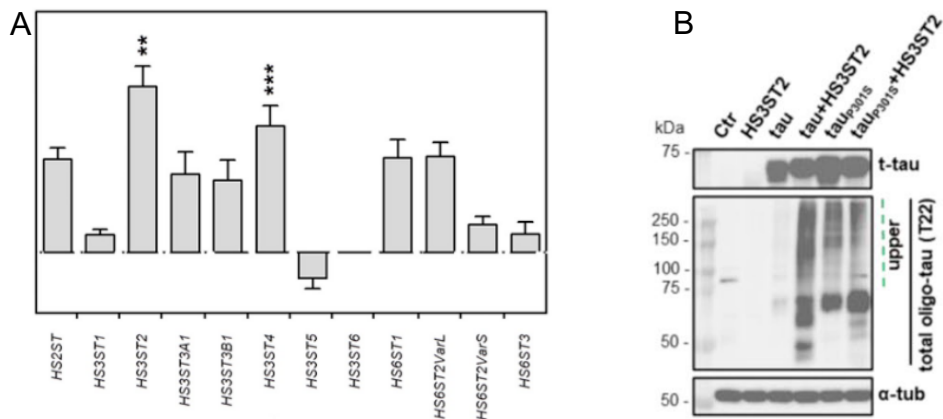


Figure 10. Heparan sulphate 3-O-sulphotransferases are increased in AD hippocampus and HS3ST2 promotes tau oligomerization. A) Expression of the main heparan sulphate sulphotransferases responsible of *N*-, 2-*O*-, 3-*O*- and 6-*O*-sulphation by RT qPCR. B) T-tau (K9JA) immunoblotting (upper blot) in RIPA cell lysates. Oligo-tau (T22) immunoblotting (medium blot) in cell lysates extracted with high salt (500 mM) Sarkosyl buffer. Stable tau aggregates are highlighted in the upper part of the blot (green dotted line). An anti- α -tubulin (α -tub) antibody was used as loading control (RIPA).

3.10. Regulation of heparan sulphate 3-O-sulphotransferases gene expression

Gene expression is tightly regulated in cells to ensure the precise and dynamic control of protein production. This regulation occurs at multiple levels. At the transcriptional level, transcription factors play a crucial role by binding to specific DNA sequences near the gene's promoter region, either enhancing or inhibiting gene transcription. Epigenetic modifications, such as DNA methylation and histone modifications, also impact gene expression by modifying chromatin structure, making genes more or less accessible to the transcriptional machinery. Non-coding RNAs, such as microRNAs (miRNAs) and long non-coding RNAs (lncRNAs), can interact with messenger RNAs (mRNAs) and regulate gene expression at the post-transcriptional level¹³.

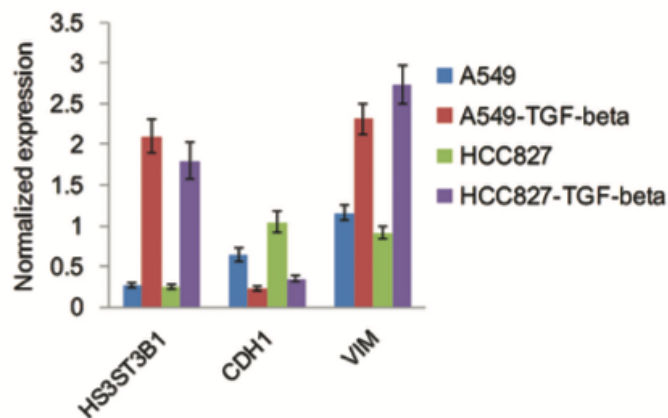


Figure 11. HS3ST3B1 is increased in transforming growth factor-beta-induced epithelial-to-mesenchymal transition process. The expression of HS3ST3B1 is significantly increased ($\times 100$) by TGF- β 1. CDH1 is the gene of E-cadherin and VIM is the gene of vimentin, they are both epithelial-to-mesenchymal transition biomarkers. Modified from Zhang Z., et al. (2018).

HS3ST2 undergoes silencing through hypermethylation in various cancer types, including cervical, ovarian, endometrial, breast, gastric, acute myeloid leukemia, colorectal, and prostate cancer⁴⁴. Consequently, its expression is significantly reduced in cancer samples compared to their matched normal counterparts. Similarly, other genes encoding HS sulphotransferases, such as HS3ST1 and HS3ST3A1, also experience hypermethylation in the proximal regions in chondrosarcoma, leading to a decrease in their transcription⁴¹. However, exposure to a demethylating agent can restore their expression, confirming the influence of aberrant methylation on their normal transcriptional activity. In contrast, HS3ST3B1 exhibits significant upregulation in non-small cell lung cancer (NSCLC) tissues when compared to matched normal tissues. This upregulation is induced by TGF- β 1, which drives the transition from an epithelial to a mesenchymal phenotype and contributes to increased HS3ST3B1 expression (Figure 11)⁴⁵. Moreover, HS3ST3B1 expression in leukemia cells is regulated by the vascular endothelial growth factor (VEGF)-dependent angiogenesis in xenografted mice. Additionally, HS3ST4 is a

transcriptional target of TRF2 (telomere repeat binding factor 2), and elevated TRF2 levels lead to the upregulation of HS3ST4 gene expression⁴⁶. To date, the relationship between heparan sulphate 3-O-sulphotransferases gene expression regulation and pathological process in AD remains an important question that remains to be addressed.

3.11. Gene regulation in Alzheimer's Disease

Gene expression is a tightly regulated process that allows cells to control which genes are turned on or off, thereby determining the production of specific proteins essential for various cellular functions. This regulation is vital for maintaining cellular homeostasis, responding to environmental cues, and ensuring proper development and tissue differentiation. At the transcriptional level, gene expression is primarily controlled by transcription factors. These are proteins that bind to specific DNA sequences in the gene's promoter region and either enhance or inhibit transcription. In AD, there is dysregulated expression of various genes that play crucial roles in brain function, neural communication, and maintenance of neuronal health¹³.

In a recent work, the comparison of gene expression between AD and old-matched patients showed a signature of 421 genes significantly upregulated in AD, while 434 genes exhibit significant downregulation. Gene Ontology (GO) analysis revealed that 'regulation of transcription' emerges as the top GO term in the Biological Process category. Further examination of genes within the 'regulation of transcription' GO term reveals the presence of several transcription factors, including SMAD4, which is the effector of the TGFB1 pathway, and chromatin structure-related genes. This provides potential insights on the importance of TGFB1 signalling pathways into the underlying mechanisms contributing to the observed gene expression changes in AD (Figure 12)⁴⁷.

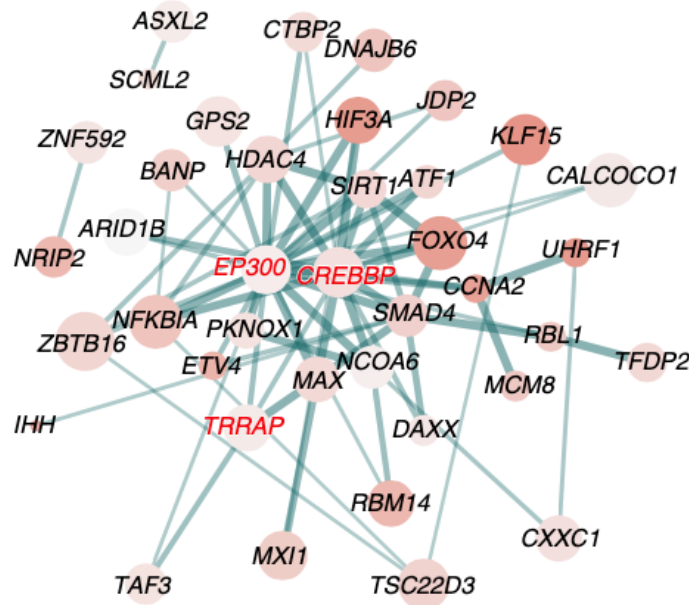


Figure 12. Transcriptomic analysis identifies upregulation of TGF- β 1 transcription related genes. StriNG analysis of the 75 transcription- and chromatin-related genes revealing a protein interaction network of 35 gene products with SMAD4, CREBBP and EP300 at the center of the network. Node size represents gene expression in AD, color intensity represents gene expression changes in AD versus old and the thickness of the lines represents the strength of the StriNG interaction. Modified from Nativio, et al. (2020).

3.12. The TGF- β signalling pathway in Alzheimer's Disease

The transforming growth factor beta (TGF- β) pathway plays a crucial role in numerous cellular processes such as differentiation, proliferation, apoptosis, and migration. The *Tgfb1* gene encodes the TGF- β 1 protein, which is a member of the TGF- β superfamily and a potent regulator of the TGF- β pathway. This pathway is initiated when TGF- β 1 binds to its type II receptor (TGFBR2), which recruits and activates the type I receptor (TGFBR1). The activated TGFBR1 then phosphorylates and activates the downstream

effectors SMAD2 and SMAD3, which form a complex with SMAD4 and translocate to the nucleus to regulate gene expression⁴⁸.

TGF- β is a pleiotropic cytokine overexpressed in the brain of AD patients playing a central role in the development and progression of the disease⁴⁹. Studies have found that the TGF- β pathway is dysregulated in AD and induces APP synthesis and promotes A β formation by a transcriptional mechanism involving the Smad3⁵⁰. TGF- β -regulated TIAF1 (TGF- β 1-induced antiapoptotic factor) aggregation leads to dephosphorylation of APP, followed by degradation and generation of APP intracellular domain (AICD), A β and amyloid fibrils, favoring the formation of senile plaques⁵¹. Furthermore, the blockade of the TGF- β –Smad2/3 innate immune signaling mitigates Alzheimer-like pathology (Figure 13)⁵². To date, it is unknown whether the TGF- β 1 signaling pathway is involved in the regulation of heparan sulphate 3-O-sulphotransferases expression, and its effect in the development and progression of AD related tau pathology.

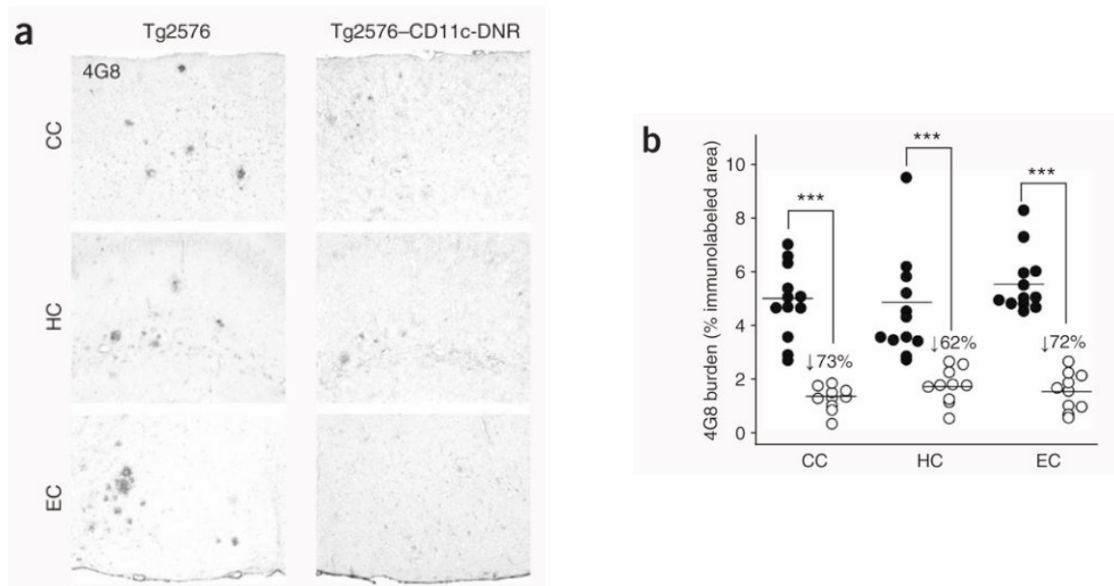


Figure 13. Reduced cerebral parenchymal β -amyloid deposits in Tg2576–CD11c-DNR mice. (a) Photomicrographs from Tg2576 or Tg2576–CD11c-DNR mouse brain

sections with median values by image analysis for human A β immunohistochemistry (antibody 4G8), bright-field photomicrographs are shown. CC, cingulate cortex; HC, hippocampus; EC, entorhinal cortex. Modified from Town T, et al (2008).

4. Rationale and aims

Alzheimer's disease is characterised by two main hallmarks in the brain: senile plaques and NFT, which play a crucial role in the development and progression of the disease. The relationship between these hallmarks is complex and not fully understood, but they are believed to interact and influence each other. Both senile plaques and NFT share a common feature: the presence of heparan sulphates, which colocalise in both structures.

To date, 143 agents have been tested in 172 clinical trials for AD. Most of these agents target amyloid plaques, inflammation/immunity, and synaptic plasticity/neuroprotection. Surprisingly, only one agent based on carbohydrates is being tested, indicating a lack of research in this area of carbohydrate-based/target molecules for Alzheimer's disease. In more than one century of research, Aducanumab and Lecanemab are the only two approved FDA disease-modifying drugs for Alzheimer's. Both approved in controversial clinical trials, minimal positive results and concerns about its safety and secondary effects, and new strategies to treat the disease are still urgently needed.

The abnormal intracellular accumulation of heparan sulfates in AD neurons occurs decades before the deposition of senile plaques and NFT. The reduction of the biosynthesis of heparan sulphates leads to a decrease in the number of senile plaques and NFT. Furthermore, the rare 3-O-sulphated heparan sulphates accumulate in brain areas vulnerable for the disease, and it has been shown that they are able to induce the aggregation of tau. The enzymes responsible for producing 3-O-sulphated heparan sulphates are called heparan sulphate 3-O-sulphotransferases. The regulation of these enzymes has been studied in cancer models, revealing a regulation by different transcriptional mechanisms, such as DNA methylation, TGF- β 1 and VEGF signalling dependent through its transcriptional factors. Regardless of the importance of these observations, to date, there is no mechanism reported that explain the gene regulation of these paralog enzymes in AD. It has been extensively described the abnormal gene expression in AD. Remarkably, genes related to the regulated of transcription are at the

top of the upregulated genes. These genes are transcription factors, including SMAD4, an effector of the TGF- β 1 pathway. The TGF- β 1 signalling pathway is involved in the development of the disease and can induce APP synthesis and prompt A β formation.

This thesis aims to study the role of 3-O-sulphated heparan sulphates in the tau aggregation process in relation to the TGF- β signalling pathway. 3-O-sulphated heparan sulphates are the product of seven enzymes, and the specific role of them in AD has not been established. We aim to determine the 3-O-sulphated heparan sulphates biosynthetic enzyme(s) involved in AD-related tau pathology. Moreover, our aim is to decipher whether and how the expression of these enzymes are regulated by the TGF- β 1 signalling pathway. Lastly, when we decipher the responsible enzyme(s), we aim to perform a loss of function of our candidate and study its effect in the AD related tau pathology.

5. Objectives of the work

- 5.1. Establishment of an *in vitro* model for the study of AD related tau pathology.
- 5.2. Investigate the role of heparan sulphate proteoglycans biosynthesis in the development of tau pathology.
- 5.3. Decipher the gene regulation of 3-O-sulphated heparan sulphates in AD related tau pathology in relation with the TGF- β 1 pathway.
- 5.4. Decipher the specificity and effect of 3-O-sulphated heparan sulphates in AD related tau pathology.

Objectives in collaboration with the GLY-CRRET Research unit

6. Material and Methods

6.1. Experimental Model

rTg4510 mice express a repressible form of human tau containing the P301L mutation under the control of a tetracycline operon-responsive element (TRE), to an activator line expressing a tetracycline-controlled transactivator (tTA) with the CaMKII α promoter. rTg4510 mice were established by crossing male C57BL/6 mice expressing the tetracycline-controlled transactivator protein under control of the forebrain-specific calcium-calmodulin-dependent kinase II (CaMK2a) promoter (CaMK2a-tTa mice; JAX® Stock#016198; RRID: MGI:5438794) with female FVB mice carrying the responder tetO-MAPT*P301L transgene under the control of the Tet-responsive element (tetO) (tetO-MAPT*P301L mice; JAX® Stock#015815; RRID: MGI:4819951). Mice hemizygous for the tetO-MAPT*P301L transgene (+/-) and for the tetracycline controlled transactivator protein (+/-) were considered rTg4510 (+/+) and non-carrier animals for the tetO-MAPT*P301L transgene (-/-) and the tetracycline controlled transactivator protein (-/-) were considered Control (-/-). For all studies, both male and female mice were used, and they were allocated randomly between experimental groups. Experimenters were blinded to the genotype/treatment of each mouse during data collection and identities were decoded later after analysis, using identification numbering based on toe tattooing. Animals were housed at the Gly-CRRET animal house in 2-5 per cage, with a light-dark cycle of 12, and food and water ad libitum. All experiments were performed in accordance with EU Directive 2010/63. The protocols were reviewed by the local animal experimentation ethics committee and authorized by the French Ministry of Research and Education (APAFIS#8375-2016123120043752 v6).

6.2. Genotyping of rTg4510 mice

Genotyping was performed using 2 mm of the tail of the animals. The tails were collected between the first 2 weeks of life. For genotyping, we used the KAPA HotStart Mouse Genotyping Kit (KAPA biosystems, KK7352). All buffers and solutions used were provided in the kit, and the procedure followed the fabricant instruction, as follows. DNA extraction was performed in a mix of 100 µl containing 10 µl of 10X KAPA Express Extract Buffer (final 1X), 1 µl of KAPA Express Extract Enzyme (2 U/reaction), the mouse tissue (2 mm of tail) and 88 µl of ultrapure water, for each sample. Lysis was performed in a water bath for 10 minutes at 75 °C and followed by 5 minutes at 95 °C to inactivate the enzyme. The samples were briefly centrifuged to pellet cellular debris and DNA extracts were diluted 10 times with 10 mM Tris-HCl (pH 8.0-8.5, Fisher BioReagents BP1758-500). Then, 25 µl PCR mix of 25 µl was made with 12.5 µl KAPA Fast genotyping mix (HotStart) with dye, 1.25 µl of forward primer, 1.25 µl of reverse primer. 10 ng of DNA crude extract and PCR grade water up to 25 µl. Then, PCR was performed following the same parameters:

Primer Sequences

	Sequences	
TA genotyping	Forward	CGCTGTGGGGCATTTTACTTTAG
	Reverse	CATGTCCAGATCGAAATCGTC
TA internal control	Forward	AAGGGAGCTGCAGTGGAGTA
	Reverse	CCGAAAATCTGTGGGAAGTC
Tau P301L genotyping	Forward	GATCTTAGCAACGTCCAGTCC
	Reverse	TGCCTAATGAGCCACACTTG
Tau internal control	Forward	CACGTGGGCTCCAGCATT
	Reverse	TCACCAGTCAATTCTGCCTTTG

PCR conditions

Steps	Temperature	Duration	Cycles
-------	-------------	----------	--------

Initial denaturation	95 °C	3 min.	1
Denaturation	95 °C	15 seconds	35-40
Annealing	60 °C	15 seconds	
Extension	72 °C	15 seconds/kb	
Final extension	72 °C	1 minute/kb	1

For PCR, the samples were loaded in 2.5 g of agarose (Invitrogen 16500-500) and heated in 120 ml of TAE buffer (Invitrogen 15558-026) and 10 µl of ethidium bromide (BET, invitrogen cat15585-011) was added to the mixture. After gel polymerisation, the first line was loaded with 10 µl of smart ladder (Eurogentec MW-1700-02), the samples were loaded and the migration was performed at 100 V. Finally, the gels were read with Licor [Odyssey-Fc) at 600 nm and analysed with Image Studio Lite software.

6.3. Primary culture of rat cortical glial cells

Primary glial cells were prepared from PND5 Sprague-Dawley rats (Janvier Labs). The cortices were dissected and processed as previously described⁴². Briefly, the head of PND5 Sprague-Dawley rats was cut to remove the brain. Both hemispheres were recovered and after removal of the meninges, the hippocampi were removed and both occipital hemispheres were dissected out in Dissection medium [HBSS (Gibco, 14170-088), 10% HEPES (Gibco, H0887). The occipital hemispheres were collected, washed twice with HBSS, and incubated for 12 minutes in 2.5% trypsin (Sigma, T6763), 2.5% DNase (Merck, 11284932001) in HBSS at 37 °C. Trypsin was inactivated with 10% FBS (Gibco, 10270-098). Cells were plated in 75 cm² flasks in Dulbecco's Modified Eagle Medium (DMEM High glucose GlutaMAX TM-I, Gibco, 61965-026) supplemented with 10% FBS (Gibco, 10270-098) and 0.1% Penicillin-Streptomycin (Life Technologies, 15140-122). Cells were maintained at 37 °C in a humidified 5% CO₂ incubator. When 80% of confluence was reached, cells were passaged to 1:2. Passages 1 and 2 were used to obtain the conditional medium as follows: Modified Eagle Medium supplement medium was replaced by pre-warmed Neurobasal medium supplemented with 2% B27

(Life Technologies, 17504044), GlutaMAX TM-I (Gibco, 35050-038), and 0.1% Penicillin-Streptomycin (Life Technologies, 15140-122). After 24 hours, the conditional medium was recovered and filtered out.

6.4. Primary cell culture of murine hippocampal neurons

Female FVB^{TetO-MAPT*P301L +/-} mice were crossed with a male C57Black6J^{CaMK2a-tTA +/-} mouse from the Gly-CRRET animal house. Primary hippocampal cell cultures were prepared from E15.5 embryonic FVB^{TetO-MAPT*P301L +/-} mice (Janvier Labs). Briefly, the head of embryos was cut to remove the brain. Both hemispheres were recovered and after removal of the meninges, the hippocampi were dissected out in Dissection medium [HBSS (Gibco, 14170-088), 10% HEPES (Gibco, H0887) supplemented with Penicillin-Streptomycin (Life technologies, 15140-122)]. Hippocampi were collected, washed twice with HBSS, and incubated for 12 minutes in 2.5% Trypsin (Sigma, T6763), 2.5% DNase (Merck, 11284932001) in HBSS at 37 °C. Trypsin was inactivated with 10% FBS (Gibco, 10270-098). Cells were dissociated and seeded in 12 well plates coated with poly-D-lysine (Sigma, P7280) or 12 well plates IBIDI chambers at a density of 200 000 cells or 35 000 cells, respectively. Cells were seeded in neurobasal medium supplemented with 2% B27 (Life Technologies, 17504044), GlutaMAX TM-I (Gibco, 35050-038), and 0.1% Penicillin-Streptomycin. Primary cultures were maintained at 37°C in a humidified 5% CO₂ incubator. After 2 hours, the medium was replaced by the glial cell-conditioned medium.

6.5. Transduction of primary hippocampal neurons

To transduce primary hippocampal neurons (PHN) in culture with lentivirus we used the Sigma Aldrich lentiviral particles (Mission Lentiviral Transduction Particles). The Lentiviral

Transduction Particles were produced from a library of sequence-verified lentiviral plasmid vectors for mouse genes. The TRC2 library consists of sequence-verified shRNAs in the TRC2-pLKO-puro vector. The TRC2 vector has the Woodchuck Hepatitis Post-Transcriptional Regulatory Element (WPRE). WPRE allows enhanced expression of transgenes delivered by lentiviral vectors. Each shRNA construct was cloned and sequenced and verified to ensure a match to the target gene. The lentiviral transduction particles are pseudotyped with an envelope G glycoprotein from Vesicular Stomatitis Virus (VSV-G). The lentiviral transduction particles were tittered via a p24 antigen ELISA assay and pg/ml of p24 are then converted to transducing units per ml using a conversion factor. At day *in vitro* 15 (DIV15), 5 viral particles per cell were added to the primary hippocampal neurons (PHN). PHN were kept under culture until 20 days (DIV20).

Clone ID	DNA sequence	P24 Antigen	Target
Non Target Control	PASS	1.4*10 ⁸ VP/ml	Non Target
TRCN0000241592	TGACTACACGCAGACTCTTTC	5.1*10 ⁸ VP/ml	Hs3st2
Hs3st4	TGAATACAATGCAGACTATGTC	1.7*10 ⁸ VP/ml	Hs3st4

6.6. Treatment of PHN

To induce or block the activation of the TGF- β 1 pathway in PHN we used the TGF- β 1 recombinant protein with a concentration of 20 ng/ml or the TGFB Inhibitor SB431542 (10 μ M) at day *in vitro* 15 (DIV15). DMSO was added as a control using the same volume in which the compounds were solubilized. PHN were kept under culture to DIV20.

6.7. Protein quantification

Protein concentration was quantified following the bicyclonic acid (BCA, Thermo Fisher Scientific) protocol. All buffers and solutions used were provided in the kit, and the procedure followed the fabricant instruction, as follows. We started by preparing the BCA working reagent by mixing BCA reagent A (copper solution) and BCA reagent B (bicinchoninic acid solution) in a 50: 1 ratio. Bovine serum albumin (BSA) was used as a set of protein concentration standards with a known protein sample, diluting it to create a range of concentrations. Protein samples were diluted 1:5 in PBS with protein inhibitors. A total volume of 5 ul of BSA for the standard concentration or sample was added to their respective wells in a 96 well plate. 200 µl of the BCA working reagent was added to each well, ensuring full coverage of the sample and avoiding bubbles. We thoroughly mixed and incubated at 37 °C for 30 minutes in the dark to form protein complexes. After cooling to room temperature, we measured the absorbance of each standard and sample at 562 nm using a spectrophotometer or microplate reader. We constructed a standard curve by plotting the absorbance values against the corresponding concentrations of the standards. Protein concentration of each sample was calculated by comparing their absorbance values to the standard curve.

6.8. Electrophoresis

To prepare an 8% SDS-PAGE gel, acrylamide and bis-acrylamide solutions, Tris-HCl buffer (pH 8.8), SDS, APS, TEMED, a gel casting tray with comb, a gel casting apparatus, and a power supply for electrophoresis were used. The volumes of acrylamide, bis-acrylamide, Tris-HCl buffer, SDS, and water needed for the resolving gel were calculated. They were mixed in a container to create the resolving gel solution, ensuring homogeneity. APS and TEMED were added as polymerization initiators, and the resolving gel was poured into the casting tray. Isopropyl alcohol was added to create a flat interphase, and we waited 30 minutes for the polymerization. The volumes of acrylamide,

bis-acrylamide, Tris-HCl buffer, SDS, and water needed for the stacking gel for an 4% SDS-PAGE gel were calculated. They were mixed to create the stacking gel solution, and APS and TEMED were added as initiators. The stacking gel was poured on top of the resolving gel, with the comb inserted to create sample wells. It was allowed to polymerize. Once fully polymerized, the comb was removed, the gel was rinsed with a running buffer, and it was placed in the electrophoresis chamber. The gel was placed in the chamber, ensuring that it was clean and properly assembled. We used the tris-glycine running buffer. Protein samples were loaded onto the gel along with a molecular weight marker. The gel chamber was connected to the power supply, the voltage was settled to 80 mV for 30 minutes, increasing to 120 mV until the end of the electrophoresis. To avoid overheating and protein degradation we settled the mA to a maximum of 150 mA. The electrophoresis was run until the dye front reached the desired protein separation based on the molecular weight marker.

6.9. Immunoblotting of RIPA-extracted proteins

The samples were harvested in RIPA buffer (50 mM tris, pH 8 .0, 150 mM NaCl, 0.1% Triton X-100, 0.5% sodium deoxycholate, 0.1% SDS; Thermo Fisher Scientific) supplemented with 1% protease inhibitor mixture (Sigma) and 1% phosphatase inhibitor cocktail I & II (Sigma). Cell lysates were centrifugated at 13,000 rpm for 20 minutes and protein contents in supernatants were determined using the BCA Protein Assay kit. Cell lysate supernatants containing 1-10 µg of proteins were suspended in Laemmli buffer (0.125 M Tris HCl, pH 6.8, 4% SDS, 20% glycerol, 0.004% bromophenol blue; Biorad) supplemented with 10% β-mercaptoethanol and heated for 5 minutes at 95 ° C. The proteins were separated in 8% acrylamide gel and transferred to a PVDF membrane with a Transblot Turbo device (BioRad) for 15 minutes. The membrane was blocked with a blocking buffer, 5% non-fat milk PBST, to prevent nonspecific binding. The membranes were incubated with their respective antibodies specific for the target protein overnight at 4 °C with gentle agitation. Blots were incubated for 1 h at room temperature with the corresponding secondary antibodies in the blocking buffer. Revelation was performed

with Immobilon Western Chemiluminescent HRP Substrate Luminata Forte (Millipore) following the manufacturer's instructions.

6.10. Immunoblotting of High salt Sarkosyl oligomers

To isolate tau oligomers, the samples were harvested in salt-rich sarkosyl buffer (50 mM HEPES pH 7.0, 250 mM sucrose, 1 mM EDTA, 0.5 M NaCl, 1% sarkosyl) supplemented with 1% protease inhibitor mixture (Sigma) and 1% phosphatase inhibitor cocktail I & II (Sigma). Lysates were centrifugated at 180000 g for 30 minutes and protein content in supernatants was determined using the BCA Protein Assay Kit (Thermo Fisher Scientific). Cell lysate supernatants containing 1-10 µg of proteins were treated or not (as indicated) in Laemmli buffer (Biorad) supplemented with β-mercaptoethanol. Samples treated with Laemmli buffer were heated for 5 minutes at 95 °C to denature the tau oligomers. The proteins were separated by electrophoresis as described above. Immunoblotting was performed as described above with their respective antibodies. Blots were incubated for 1 h at rt with the corresponding secondary antibodies in blocking buffer. Revelation was performed with Immobilon Western Chemiluminescent HRP Substrate Luminata Forte (Millipore) following the manufacturer's instructions.

Antibody	Dilution	Catalog number
GAPDH	1:10000	Thermo Fisher Scientific
PHF1	1:500	Peter Davis
T22	1:1000	Millipore
pSMAD2/3	1:500	Abcam
AT8	1:500	Thermo Fisher Scientific
MC1	1:500	Peter Davis
ACTB	1:5000	Thermo Fisher Scientific

6.11. RNA isolation from HPN

RNA was extracted using NucleoSpin RNA XS, Micro kit for RNA purification (Macherey-Nagel; 740902.50). Medium was aspirated and cells were washed two times with PBS. lysed by adding the RA1 buffer with the reducing agent TCEP to the well. The lysate was pipetted and mixed in an Eppendorf with a vortex. Then, the lysate was homogenized for 30 seconds (s) and 70% ethanol was added to the mix by pipetting. The samples were then transferred to the nucleospin column placed in a 2 ml collection tube, centrifuged for 15s at 11000 g and the flow was discarded. After this step, MDB buffer was added to the spin column to desalt the column and the samples were centrifuged for 15 s at 11000 g and the flow through was discarded. rDNase was added directly to the membrane of the column and incubated for 15 minutes at room temperature. To wash and dry the silica membrane, RA2 buffer was added to the spin column and samples were centrifuged again for 30 s at 11000 g and the flow through was discarded. This step was repeated two times. Highly pure RNA was eluted in a volume of 15 µl of H₂O (RNase free) and centrifuged at 1100 g for 30 s. RNA was either stored directly at -80 °C or directly quantified.

6.12. RNA isolation from hippocampal formation, 2 and 4 months.

RNA was extracted using Trizol (Qiazol) followed by the RNeasy mini kit (Qiagen; 74004). Hippocampal formation tissue was lysed with a rotor-station homogenizer by addition of Trizol and tissue was homogenized. Chloroform was added and mixed till a homogeneous solution was formed. Microcentrifuge tubes were centrifugated at 12000 g for 10 minutes. The super aqueous phase was transferred to a new microcentrifuge tube. Then, 100% ethanol was added to the super aqueous phase and mixed by pipetting. Samples were then transferred to RNeasy spin column placed in a 2 ml collection tube, centrifuged for 15 s at 8000 g and the flow-through was discard. After this step, RW1 buffer was added to the RNeasy spin column and samples were centrifuged for 15 s at 8000 g to wash the spin column membrane and the flow-through was discarded. DNase was added directly

into the silica membrane and incubated for 15 minutes at room temperature. To wash the spin column membrane, the RPE buffer was added to the RNeasy spin column and samples were centrifuged again for 2 minutes at ≥ 8000 g. The long centrifugation dries the spin column membrane, ensuring the removal of any traces of ethanol for RNA elution. Finally, RNase spin column was placed in a new microcentrifuge tube, and 15 μ l of H₂O (RNase free water) were added directly into the column and centrifuged for 1 min. at 8000 g. RNA was either stored directly at -80 °C or directly quantified.

6.13. RNA quantification

The RNA quantification was done with the Nanodrop spectrophotometer. The Nanodrop was calibrated, and the sample measurement surface was cleaned with ethanol and a lint-free wipe. First, 1 μ l of nuclease-free water was pipetted onto the clean measurement surface of the Nanodrop for the blank measurement, and the instrument was zeroed. Then, 1 μ l of the RNA sample was pipetted onto the measurement surface, and the absorbance was measured by closing the surface. The absorbance values at 260 nm (for RNA quantification) and 280 nm (for protein contamination assessment) were recorded. The RNA concentration was calculated using the appropriate nucleic acid extinction coefficient, and the purity of the RNA sample was assessed by examining the A260/A280 ratio.

6.14. RNA expression analysis

RNA analysis RNA was isolated as described above. 200 ng of RNA per sample was converted to cDNA using the AffinityScript Multiple Temperature cDNA synthesis kit according to the manufacturer instructions at 25 °C for 10 min, at 50 °C for 60 min, and at 70 °C for 15 min. All buffers and solutions used were provided in the kit, and the procedure followed the fabricant instruction. Reactions were prepared using 250 nM of

upstream primer and 250 nM of downstream primer. Nuclease-free PCR-grade water was added to adjust the final volume to 20 μ l. Gene expression was analysed in template cDNA by quantitative real time polymerase chain reaction (qPCR) using the Brilliant III Ultra-fast SYBR* kit (Agilent Technologies) in an Agilent AriaMx thermocycler. Analysis was performed with the Agilent AriaMx 1.0 software.

Primer	Forward	Reverse
Hs3st1	GGGTACGCGACTCAGTAAT	GGTGGGAATGCACAAGCTG
Hs3st2	TGGA CTGGTACAGGAGC	TGACGAAATAGCTGGGC
Hs3st3a1	CCTTACTTCTGGACGAGGG	TGGGCATCAAATCCCGGT
Hs3st3b1	ATCTCCAGCTTCTTCAGCGG	CTGGGCATCAAGTCTCGGTA
Hs3st4	ATGGTACAGAAATGTGATGCC	AAGGTGGGGATCTCTGG
Hs3st5	AAGATGTGAAGGCTGCTGC	GGCACCACCAAATCGACT
Rplp0	TCTCGCTTTCTGGAGGGTG	TCCACAGACAATGCCAGGAC

6.15. Immunofluorescence of PHN

Primary neurons maintained in culture for 20 days *in vitro* were rinsed with cold PBS and then fixed at 4 °C in cold methanol for 5 minutes. Cells were rinsed with cold PBS (three times). For immunofluorescence staining, cells were washed with PBS or alternatively with PBS containing 0.01%, Triton-x100 (PBS-T) for permeabilization during 15 minutes at room temperature. Unspecific sites were blocked with PBS (or PBS-T) containing 3% fetal bovine serum (FBS) for 60 minutes at room temperature prior to incubation with primary antibodies. Cells were incubated with the first antibody in blocking solution (3% FBS PBS-T) overnight at 4 °C. Cells were then washed with PBS (or PBST) and incubated with the secondary antibody for 60 minutes at room temperature. After washing with PBS, nuclei were stained with DAPI (1 μ g/mL in PBS) for 5 minutes and washed with PBS before mounting with Prolong Gold antifade reagent. Stack images were obtained with

the software CellSens from a spinning disk inverted confocal microscope (IX81 DSU Olympus, 60 × N.A.1.35) coupled to an Orca Hamamatsu RCCD camera.

Antibody	Dilution	Catalog number
MAP2	1:1000	Abcam
NeuN	1:500	DAKO
PHF1	1:500	Peter Davis
T22	1:1000	Millipore
pSMAD2/3	1:500	Abcam
AT8	1:500	Thermo Fisher Scientific
Hs3st2	1:500	Thermo Fisher Scientific
Synaptophysin	1:5000	Thermo Fisher Scientific
HS4C3	1:100	Ten Dam
Alexafluor 488	1:2000	Thermo Fisher Scientific
Alexafluor 488	1:2000	Thermo Fisher Scientific
VSV	1:5000	Ten Dam
VGLUT1	1:1000	Abcam
PSD95	1:1000	Thermo Fisher Scientific

6.16. Transcardial perfusion, fixation and brain dissection

Mice were anesthetized in a close chamber with 5 % isoflurane, ensuring the absence of reflexes and prepared for the intracardiac perfusion. The perfusion system consisted of a pump connected to a needle and tubing filled with phosphate-buffered saline (PBS). A midline incision was made through the thoracic region, extending toward the neck, to expose the chest cavity. The heart was exposed by dissecting the muscles and holding

the ribs aside. A needle connected to the perfusion tubing was inserted into the left ventricle of the heart and the right atrium was sectioned. The perfusion pump was started, perfusing PBS through the heart at a rate of approximately 10 mL/min to flush out the blood. Once the blood was cleared, the perfusion solution was switched to a 4% paraformaldehyde (PFA) solution, and perfusion was continued for 10-15 minutes to fix the tissues. The fixation was followed up by checking the coloration of the liver and rigidity of the mouse. After completion, the brain was carefully dissected, removed, and transferred to a container with fresh 4% PFA solution for post-fixation overnight at 4°C.

6.17. Fixation, cryoprotection and long-term storage

To fix brain tissue, brains that followed an overnight incubation at 4 °C in PFA 4%, were transferred to sucrose 10% for 24 hours at 4 °C with agitation. Then, brains were transferred to sucrose 20% and kept again for 24 hours at 4 °C with agitation. This was repeated for sucrose 30% during 24 hours at 4 °C with agitation. Finally, brains were soaked for 1 minute in isopentane at -30 °C, and placed in foil paper to be conserved at -80 °C.

6.18. Brain slicing

The mouse brain was prepared for slicing by embedding it in sucrose 30% and freezing it on dry ice. The microtome plate and blade were pre-cooled to -20 to -25°C using dry ice. The frozen brain block was securely mounted onto the microtome plate using sucrose 30%. Trimming cuts were made to obtain a flat surface, and thin sections of the brain tissue of 30 µm were sliced. The sections were carefully transferred with a fine brush onto cryo-tubes containing 10% DMSO in PBS. Cryo-tubes were stored at -20 °C.

6.19. Histopathological analysis of mice brain with the chromogen DAB

The fixed mouse brain tissue was prepared from free-floating brain tissue. The brain sections were collected in a washing buffer (PBS) containing 25% Triton X-100. To quench endogenous peroxidase activity, slides were incubated for 10 minutes in 3% hydrogen peroxide in 20% methanol. After rinsing the slides two times with milliQ water for 5 minutes, slides were washed two times more in PBS containing 0.25% Triton X-100 for 10 minutes each time and slides were incubated with 5% goat serum (Thermo Fisher #16210072) in PBS for 30 minutes at room temperature and washed. Slides were then incubated with AT8 primary antibody (P. Davies, 1:500) in 0.1 M PBS containing 0.25% Triton X-100 and 0.2% overnight. After washing 3 times (5 minutes each time) in PBS containing 0.25% Triton X-100, samples were incubated for 60 minutes in a secondary goat anti-mouse biotinylated IgG1 in PBS 0.25% Triton X-100. Then, after washing 3 times (5 minutes each time) in PBS 0.25% Triton X-100, slides were treated with the Elite ABC KIT following fabricant instructions, rinsed for 10 minutes with PBS 0.25% Triton X-100 and then 50 mM tris buffer containing 150 mM NaCl (pH 7.4) twice (10 minutes each). Slides were developed by a short incubation in 0.1% 3,3'-diaminobenzidine (DAB) peroxidase substrate solution containing 0.05% hydrogen peroxide diluted in tris buffer saline and the reaction was stopped by dilution. Slides were mounted in Superfrost Plus slides in 0.3% gelatin diluted in PBS. The day after, slides were rehydrated and dehydrated in water, ethanol 30%, ethanol 70%, ethanol 90%, ethanol 100%, and finally xylene. Sections were scanned by using a Nanozoomer (Hamamatsu).

6.20. Immunofluorescence analysis of mice brain

Tissue samples were used for immunofluorescence analysis. Briefly, OCT tissue sections were washed with PBS containing .25% Triton X-100 and incubated for 60 minutes in blocking buffer (PBS, 5% BSA) and immunostaining was performed using primary antibodies against human tau (K9JA) and pTau S202/205 (AT8) overnight. Tissue

sections were washed with PBS containing .25% Triton X-100 3 times and incubated for one hour with the correspondent secondary antibody (Alexafluor 488 555) followed by extensive PBS washes and nuclei were labelled with 1 µg/mL DAPI for 5 minutes. Then, slides were mounted with Prolong (Invitrogen) and images were imaged using an inverted microscope IX81 Olympus coupled to an Orca Hamamatsu RCCD using the CellSens software. Images were processed with the ImageJ software.

Antibody	Dilution	Catalog number
K9JA	1:5000	DAKO
AT8	1:500	Thermo Fisher Scientific
Alexafluor 488	1:2000	Thermo Fisher Scientific
Alexafluor 488	1:2000	Thermo Fisher Scientific

6.21. Human post-mortem material

Tissue samples from hippocampal formation were obtained by the Gly-CRRET Research unit from The Netherlands Brain Bank of the Netherlands Institute for Neuroscience (www.brainbank.nl). All material has been collected from donors for or from whom a written informed consent for a brain autopsy. Use of the material and clinical information for research purposes was obtained by the NBB. No significant differences in age and PMI were observed between the Ctr and AD groups. Use of human brain post-mortem samples was approved by the Université Paris-Est Créteil (UPEC) CEDIS ethics committee.

6.22. Immunofluorescence of human brain

Tissue samples were used for immunofluorescence analysis. Briefly, 4 µm thick FFPE tissue sections (hippocampus) were deparaffinized and treated for 5 minutes with 88%

formic acid. Then, sections were incubated for 30 minutes in a blocking buffer (PBS, 5% BSA) and immunostaining was performed using primary antibodies against pSMAD2/3 and AT8. For immunofluorescence experiments, lipofuscin autofluorescence was quenched by preincubating tissue slides with 0.1% Sudan Black B (in 70% ethanol) for 5 minutes followed by extensive PBS washes and nuclei were labelled with 1 µg/mL DAPI (Sigma) for 5 minutes. Then, slides were mounted with Prolong (Invitrogen) and images were imaged using an inverted microscope IX81 Olympus coupled to an Orca Hamamatsu RCCD using the CellSens software. Images were processed with the ImageJ software.

Antibody	Dilution	Catalog number
pSMAD2/3	1:2000	Abcam
AT8	1:500	Thermo Fisher Scientific
Alexafluor 488	1:2000	Thermo Fisher Scientific
Alexafluor 488	1:2000	Thermo Fisher Scientific

6.23. Statistical analysis

Statistical analyses were performed using GraphPad Prism software version 5.01. Values are expressed as the standard error of the mean (SEM). Statistical significance was analyzed Student's t-test, or two ways ANOVA when several variables were considered, as indicated. Post-tests analyses were performed as indicated; P values are indicated; ns = not significant.

6.24. RNA Sequencing and Data Analysis

Total RNA and library integrity were verified on LabChip Gx Touch 24. Between 197.97 - 276.9 ng of total RNA were used as input for SMARTer Stranded Total RNA Sample Prep Kit-HI Mammalian (Clontech). Sequencing was performed on the Novaseq 6000 ILLUMINA with S1 cartridge (200 cycles) of 1600 million reads in Paired-ends. Raw reads were visualized by FastQC to determine the quality of the sequencing. Trimming was performed using trimmomatic with the following parameters LEADING:3 TRAILING:3 SLIDINGWINDOW:4:15 HEADCROP:4, MINLEN:4. High quality reads were quantified with Salmon. Briefly, a transcriptome index is constructed using a reference genome (GRCm39). Salmon uses an indexing method that allows for rapid alignment-free quantification. For quantification, the processed reads are aligned to the transcriptome index, and the software estimates the abundance of transcripts or isoforms. The output of Salmon provides estimated counts or normalized values of transcript abundance. Differential gene expression was done with Deseq2. Deseq2 normalizes raw read counts, estimates dispersion to model variability, and employs negative binomial distribution to statistically assess differential expression. It computes p-values and fold changes, which are adjusted for multiple testing using methods like FDR. For Gene ontology (GO) enrichment analysis we used EnrichGO, taking a list of genes and assessing their enrichment in specific biological processes, molecular functions, and cellular components. The tool utilizes statistical methods to compare the input gene list with the GO annotations in a reference database. EnrichGO calculates p-values and applies multiple testing corrections to identify significantly enriched GO terms.

6.25. Modelling of tau protein and 3-O-heparan sulphates

The 3D model of the human tau protein was created using i-TASSER (Iterative Threading ASSEmbly Refinement) utilizing the FASTA sequence that was obtained from the protein data bank (PDB ID: 6HRE) as the input, the model building was processed in three stages. TASSER employs a PDB library, LOMETS (Local Meta-Threading Server, version 3 to retrieve templates of protein's super secondary folds matching the primary sequence. The templates from the previous step are used as the reference to build the secondary

structure to initiate the full-length modeling of the submitted FASTA sequence through replica-exchange Monte Carlo simulations. The third step involves structure re-assembly; starting from the SPICKER cluster centroid, the fragment assembly simulation is repeated. TM-align employs the spatial restraints collected from LOMETS and PBD structures to guide the stimulation. For conformation and binding free energy calculations during docking simulation we used AutoDock4. The preprocessed ligand library was prepared to perform blind docking of heparan sulphate dimers with Tau protein model with standard protocol. The dimer structure for heparan sulphate was selected after thorough examination through scientific articles. The atomic coordinates of the dimers were obtained using the Glycam GAG builder.

6.26. STAR METHODS

Key Resources Table

REAGENT RESOURCE	or	SOURCE	IDENTIFIER
Antibodies			
GAPDH		Thermo Scientific	2597
PHF1		Peter Davis	Gift
T22		Sigma-Aldrich	ABN454
pSMAD2/3		Abcam	ab272332
AT8		Thermo Fisher	MN1020
ACTB		ThermoFisher	ACTN05-C4
Neun		Dako	C5b-9
VGLUT1		Abcam	ab77822
PSD95		Thermo Scientific	6G6-1C9
HS3ST2		Thermo Scientific	PA5
MAP2		Abcam	AB5392
HS4C3		Ten Dam et al., 2006	Gift
Synaptophysin		Invitrogen	MA5-14532
K9JA		DAKO	A0024
Chemicals and Reagents			
Neurobasal medium		Gibco	21193-049
B-27 Supplement 50x		Life Technologies	17504044
HBSS		Gibco	14170-088

DNase I	Merck	11284932001
Trypsin-EDTA Solution	Sigma	T3924
HEPES	Gibco	H0887
GlutaMAX TM-I	Gibco	35050-038
DMEM + GlutaMAX-I	Gibco	61965-026
FBS	Gibco	10270-098
Penicillin-Streptomycin	Life technologies	15140-122
Trypsin	Sigma	T6763
Poly-D-lysine hydrobromide	Sigma	P7280
DPBS	Thermo Scientific	14190250
RIPA	Thermo Scientific	89901
Protease Inhibitor	Sigma	P8340
Phosphatase Inhibitor	Sigma	P5726
Phosphatase Inhibitor	Sigma	P0044
Beta-Mercaptoethanol	Sigma	M6250
4x Laemmli SDS	GeneTex	GTX16355
Tween-20	VWR	-
Triton-x100	VWR	-
DAB	Sigma Aldrich	D5637
BSA	Vector laboratories	SP-5050-500
DAPI	Thermo Scientific Fischer	-

ProLong Gold Antifade Mountant	Thermo Scientific	Fischer	P10144
Nuclease-free water	Thermo Scientific	Fisher	AM9937
TRIzol® Reagent	Thermo Scientific	Fisher	15596018
TGFB Inhibitor	Sigma/MERCK		SB431542
TGFB1	PEPROTECH		100-21C
Critical Commercial Assays and Kits			
AffinityScript cDNA Synthesis Kit	Agilent		-
qPCR Brilliant SYBR	Agilent		-
NucleoSpin RNA XS	Macherey-Nagel		-
RNeasy Minikit	QIAGEN		-
Elite ABC KIT	Vector Laboratories		PK-6100
BCA Kit	Thermo Scientific		-
Clarity Western ECL Substrate	Bio-Rad		1705060
Recombinant DNA			
MISSION Lentivirus Transduction Particles	Sigma		TRCN0000241592

MISSION Lentivirus Transduction Particles Non-Target Control	Sigma	PASS
MISSION Lentivirus Transduction Particles	Sigma	TRCN0000241592

7. Results

7.1. Establishment and characterisation of tauopathy in primary hippocampal neuronal cultures from rTg4510 mice model.

7.1.1. Neurons are the predominant cell type in dissected hippocampus from 16 days mouse embryos

To study the gene regulation and role of 3-O-sulphated heparan sulphates and their implication during tauopathy development, we first aimed to develop an *in vitro* cell model of tau pathology in neural cells. Primary hippocampal neuron (PHN) cell culture is a widely used experimental model that offers several advantages for studying various aspects of neuronal biology and neurodegenerative diseases. Derived directly from brain tissue, primary hippocampal neurons provide a physiologically relevant model for investigating the physiopathology of neurons in the hippocampus. These neurons form functional synaptic connections, enabling the study of synapse formation, neurotransmitter release, and synaptic plasticity⁵³. They allow long-term studies on neuronal development and maintenance, and their gene expression can be manipulated to investigate the roles of specific proteins and signalling pathways. Additionally, they serve as valuable tools for creating disease models of neurodegenerative disorders including AD and Parkinson's diseases. Moreover, PHN cultures reduce reliance on animal experiments, providing an ethical alternative for studying neuronal biology and disease processes. Thus, we selected this model and implemented the conditions to first obtain highly pure wild type (WT) hippocampal neuronal cell populations. With this aim, we dissected embryonic day 16 (E16) hippocampal neurons and cultivated them *in vitro* for 20 days (DIV-20). PHN were kept in glial cell conditioned medium (GCCM). GCCM is a specialized culture medium containing secreted factors from glial cells. When applied to neurons, GCCM supports their survival, growth, synaptic function, and plasticity. At DIV-20, PHN were fixed and immunostained with the antibodies MAP2 and NeuN, two widely used mature

neuronal markers. NeuN is a protein encoded by the RBFOX3 gene, while MAP2 is a protein encoded by the MAP2 gene. We showed a specific staining and colocalization between the two neuronal markers in the WT cells, with absence of other cell types, as expected confirming that neuronal cells are predominant in our model.

Neurons are the predominant cell type in dissected E16 hippocampus cell culture

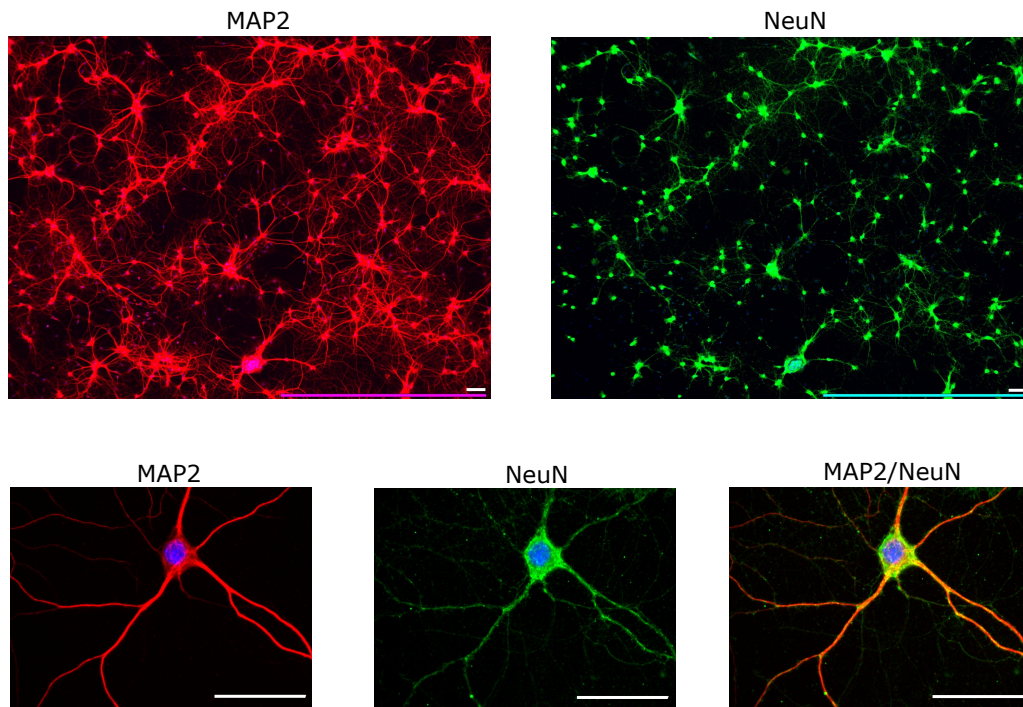


Figure 1. Primary hippocampal neuron cell culture characterisation. Immunostaining with the antibodies MAP2 and NeuN (4x), and colocalization between MAP2 and NeuN (60x) at day in vitro 20 in PHN supplemented with GCCM. Nuclei were counterstained with DAPI (blue). Confocal slices images were acquired by a confocal microscope IX81 Olympus (magnification 60x, immerse oil). Representative images (n=3). Scale bars represent 50 μm .

7.1.2. Primary hippocampal neurons from the rTg4510 mice model are a good model to study AD-related tau pathology

To implement a neuronal cell model of tauopathy, we then used primary hippocampal cells from the rTg4510 mice model of tauopathy. The rTg4510 mouse is a widely used transgenic mouse model for studying AD-related tau pathology, as this mouse shows specific pathological features observed in human AD⁵⁴. The rTg4510 mouse overexpresses the human tau protein carrying the P301L mutation (hTauP301L) responsible of frontotemporal dementia with parkinsonism in chromosome 17 (FTDP17), characterized by rich tau pathology, as observed in the AD brain. In this model, TauP301L is expressed under the control of the tetracycline-regulated promoter system under the control of the CAMK2A promoter, providing neuron specificity. The expression of the mutant tau protein leads to the formation of NFTs in the neurons of the mice. To investigate whether the rTg4510 cultured neurons develop tau pathology, we dissected PHN as described for the WT cells (see above). PHN were kept under cell culture for 20 days. At DIV-20 cells were harvested in RIPA buffer and fixated for immunohistochemical analysis. Western blot analysis demonstrated the characteristic abnormal phosphorylation of tau in the rTg4510 PHN (+/+) compared to the WT (-/-) at two different domains of the protein. The antibody pTau (s202/205, known as AT8) in the proline-rich domain, and the pTau (s396/404, known as PHF1) in the C-terminus domain (Figure 2 A, B). Both phosphorylation sites are known to be pathological and characteristic of the abnormally phosphorylated tau that accumulates in AD. Similarly, immunofluorescence in the rTg4510 (+/+) PHN showed an increase in the abnormal phosphorylation of s396/404 in the rTg4510 (+/+) PHN compared with the WT (Figure 2 C). Because in AD the abnormal phosphorylation of tau has been related a loss of synapses, we investigated whether the rTg4510 PHN recapitulate this pathological characteristic. Synaptophysin is a protein that plays a crucial role in the formation and maintenance of synaptic connections, and it has been extensively used as a marker to assess synaptic density and function.

Figure 2 C shows that in the rTg4510 (+/+) PHN there is an increase of pTau (s396/404) compared with WT (-/-) PHN. Remarkably in figure 2 D, we found a general decrease of synaptophysin, as well as a decrease in synaptic density in rTg4510 (+/+) PHN, whereas co-immunostaining of synaptophysin with pTau (s396/404) in WT (-/-) littermates revealed an almost negligible staining of pTau (s396/404), and a normal pattern of synaptophysin localization and synaptic density. These results confirm that the rTg4510 PHN recapitulates central aspects of AD, allowing the validation of the use of these cells for the *in vitro* study of AD-related tauopathy.

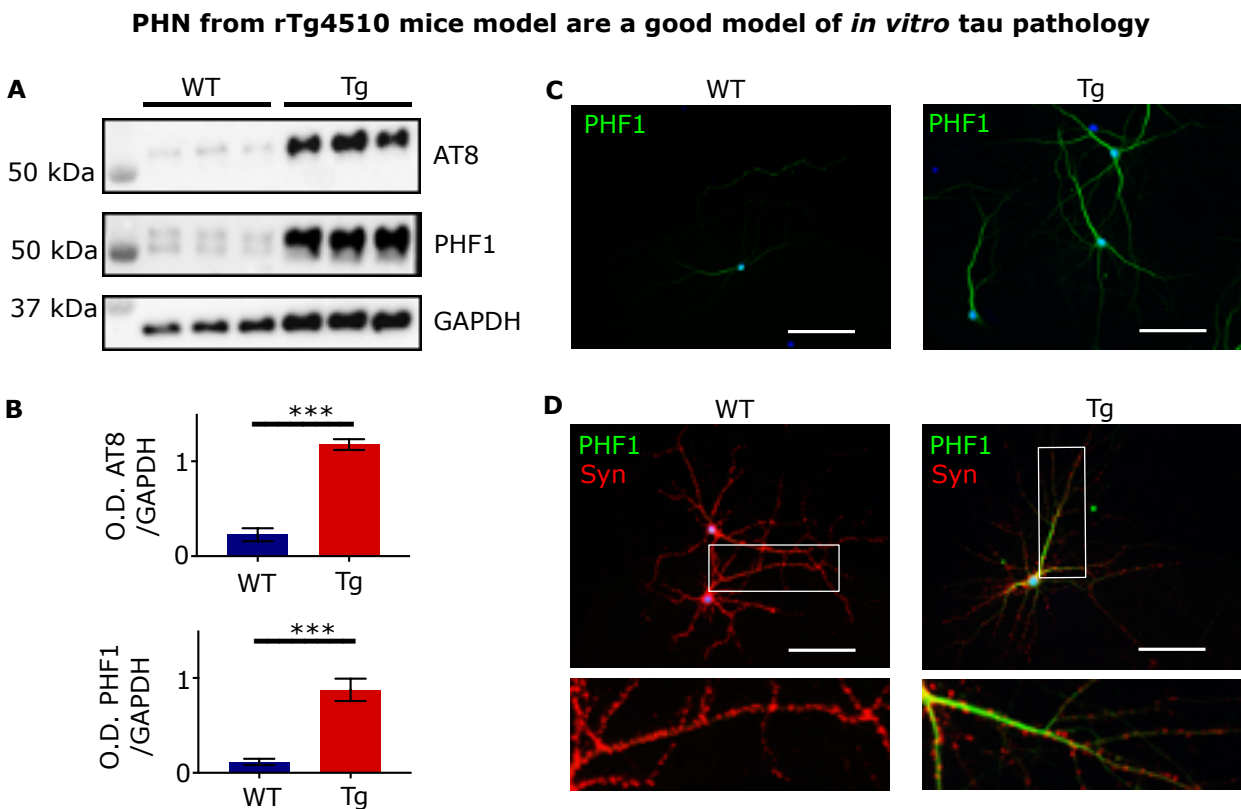


Figure 2. Tau pathology in the rTg4510 primary hippocampal neuronal cells. A. Immunoblotting of pTau (s202/205) and pTau (s396) in WT and rTg4510 PHN. B. Quantification of pTau (s202/205) and pTau (s396) normalized with GAPDH as loading control. C. Immunostaining of pTau (s396/404) in rTg4510 and WT PHN. D. Co-

immunostaining of pTau (s396/404) with Syn in rTg4510 and WT PHN. All results are shown at DIV-20 in PHN supplemented with GCCM. Nuclei were counterstained with DAPI (blue). Confocal slices images were acquired by a confocal microscope IX81 Olympus (magnification 40x, immerse oil). Representative blots and images (n=3). Scale bars represent 80 μ m. Error bar in plots is represented as SEM. * 0.05<p-value, **0.01<p-value, *** 0.001<p-value.

7.1.3. Tau oligomerisation evolves during time in cultured rTg4510 PHN.

Tau oligomerization is a multi-step process central to the development of AD. It begins with the abnormal hyperphosphorylation of tau, followed by its detachment from tubulin and prompting its misfolding³². Misfolded tau proteins form stable nuclei or seeds that serve as templates for the assembly of small, soluble tau oligomers. These oligomers, detectable with the T22 antibody, are highly toxic to neurons, disrupting cellular functions and hindering synaptic activity²⁵. A growing number of studies have demonstrated that soluble oligomers of tau are critical players in the AD progression. Tau soluble oligomers are formed by tau dimers/trimers of 120-180 kDa and are toxic to hippocampal neurons, as they induce the loss of dendritic spines and neurites⁵⁵. Over time, tau oligomers evolve into larger, more stable insoluble aggregates that form protofibrils and fibrils, ultimately culminating in the formation of neurofibrillary tangles. Using cell lysates of the rTg4510 (+/+) and WT (-/-) PHN, we performed a high salt Sarkosyl-fractioning method to separate soluble tau oligomers from insoluble tau protein fractions in PHN at DIV 5, 10, 15, 20. Immunoblotting of the insoluble protein extract allowed us to detect a specific band of tau oligomers at 120 kDa pTau oligomers in the rTg4510 (+/+) and WT (-/-) PHN, consistent with reported bibliography⁵⁵.

Immunoblotting of the soluble tau oligomer fraction revealed a kinetics of tau oligomerization. Tau oligomerisation in WT (-/-) is detectable but non-significantly. Previous results have shown that endogenous tau can form small oligomers under physiological conditions in neurons⁵⁶. They can potentially mediate microtubule bundling

and regulate the function of microtubule motors. In rTg4510 (+/+) PHN the oligomerisation of tau evolves overtime with a peak observed at DIV-15, followed by a decrease, as detected at DIV-20 (Figure 3). This data allows us to establish the time window between DIV-15 and DIV 20 as the optimal time for the following experiments.

Tau oligomerization evolves overtime in rTg4510 PHN

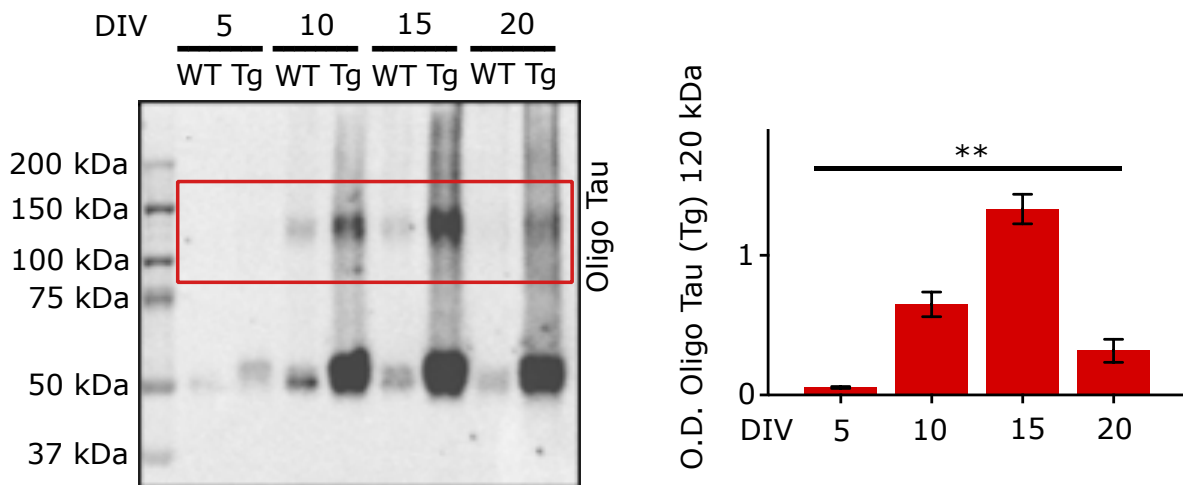


Figure 3. PHN rTg4510 (+/+) produce tau oligomers in a time dependent manner. Immunoblotting of High salt Sarkosyl soluble fraction (tau oligomers) at DIV 5, 10, 15 and 20. T22 antibody was used to detect oligomeric tau (Oligo Tau). Quantification of Oligo Tau in Tg. * 0.05<p-value, ** 0.01<p-value, *** 0.001<p-value. All results are shown in PHN supplemented with GCCM. Representative blot (n=3). Error bar in plots is represented as SEM. Two-Way ANOVA (post-hoc test TukeyHSD). * 0.05<p-value, **0.01<p-value, *** 0.001<p-value.

7.2. Increased levels of heparan sulfate proteoglycans biosynthetic machinery correlate with an increase in tau oligomerization

7.2.1. rTg4510 mice model develops tauopathy in pyramidal layer of CA1 region

In AD the progression of tau deposition follows a hierarchical pattern, initially impacting regions receiving hippocampal input and projection zones (e.g., lateral entorhinal cortex, CA1/subiculum border, and outer molecular layer of dentate gyrus). This process occurs in an anterograde manner through the hippocampal circuitry, in which CA1 and CA2 are strongly affected⁵⁷. However, in the rTg4510 mice model, the tau pathology evolves differently, as the transgene hTauP301L expresses in all neurons of the hippocampal formation and cortical areas⁵⁸. Thus, to characterize the involvement of CA1 in the AD-related rTg4510 mouse model of tauopathy, we generated and crossbred the male C57BL/6 mice expressing the tetracycline-controlled transactivator protein under control of the forebrain-specific calcium-calmodulin-dependent kinase II (CaMK2a) promoter with female FVB mice carrying the responder tetO-MAPT*P301L transgene at the animal house of the Gly-CRRET. We first immunolabel free floating full brain sections from 4 months old (4M) rTg4510 and WT mice. AT8 (P-tau-s202/205) immunohistochemistry with the 3,3'-Diaminobenzidine (DAB) chromogen revelation revealed a high immunoreactivity in cortex and hippocampus, and in a greater degree in the hippocampal region CA1. Co-immunostaining with the hTau (K9JA) and pTau (s202/205) showed the colocalization between both antibodies, confirming the transgene mice model, and the presence of abnormally hyperphosphorylated tau in the CA1 pyramidal layer of the hippocampus, one of the first areas affected by the tau pathology in AD.

CA1 region is affected in rTg4510 mice model

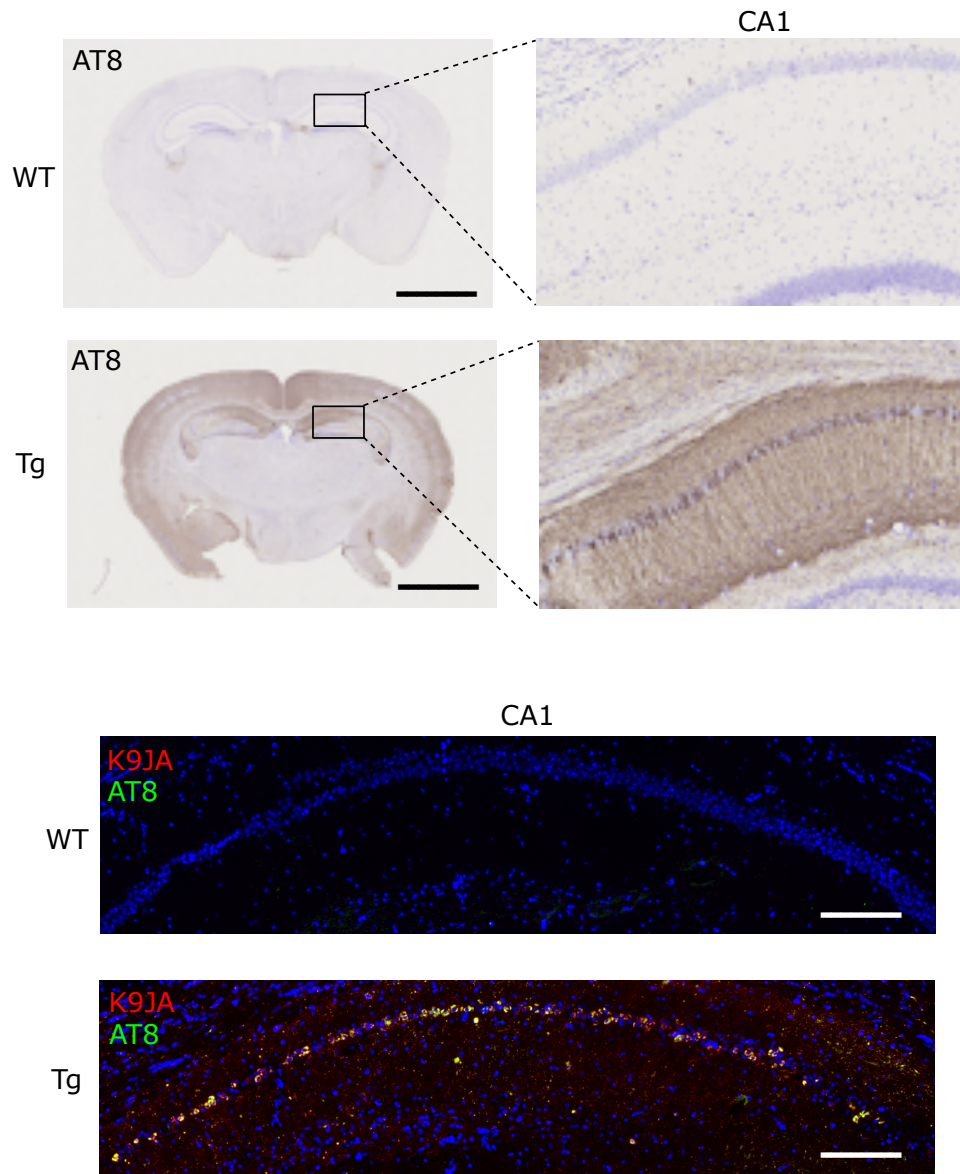


Figure 4. Tau pathology affects the CA1 region in the rTg4510 mouse. Full brain mice slices sections of rTg4510 (+/+) / WT (-/-) at 4 months old. A. Immunohistochemistry with the chromogen DAB of pTau (AT8). Magnification to the CA1 hippocampal region. Nuclei were counterstained with cresyl violet (blue). Scale bar 2 mm. B. Hippocampal CA1 formation immunofluorescence co-staining of hTau (K9JA) and pTau (AT8). Scale bar 200 μ m. Nuclei were counterstained with DAPI (blue). Representative images (n=3).

7.2.2. Tau oligomerization starts at early stages of tau pathology development in rTg4510 mice brain.

The rTg4510 mice is characterized by deficits in spatial navigation, spatial memory, and fear conditioning seen as early as 1.5 months of age, although, NFT lesions could be detected at 4 months in the hippocampus, and 60% neuronal decrease is observed in hippocampal CA1 neurons by about 5.5 months⁵⁸. Thus, we decided to evaluate the presence of tau oligomers at early stages of the pathology evolution. We recovered the brain and dissected the hippocampal formation in rTg4510 and WT mice aged 2 and 4 months. As described above, we performed a high salt Sarkosyl-fractionation to separate soluble oligomers from insoluble advanced aggregates. As expected, we did not find any soluble oligomer in the WT animals whereas analysis of the rTg4510 at same ages showed high levels of tau oligomers at 2 months followed by a decrease at 4 months (Figure 5 A). When analyzing the phosphorylation of tau at epitopes s396 and 404 (PHF1), a common phosphorylation site found in NFTs, we found an increase of the abnormally phosphorylated tau that evolved with time (Figure 5 B), as previously reported⁵⁴. These results confirms that the rTg4510 mice model can be used to study whether HSPG and their heparan sulphate chains are involved in the development and evolution of tau pathology in the mouse brain, particularly in the CA1 region of the hippocampus, as in the primary cultures of the rTg4510 hippocampal neurons.

Tau oligomerization starts at early stages of the disease

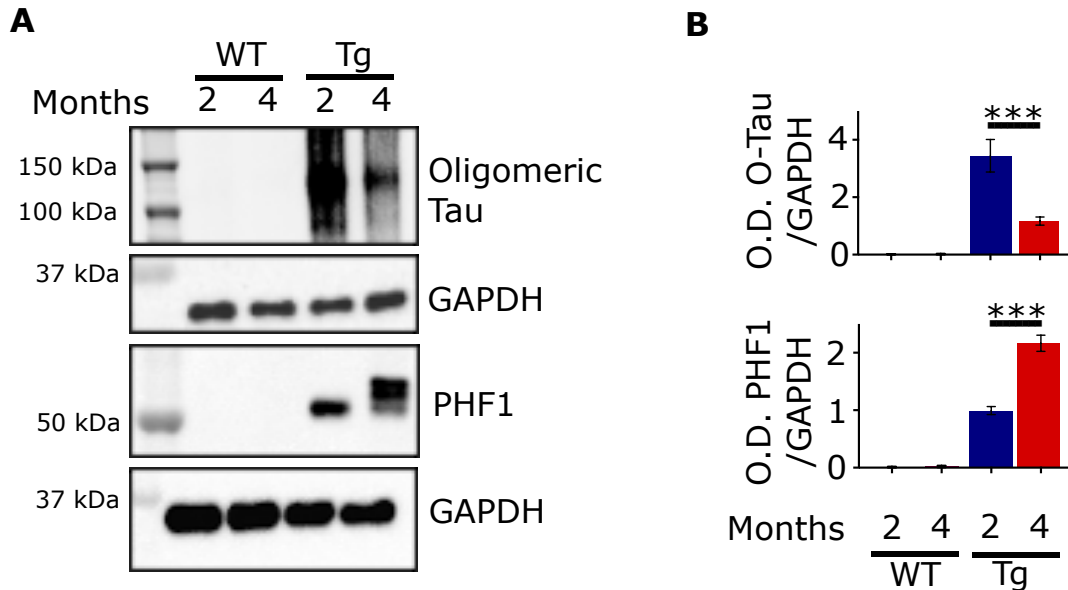


Figure 5. Tau oligomerization evolves in the rTg4510 mouse brain. Immunoblotting of high salt Sarkosyl soluble fraction from 2 and 4 months rTg4510 and WT hippocampal formation with the Oligo Tau antibody and pTau (s396/404). Quantification of Oligo Tau and pTau (s396/404) normalized with the loading control GAPDH. Representative blots (n=3). Error bar in plots is represented as SEM. * 0.05<p-value, **0 .01<p-value, *** 0.001<p-value.

7.2.3. Transcriptomics analysis identifies an upregulation of heparan sulfate proteoglycans biosynthetic machinery related genes at early stages of tau pathology development

Proteoglycans show remarkable functional versatility, influenced by both the core protein's identity and the structure of the attached glycanic chain. This diversity is evident

in the array of diseases arising from gene defects in their biosynthesis. Among these molecules, heparan sulphate proteoglycans (HSPG) stand out as the most complex in terms of structure and function⁴⁰. Notably, certain genes are pivotal for normal development and tissue balance, while others are not, highlighting the diverse roles of HSPG. The biological roles of HSPG are dictated by their specific core protein and associated heparan sulphate chains generated by an HSPG biosynthetic machinery unique to each tissue or cell³⁹. This machinery is composed of about 45 genes that, depending on their expression levels and patterns, can form a diversity of HSPG able to specifically interact with a diversity of proteins, including those that have tendency to aggregate. Thus, HSPG are linked to various types of amyloid deposits within the human body and have also been connected to several aspects of AD pathogenesis, including the formation of senile plaques, cerebrovascular amyloid, and NFT¹⁸. To explore whether the HSPG biosynthetic machinery is altered during the development and progression of AD-related tau pathology, we recovered brains and dissected the hippocampus of rTg4510 (+/+) and WT (-/-) mice aged 2 and 4 months old and isolated high-quality RNA. Then, we performed paired RNA-sequencing after ribosomal depletion. Gene expression of the HSPG biosynthetic machinery was done by comparing rTg4510 (+/+) against WT (-/-) littermates in the 2- and 4-months old mice. This allowed us to find an increased expression of 37 out of 45 genes involved in the HSPG biosynthesis, including EXT1, HS6ST2, HS6ST3, HS3ST2 and HS3ST, previously reported to be involved in AD physiopathology (Figure 6 A). Furthermore, at 2 months, we observed a highly significant increase of several genes in the HSPG biosynthetic machinery followed by a decrease at 4 months (Figure 6 B). Remarkably, this data correlates with the increase of tau oligomerization at 2 months (Figure 5), suggesting the involvement of the HSPG in development of AD related tau pathology.

Interestingly, the highly 3-O-sulphated heparan sulphates prototype, heparin, has been largely used to induce the aggregation of tau *in vitro*, suggesting that the interaction of 3-O-sulphated heparan sulphates might participate to the development of the tau pathology. However, it is unknown 3-O-sulphated heparan sulphates interact with the tau protein.

Heparan sulphate proteoglycans biosynthetic genes are upregulated at early stages of tau pathology

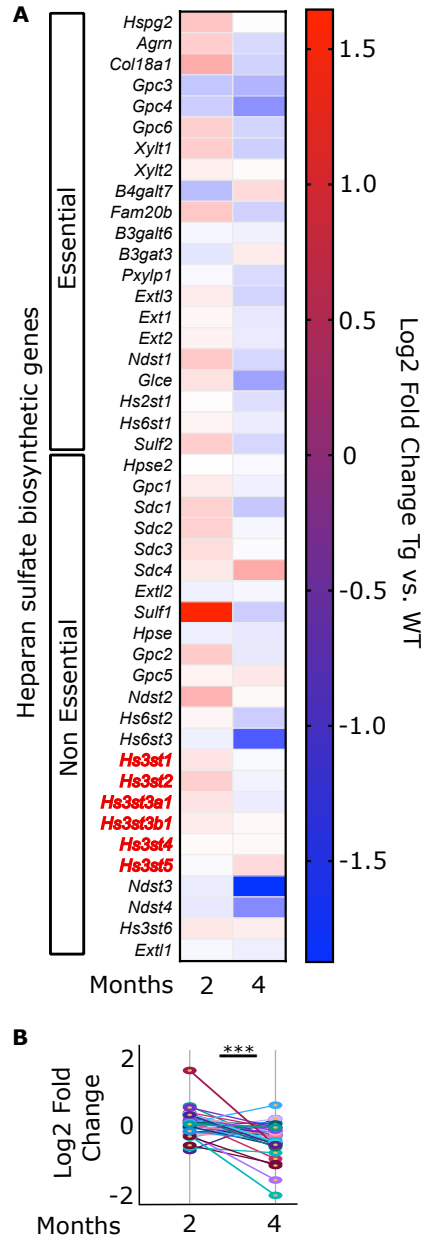


Figure 6. HSPG biosynthetic machinery is upregulated at 2 months in rTg4510. A. Heatmap revealing an increase of expression in rTg4510 (+/+) versus WT (-/-) hippocampus at 2 months, followed by a downregulation at 4 months. **B.** Group comparison of differentially expressed genes at 2 and 4 months revealing a general decrease in HSPG biosynthesis at 4 months. * 0.05<p-value, ** 0.01<p-value, *** 0.001<p-value. n=3.

7.2.4. Protein modelling of 3-O-sulphated heparan sulphates disaccharide units bind to tau residues susceptible to abnormal hyperphosphorylation

In vitro, tau filaments form within hours when tau is incubated with heparin. While heparin is not an exact model of the heparan sulphates that are present in neurons, in where they can interact with tau protein, both heparin and heparan sulphates trigger the structuration of tau into filaments exhibiting remarkably similar structures. Indeed, the interaction of heparin with full-length human tau protein prompts the tau assembly into filaments closely resembling those found in the brain tissue of individuals with AD. Therefore, to study the putative role of endogenous 3-O-sulphated heparan sulphates proteoglycans, which by interacting with tau in neurons can induce the formation of tau fibrils, we modelled the interaction between tau protein in its native form with 3-O-sulphated heparan sulphates disaccharide units. By *in silico* docking simulation, we remarkably found that 3-O-sulphated heparan sulphates specifically interacts with the tau microtubule assembly domain (Figure 7), containing most of the pathological phosphorylation sites characteristic of AD.

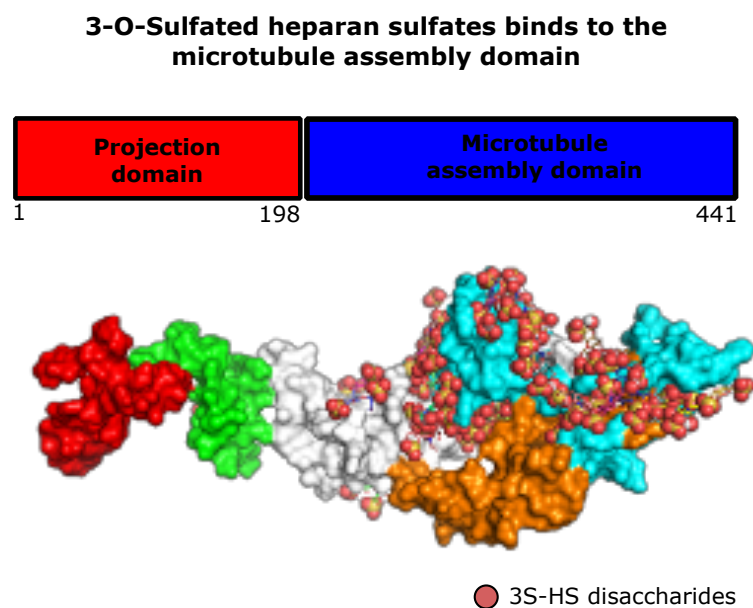


Figure 7. 3-O-sulphated heparan sulphates interact with tau at the microtubule assembly domain. Protein modelling simulation of tau native protein with the 3-O-sulphated heparan sulphates disaccharides interacting specifically with the microtubule assembly domain (199-441).

These results suggest that the intracellular 3-O-sulphated heparan sulphates might interact with tau and participate to the development of tau pathology. Previously, our team demonstrated that 3-O-sulphated heparan sulphates produced by the enzyme HS3ST2 accumulate inside cells in the AD brain (under submission) and in cellular models of AD-related tauopathy. Moreover, we showed that the expression of the 3-O-sulphated heparan sulphates biosynthetic enzyme HS3ST2 and HS3ST4 is increased in AD. However, the factors that induce the increased expression of these enzymes, and thus synthesize 3-O-sulphated heparan sulphates in neural cells are unknown.

7.3. TGF- β 1 controls the expression of the heparan sulphate 3-O sulphotransferases and regulates tau abnormal phosphorylation

7.3.1. SMAD2 and SMAD3 phosphorylation increases in AD human brain hippocampal formation

TGF- β is primarily expressed in neurons and microglia⁴⁹. Under physiologic conditions, it plays a role in maintaining neuronal equilibrium, promoting axon growth, fostering synaptogenesis, and maintaining microglial Smad2 and Smad3 pathways⁵⁹. However, in AD aberrant localization of phosphorylated Smad2 proteins indicates a disturbance in the TGF- β 1/Smad signaling pathway⁶⁰. Smads are the downstream effectors of TGF- β within the cytoplasm. SMAD2/3, known as R-SMADs, form heterotrimeric or dimeric complexes with the co-SMAD, SMAD4. SMAD4 is a transcription factor that interacts with DNA

specific sequences after translocation of these protein complexes into the nucleus, in which they partner with transcription factors to regulate gene expression by either activating or repressing target genes. R-Smads remain in the cytoplasm during cell resting, avoiding the nuclear translocation of the co-Smad into the nucleus⁴⁸. This signalling pathway is activated during chronic inflammation, such as AD⁵².

TGF- β 1 pathway has been associated with the transcription activation of the A β precursor protein gene APP, as well as the TIAF1 self-aggregation, leading to the generation of A β plaques in AD⁵¹. However, little is known about its role in the development and progression of NFTs. To decipher the role of the TGF- β 1 pathway in AD, we decided to immunolabel healthy and AD human brain hippocampal formation with antibodies against pSMAD/3 (T8) and pTau (s202/205). As expected, labelling with the pTau revealed the presence of NFT in the AD CA1 region but not in the control brain. Remarkably, co-staining with pSMAD2/3 revealed a specific nuclear localization, suggesting a crucial role of TGF- β 1 pathway in the gene expression regulation in AD (Figure 8).

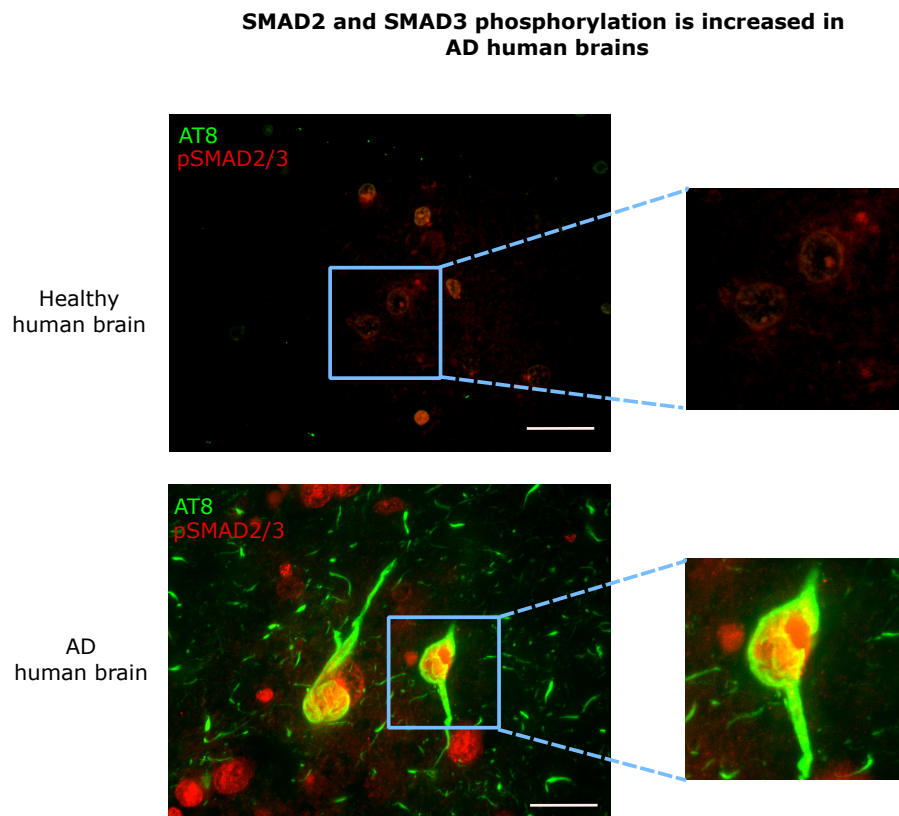


Figure 8. Activated R-SMADs (SMAD2/SMAD3) localize in neuronal nuclei in AD neurons. Co-immunolabelling of pSMAD2/3 and pTau (AT8) in healthy and AD hippocampal CA1 region, revealing an activation of the TGF- β 1 pathway in AD brains. Confocal slices images were acquired by a confocal microscope IX81 Olympus (magnification 60x, immerse oil). Representative images (n=3). Scale bar is 40 μ m.

7.3.2. Smad2 and Smad3 phosphorylation increases in rTg4510 PHN

As described above, the abnormal localization of phosphorylated Smad2/3 proteins in AD CA1 tissue indicates a disturbance in the TGF- β 1/Smad signaling pathway. Although this has been previously shown in the context of A β pathology, the effect in tau pathology remained unknown. To investigate this event in a pure model of tauopathy, we dissected PHN as described above. At DIV-20, cells were harvested in the RIPA buffer and fixed for immunohistochemical analysis. Immunofluorescence with pSMAD2/3 revealed high levels of pSmad2/3 in the rTg4510 (+/+) PHN compared with the WT (-/-). Moreover, pSmad2/3 mainly showed a nuclear localisation, suggesting a crucial role in gene regulation during AD-related tau pathology. This data was corroborated by western blot analysis, confirming the increased phosphorylation of Smad2/3 in the rTg4510 PHN.

Increased phosphorylation of Smad2 and Smad3 in rTg4510 PHN

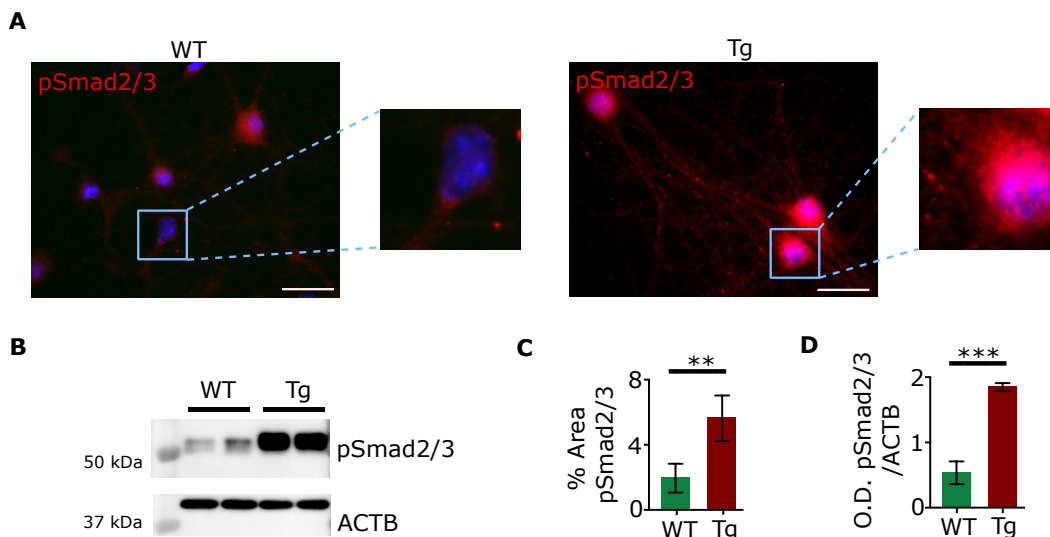


Figure 9. Increased phosphorylation of Smad2/3 in rTg4510 PHN. A. Immunostaining of pSmad2/3 in PHN revealing an increased phosphorylation and nuclear localization of Smad2/3 in rTg4510 compared with WT model. B. Immunoblotting of pSmad2/3 in WT and rTg4510 PHN revealing an increased phosphorylation of Smad2/3 in the rTg4510 PHN. C. Semi-quantification of pSmad2/3 in PHN. D. Quantification of pSmad2/3 normalized with the housekeeping gene ACTB. All results are shown at DIV-20 in PHN supplemented with GCCM. Nuclei were counterstained with DAPI (blue). Confocal slices images were acquired by a confocal microscope IX81 Olympus (magnification 60x, immerse oil). Scale bar is 20 μ m. Representative blots and images (n=3). Error bar in plots is represented as SEM. * 0.05<p-value, **0.01<p-value, *** 0.001<p-value.

7.3.3. TGF- β 1 controls gene expression of Heparan sulphate 3-O sulphotransferases

Receptor-activated Smads (R-Smads) by TGF- β 1 create heterotrimeric complexes with Smad4, an essential component for the transcriptional control of the majority of target genes⁴⁸. Smad4 exhibits an affinity for GC-rich motifs. The Smad MH1 domains has a remarkable conservation across diverse metazoans, where the DNA-binding β -hairpin showcases no amino-acid sequence differences. The β -hairpin's is flexible and adaptable, enabling it to achieve high-affinity binding with multiple variants of the consensus sequence GGC(GC)|(CG). Noteworthy, it has been described that the expression of HS3ST3B1 is under the regulation of the TGF- β pathway⁴⁵. The seven heparan sulphate 3-O-sulphotransferases are paralog genes, arising from gene duplication events from a common gene ancestor. Therefore, by using the crystal structure of the MH-1 domain of Smad4, previously described to be upregulated in AD, we decided to model its interaction with the Hs3st2 gene promoter. We show here that Smad4-MH1 can bind to several consensus sequences along the Hs3st2 promoter (Figure 10 A). Moreover, the *in silico* comparison of Hs3st2 promoter with other heparan sulphate 3-O-sulphotransferases promoters revealed a high homology between these

paralog genes (Figure 10 B), suggesting that TGF- β 1 can regulate the expression of different heparan sulphate 3-O-sulphotransferases genes. Thus, to confirm that heparan sulphate 3-O-sulphotransferases gene expression can be regulated by TGF- β 1, we dissected rTg4510 PHN as described above, and at DIV-15 we activated the TGF- β pathway with the recombinant protein TGF- β 1 or blocked its activation by the inhibition of TGFBR1. Remarkably, we found that the expression of these paralog genes is under the control of TGF- β 1, including the previously described HS3ST3B1 (Figure 10 C). Altogether, we show that TGF- β 1 regulates the expression of all heparan sulphate 3-O-sulphotransferases enzymes and therefore, their 3-O-sulphated heparan sulphates product.

Smad4 regulates HS 3-O-sulfotransferases gene expression

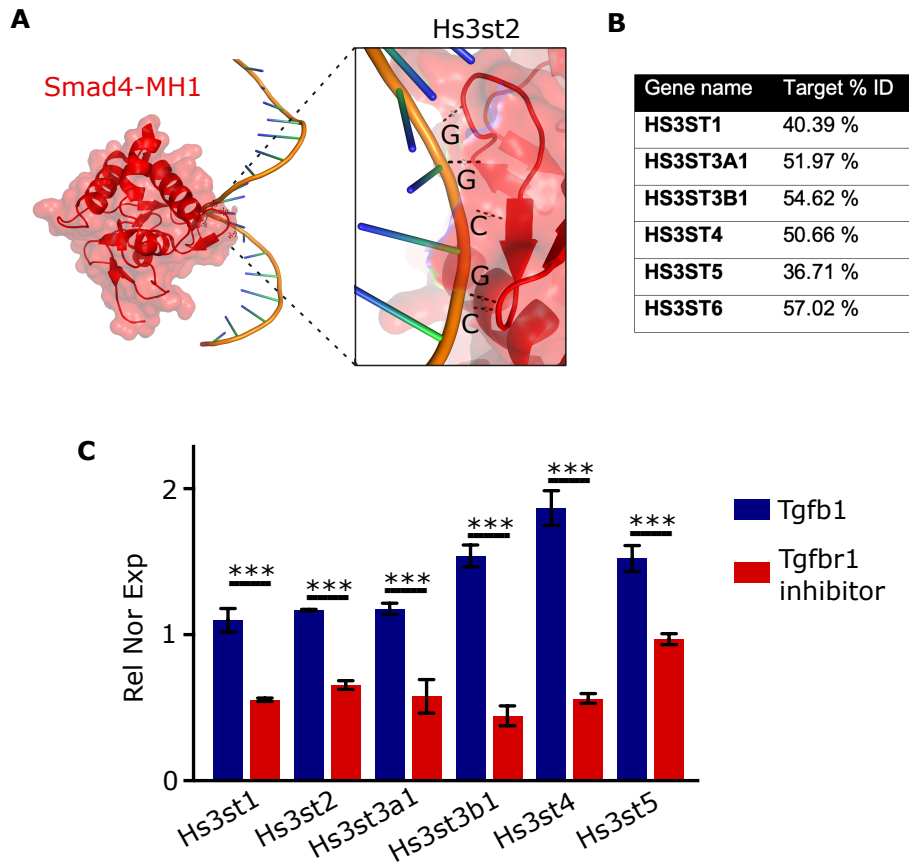


Figure 10. Smad4 regulates gene expression of HS3ST paralog genes in rTg4510 PHN. A. Crystal structure of Smad4-MH1 binding to the consensus sequence GGCGC in the gene promoter of Hs3st2. B. In silico analysis of gene sequence homology of Hs3st paralog genes compared with Hs3st2. C. qPCR of 3-O-sulphated heparan sulphates paralog genes in rTg4510 PHN (+/+) treated with Tgfb1 recombinant protein, or Tgfb1 inhibitor (SB431532). Gene normalization against Rplp0 housekeeping gene. n=3. Error bar in plots is represented as SEM. * 0.05<p-value, **0 .01<p-value, *** 0.001<p-value.

7.3.4. Selective inhibition of TGF- β 1 signaling decreases tau pathology

The precise role of TGF- β 1 signalling pathway in the pathophysiology of AD remains uncertain, with recent studies yielding conflicting findings. The inhibition of TGF- β 1 signalling pathway and downstream Smad2/3 results in a reduction in brain parenchymal and cerebrovascular A β deposits in a mouse model overexpressing a mutant form of APP resulting in elevated levels of A β and ultimately, in the formation of amyloid plaques (A β abundance were markedly reduced by up to 90%)⁵². However, the effect of TGF- β 1 inhibition in tau aggregation has not been studied. Thus, we used PHN to investigate the effect of selective inhibition of the TGF- β 1 signalling pathway in tau pathology. rTg4510 PHN were dissected as described above and treated with the selective Tgfb1 inhibitor (SB431532) at DIV-15, during the peak of tau oligomerization (Figure 3). PHN were kept under cell culture for 20 days. At DIV-20, cells were harvested in the RIPA buffer and fixed for immunohistochemical analysis. Immunoblotting of pTau (s396/402/PHF1) in control (DMSO) or treated (SB431532) rTg4510 PHN (+/+) showed a significant decrease in tau abnormal phosphorylation. Co-staining with pSmad2/3 and pTau (s396/402/PHF1) confirmed the effect of the Tgfb1 inhibitor by a decrease in Smad2/3 phosphorylation with a remarkable reduction of the tau abnormal phosphorylation, confirming the anti-tau pathology effect observed by western blot. This was confirmed by high levels of pSmad2/3 in the rTg4510 PHN compared with the WT. Additionally, immunolabeling

using the anti-oligomeric tau antibody T22 showed a decrease in tau oligomerization. Altogether, this data shows a decrease in tau pathology by the selective inhibition of TGF- β 1 signalling pathway. Thus, we hypothesized that this effect could occur through a downregulation of the 3-O-sulphated heparan sulphates enzymes, which have been previously found to be involved in tau pathology⁴³.

TGF- β 1 inhibition decreases tau abnormal phosphorylation and oligomerization

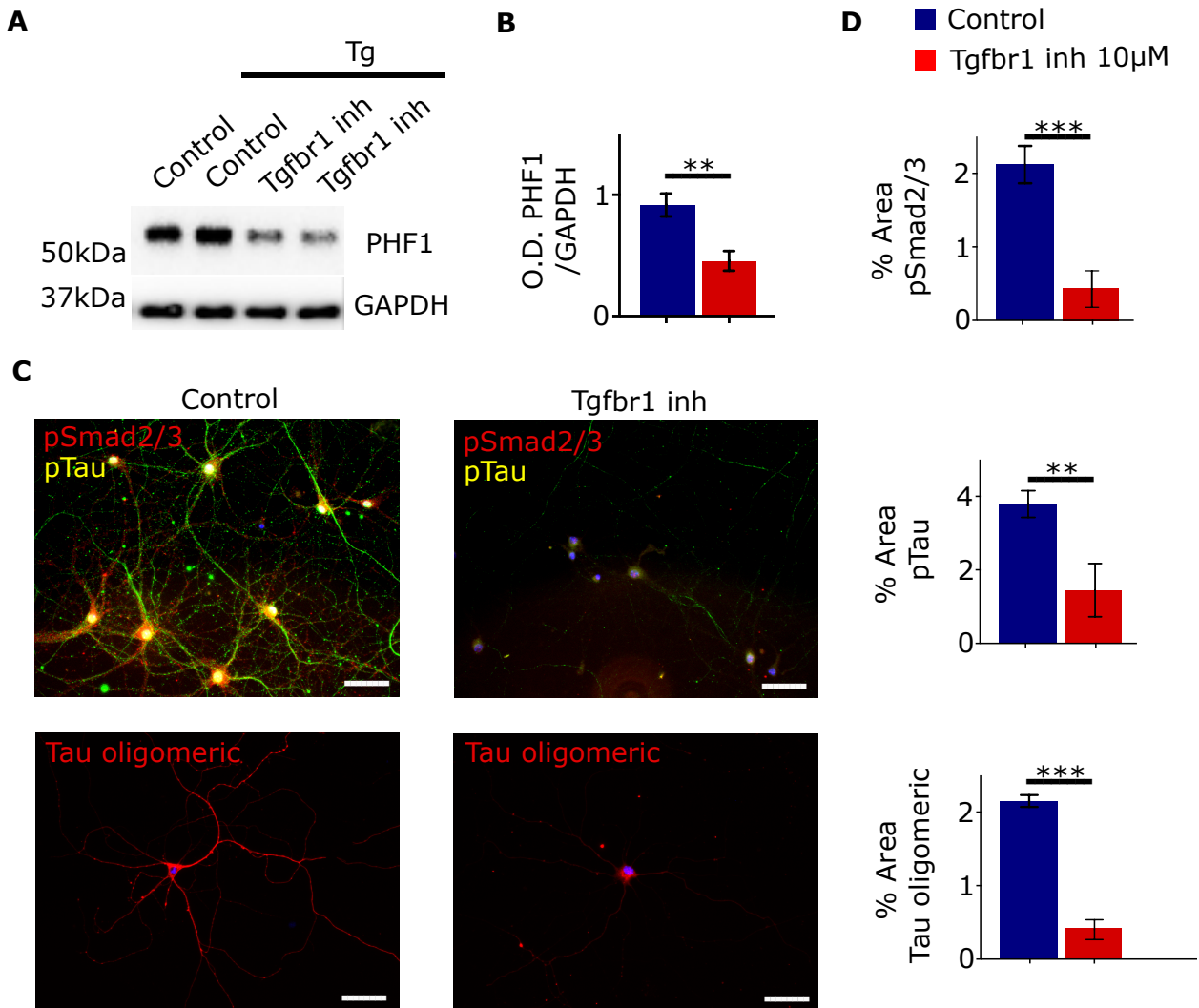


Figure 11. Tgf- β 1 inhibits tau abnormal phosphorylation and oligomerization in rTg4510 PHN. A. Immunoblotting of pTau (s396/402/PHF1) in rTg4510 PHN treated with the Tgfr1 inhibitor SB431532 revealing a decreased abnormal phosphorylation of tau. B. Quantification of pTau in PHN protein lysates, normalized with the loading control GAPDH. C. Co-Immunostaining of pSmad2/3 and pTau (s396/402/PHF1) in PHN revealing a decreased phosphorylation and nuclear localization of Smad2/3, and a decrease in abnormal phosphorylation and oligomerization of tau in rTg4510 PHN treated with the Tgfr1 inhibitor SB431532, D. Semi-quantification of pSmad2/3, pTau (s396/402/PHF1) and oligo tau in rTg4510 PHN. All PHN were treated with 10 μ M of SB431532 at DIV-15. Results are shown at DIV-20 in PHN supplemented with GCCM. Nuclei were counterstained with DAPI (blue). Confocal slices images were acquired by a confocal microscope IX81 Olympus (magnification 60x, immerse oil). Representative blots and images (n=3). Scale bar is 50 μ m. Error bar in plots is represented as SEM. * 0.05<p-value, **0 .01<p-value, *** 0.001<p-value.

7.4. 3-O-sulphated heparan sulphates synthesized by Hs3st2 are involved in tau abnormal phosphorylation and oligomerization

7.4.1. Hs3st2 and Hs3st4 are involved in AD

Recent studies have highlighted a specific subgroup of heparan sulphates known as 3-O-sulphated heparan sulphates, which exhibited a strong binding affinity to tau protein, leading to increased cellular internalization. The 3-O-sulphated heparan sulphates interaction with tau results in abnormal phosphorylation of tau and triggers its aggregation, a hallmark of neurodegenerative diseases, such as AD. The biosynthesis of

3-O-sulphated heparan sulphates is done by a family of heparan sulphate biosynthetic enzymes known as heparan sulphate 3-O-sulphotransferases, which transfer sulpho groups to the 3-hydroxyl (3-OH) positions of glucosamine residues. Although 3-O-sulphation is a rare modification in heparan sulphates, it plays a crucial role in its biological functions. In humans, there are seven heparan sulphate 3-O-sulphotransferases encoded by HS3ST1, HS3ST2, HS3ST3A, HS3ST3B, HS3ST4, HS3ST5, and HS3ST6 coding genes, each one exhibiting unique substrate specificity and producing heparan sulphates with distinct 3-O-sulphated domains. The challenge of measuring the levels of 3-O-sulphated heparan sulphates has impeded efforts to correlate the expression of heparan sulphate 3-O-sulphotransferases genes and the heparan sulphate subpopulation with AD. Using data publicly available from the Genotype-Tissue Expression (GTEx) project, we analyzed the expression levels of heparan sulphate 3-O-sulphotransferases coding genes in the hippocampus of healthy patients, finding that HS3ST2 and HS3ST4 are the highest expressed (Figure 12 A). Furthermore, WT (-/-) and rTg4510 (+/+) PHN were dissected as described above and high-quality RNA was isolated at 20-DIV. After ribosomal depletion, we performed paired end RNA-sequencing. Transcripts were quantified and differential gene expression analyzed comparing the WT (-/-) and rTg4510 (+/+) PHN RNA samples. Although in human tissue HS3ST2 and HS3ST4 showed the higher expression, in our WT PHN we found that Hs3st1, Hs3st2 and Hs3st4 have the higher level of expression. Remarkably, Hs3st2 and Hs3st4 were the only ones upregulated in the rTg4510 cells. Altogether, this data shows a good correlation between the pattern of expression of human healthy hippocampus and WT PHN. Moreover, this data suggests a potential crucial role of both Hs3st2 and Hs3st4 in the development of tau pathology.

Hs3st2 and Hs3st4 are upregulated in the hippocampus of AD related taupathy

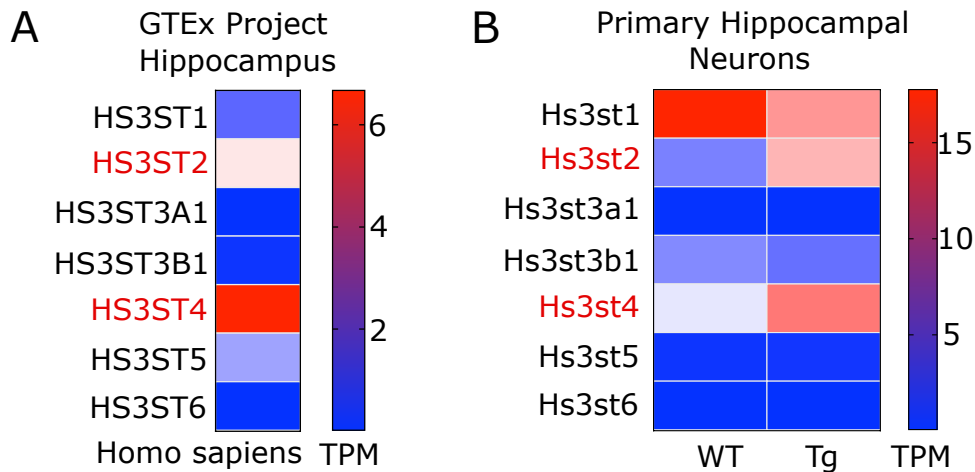


Figure 12. Hs3st2 and Hs3st4 are predominantly expressed in the human healthy hippocampus and are upregulated during the development of the tau pathology. A. Heatmap revealing Hs3st2 and Hs3st4 higher levels of expression in human healthy hippocampus compared to other heparan sulphate 3-O-sulphotransferases. B. Heatmap revealing the upregulation of Hs3st2 and Hs3st4 in rTg4510 compared with WT PHN, n=3.

7.4.2. Hs3st2 and not Hs3st4 decreases tau abnormal phosphorylation and aggregation

The involvement of heparan sulphate 3-O-sulphotransferases in binding and prompting tau aggregation highlights its role in facilitating their cellular uptake, presenting a promising avenue for potential modulation of tau-related pathogenesis. Several studies

have associated the specific role of 3-O-sulphated heparan sulphates in the AD-related tauopathy. HS3ST1 was found to be upregulated in the frontal cortex in AD patients. Moreover, the inhibition of its 3-O-sulphation domains in heparan sulphate chain inhibits tau internalization. The mRNA levels of HS3ST2 and HS3ST4 have been reportedly upregulated in the hippocampus of AD patients, and the expression of Hs3st2 was shown to be critical for the abnormal hyperphosphorylation of tau. Recently, it was shown that HS3ST2 gain of function induces the cell autonomous aggregation of tau not only in cells expressing tauP301S, but also in cells expressing the wild type tau. As described above, Hs3st2 and Hs3st4 are upregulated in the AD-related tauopathy. Thus, we decided to decipher its role in the process of tau aggregation in relation with TGF- β 1 signalling pathway. With this aim, WT (-/-) and rTg4510 (+/+) PHN were dissected as described above and at DIV-15 to induce a loss of Hs3st2 and/or Hs3st4 functions. We transduced lentivirus containing a shRNA for Hs3st2, Hs3st4, a combination of both, and a non-target control. PHN were fixed, high-quality RNA and proteins were isolated at 20-DIV. The efficiency of lentiviral transduction was evaluated by qPCR, showing a high efficiency of lentiviral transduction and gene silencing for both constructs, shHs3st2 and shH3st4 (Figure 13 A). The loss of function (LOF) of Hs3st4 did not decrease the levels of abnormally phosphorylated tau. However, Hs3st2 along or combined Hs3st2/Hs3st4 LOF resulted in a highly significant decrease of the abnormal hyperphosphorylation of tau. Furthermore, we used a high salt Sarkosyl-fractionated method to extract soluble protein fractions containing tau oligomers, additionally revealing a decrease in tau oligomerization (Figure 13 B,C). Immunofluorescence confirmed the increased levels of Hs3st2 in rTg4510 PHN (Figure 13 D). As heparan sulphates are the product of the seven 3-O-sulphated heparan sulphates and several other heparan sulphate sulphotransferases, it is expected that 3-O-sulphated heparan sulphates coexists with other sulfation types, including *N*-sulfation, 6-O-sulfation, and 2-O-sulfation. Nevertheless, LOF of Hs3st2 in rTg4510 (+/+) PHN led to a specific decrease in the 3-O-sulphated heparan sulphates (Figure 13 E), confirming the specificity and relevance of Hs3st2 in 3-O-sulphated heparan sulphates biosynthesis in neurons from the hippocampus, one of the first and most affected areas in AD.

Hs3st2 loss of function decreases tau abnormal phosphorylation and aggregation

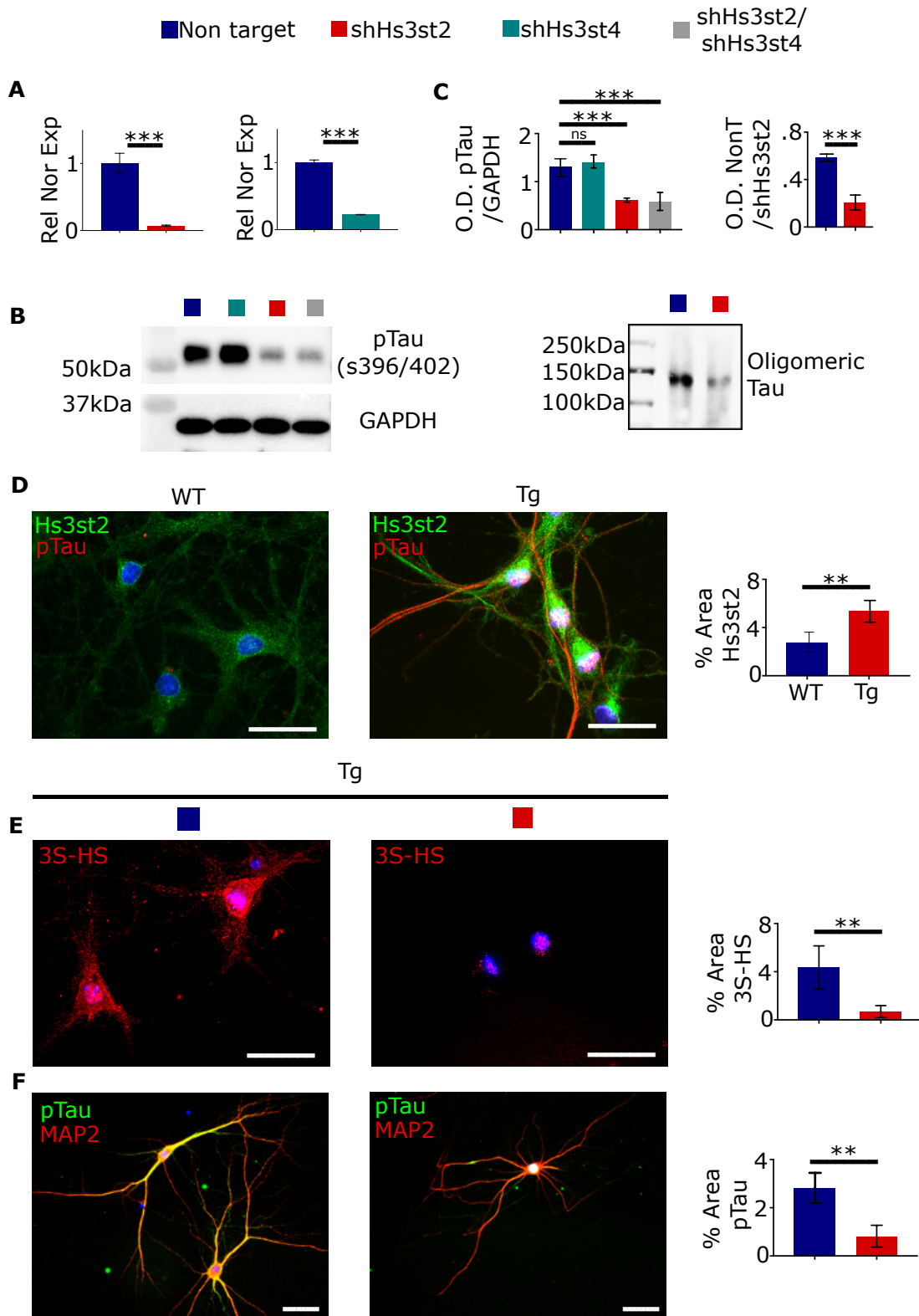


Figure 13. Hs3st2 and no Hs3st4 inhibits abnormal tau phosphorylation and oligomerization in rTg4510 PHN. **A.** qPCR of Hs3st2 and Hs3st4 after LOF showing the efficiency of the lentiviral transduction and shRNA in rTg4510. Gene normalization against Rplp0 housekeeping gene. **B.** Immunoblotting of pTau (s396/402) and oligo tau for Sarkosyl-extraction in rTg4510 PHN transduced with the Lv-shHs3st2 and Lv-shHs3st4. **C.** Quantification of pTau and oligo tau normalized with the housekeeping gene GAPDH. **D.** Co-Immunostaining of Hs3st2 and pTau (s396/402/PHF1) in PHN revealing higher levels of Hs3st2, and tau abnormal hyperphosphorylation in rTg4510 compared with WT. Scale bar is 40 μ m. **E.** Immunostaining with the antibody HS4C3 revealing a decrease in 3-O-sulphated heparan sulphates in rTg4510 PHN after Hs3st2 LOF. Scale bar is 40 μ m. **F.** Co-Immunostaining of MAP2 and pTau (s396/402/PHF1) in rTg4510 PHN after Hs3st2 LOF revealing a decrease in tau abnormal hyperphosphorylation, and no effect in MAP2. All PHN were treated with 3 LV of their respective construct at DIV-15. Results are shown at DIV-20 in PHN supplemented with GCCM. Nuclei were counterstained with DAPI (blue). Confocal slices images were acquired by a confocal microscope IX81 Olympus (magnification 60x, immerse oil). Representative blots and images (n=3). Scale bar is 60 μ m. Error bar in plots is represented as SEM. * 0.05<p-value, **0.01<p-value, *** 0.001<p-value.

The tau protein, or microtubule associated protein 2 (MAP 2), belongs to a family of proteins that functions to stabilize neuronal shape by promoting microtubule synthesis and cross-linking with other components of the cytoskeleton and has been involved in the growth, differentiation, and plasticity of neurons, with key roles in neuronal responses to growth factors, neurotransmitters, and synaptic activity⁶¹. Co-immunostaining of pTau (s396/402/PHF1) with MAP2 confirmed the effect of Hs3st2 LOF in decreasing the abnormal hyperphosphorylation of tau without affecting MAP2 levels. Furthermore, LOF of Hs3st2 did not change the localization of the MAP2 marker in the neural cells, ruling out a negative effect of loss of function (LOF) of Hs3st2 in neuronal homeostasis. Altogether, this data shows for the first time the specificity of the Hs3st2 enzyme in the

reduction of 3-O-sulphated heparan sulphates and show for the first time its critical role in the tau abnormal phosphorylation and oligomerization in neurons and the context of AD-related tau pathology.

7.5. Hs3st2 loss of function enhances glutamate synapse size and connectivity, cognition and learning or memory in Alzheimer's disease related tauopathy

7.5.1. Transcriptomic analysis of Hs3st2 LOF in rTg4510 PHN reveals pathways involved in cognition and learning of memory

Tau interaction with microtubules is essential for maintaining proper neuronal structure and intracellular transport. However, in AD, tau abnormal phosphorylation leads to its detachment from microtubules. This altered tau is prone to self-aggregation, forming toxic oligomers and insoluble fibrils. The presence of pathological tau at synapses correlates with synaptic impairment in AD. Tau aggregates disrupt synaptic vesicle trafficking, impair neurotransmitter release, and hinder synaptic plasticity, the brain's ability to adapt and learn. Furthermore, tau-induced inflammation and oxidative stress contribute to synaptic damage. Moreover, tau aggregates contribute to the loss of dendritic spines, which are essential for synapse formation and function. After demonstrating the specific role of Hs3st2 in the AD-related tau pathology, we decided to investigate the transcriptomic landscape of rTg4510 PHN after Hs3st2 LOF (Figure 14 A). Remarkably, gene ontology from the differential gene expression cluster of upregulated genes in rTg4510 after Hs3st2 LOF revealed, at the top of the “Biological process”, genes associated with cognition and learning or memory. Furthermore, by analyzing the genes involved in “Cellular component”, most of these processes are associated with healthy synapses, such as, neuron to neuron synapse, postsynaptic specialization and postsynaptic density. Together, this shows that the LOF of Hs3s2 in AD-related tau pathology can recover synaptic homeostasis.

Hs3st2 loss of function enhances cognition and synaptic homeostasis

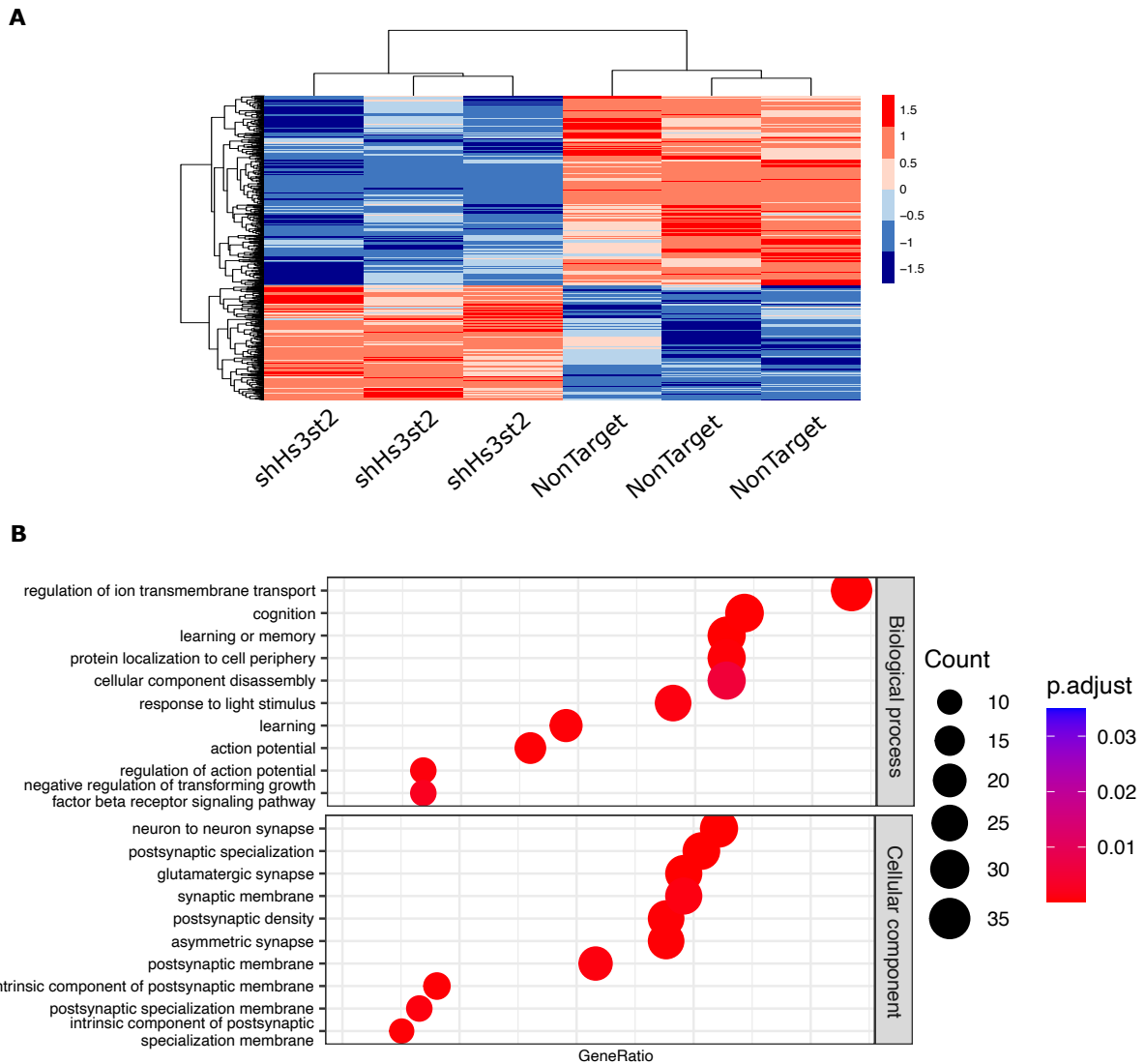


Figure 14. Hs3st2 LOF recovers synaptic homeostasis. A. Heatmap of differentially expressed genes after Hs3st2 LOF in rTg4510 PHN. **B.** Gene ontology and KEGG pathways analysis for biological process and cellular component in the upregulated genes after Hs3st2 LOF. All PHN were treated with 3 LV of their respective construct at DIV-15. Results are shown at DIV-2. PHN were supplemented with GCCM. Reads were aligned with STAR and an over-representation test was done with enrichGO in R. n=3.

7.5.2. Hs3st2 LOF enhances synaptic size and connectivity

In AD there is a significant relationship between synaptic size and the progression of the disease³⁶. Synapses are critical connections between neurons where communication occurs, and they play a fundamental role in cognitive functions like learning and memory. Synaptic loss is a hallmark of AD pathology, and this loss is closely linked to changes in synaptic size. As the disease advances, synapses shrink in size, leading to a reduction in synaptic density. This reduction in synaptic density has been observed in brain regions implicated in memory and cognitive functions, such as the hippocampus. This synaptic atrophy results in impaired neuronal communication and disrupts neural circuits that underlie memory formation and retrieval. The relationship between synaptic size and AD is further underscored by the fact that synaptic dysfunction and loss often occur early in the disease process, even before significant neuronal loss is evident. Synaptic deficits contribute to cognitive impairment and are thought to strongly correlate with memory decline in AD⁶². Having shown that Hs3st2 LOF recovers synaptic homeostasis at the transcriptome level, we decided to investigate the effect at the synapse in the PHN. Thus, rTg4510 PHN were dissected as described above and, at DIV-15, we started Hs3st2 LOF using lentiviral particles carrying *shHs3st2*, as shown above. At DIV-20 we fixed the cells to perform immunofluorescence focusing on synaptic markers. Immunostaining with Synaptophysin (Syn) revealed an increase in synapse number after Hs3st2 LOF. Furthermore, co-staining with the presynaptic marker Vesicular glutamate transporter 1 (VGLUT-1) and postsynaptic marker Postsynaptic density protein 95 (PSD95) revealed a significant increase and recovery in synaptic density, as well as colocalization between both markers, indicating active synapses. Taken together, this data shows in a model of AD-related tauopathy that LOF of Hs3st2 enhances synaptic size and connectivity.

Hs3st2 loss of function enhances synaptic size and connectivity

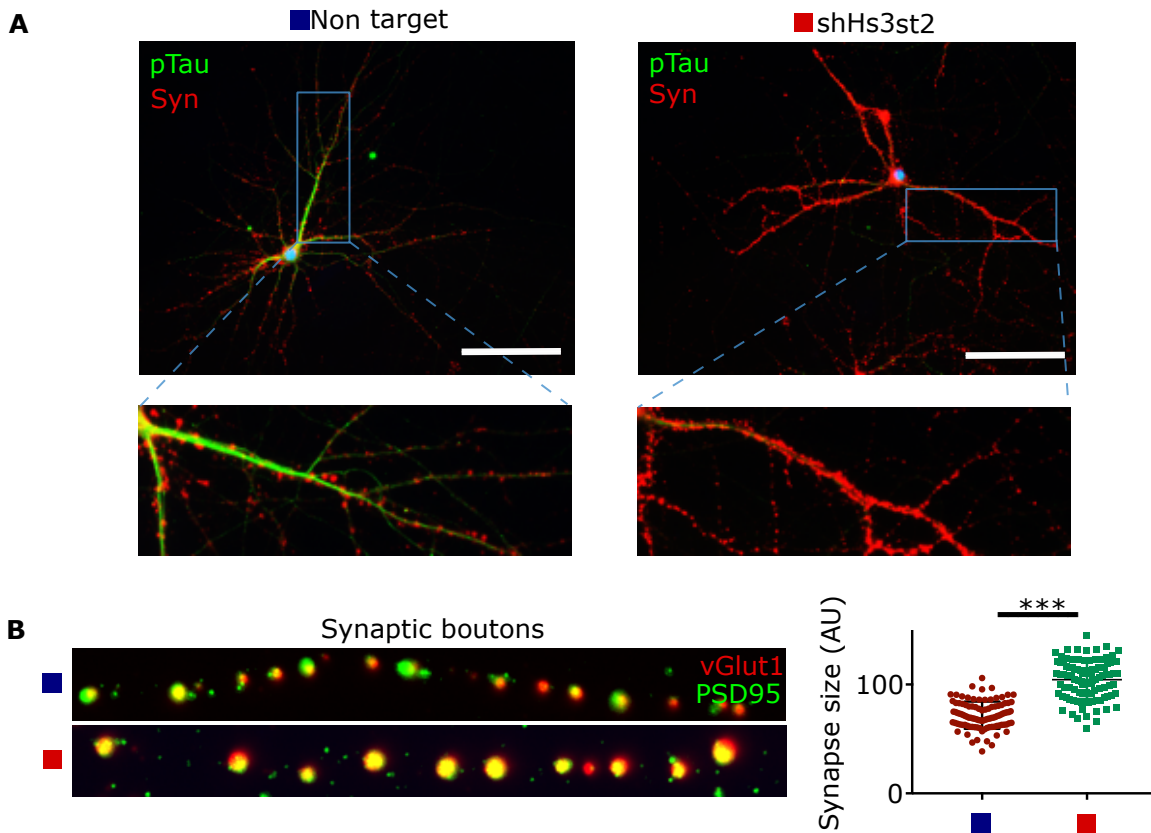


Figure 15. Hs3st2 LOF enhances synaptic size and connectivity in rTg4510 PHN. A. Co-Immunostaining of Syn and pTau (s396/402) in rTg4510 PHN after Hs3st2 LOF revealing a decrease in tau abnormal hyperphosphorylation, and an increase in synaptic number. **B.** Co-immunostaining of vGLUT1 with PSD95 after Hs3st2 LOF in rTg4510 shows an increase in synaptic density and co-localization between both markers, demonstrating active synapses. Quantification of synapse size in WT and rTg4510. All PHN were treated with 3 LV of their respective construct at DIV-15. Results are shown at DIV-20 in PHN supplemented with GCCM. Nuclei were counterstained with DAPI (blue). Representative images (n=3). Confocal slices images were acquired by a confocal microscope IX81 Olympus (magnification 60x, immerse oil). Representative blots and images (n=3). Scale bars represent 80 μ m. Error bar in plots is represented as SEM. * 0.05<p-value, **0 .01<p-value, *** 0.001<p-value.

Altogether, our results shows that the increase of TGF- β 1 signalling pathway observed in AD can induce tau pathology mediated by 3-O-sulphated heparan sulphates through Hs3st2 expression upregulation by the activation of its promoter in cultured hippocampal cells. We showed that Hs3st2 specific LOF, and no other 3-O-sulphated heparan sulphates results in the arrest of tau pathology and recovers synaptic density and connectivity, leading to an increase in gene pathways related to cognition and learning or memory. This data positions the 3-O-sulphated heparan sulphates and Hs3st2 in the center of the disease and potential therapeutic target.

8. Discussion

We show that 3-*O*-sulphated heparan sulphates can bind to tau in the microtubule assembly domain. This domain contains the majority of the pathological phosphorylation sites responsible for tau abnormal hyperphosphorylation¹. In a model for Alzheimer's disease related tau pathology the heparan sulfate proteoglycan (HSPG) biosynthetic genes³⁹, including the heparan sulfate 3-*O*-sulphotransferases coding genes, are upregulated in the hippocampus at an early stage, correlating with the peak of tau oligomerization. Remarkably, it has been shown by others that tau soluble oligomers are the most toxic tau species in AD³². Moreover, we show here that heparan sulfate 3-*O*-sulphotransferases expression is under the control of TGF- β 1 pathway, which we found to be activated in AD brains. R-SMADs are the downstream effectors of TGF- β 1 pathway, leading to the nuclear translocation of SMAD4, a transcription factor upregulated in AD⁴⁷. Based on our results, we propose a mechanism in which the inhibition of TGF- β 1 pathway leads to a decrease in tau abnormal phosphorylation and oligomerization through the downregulation of heparan sulfate 3-*O*-sulphotranferases expression. We found that from the seven heparan sulfate 3-*O*-sulphotranferases, Hs3st2 and Hs3st4 are upregulated in the hippocampus and that Hs3st2 is involved in the events leading to tau pathology, as loss of function of Hs3st2, and not Hs3st4, decreased the tau abnormal phosphorylation and oligomerization. Synaptic loss is a hallmark of AD pathology, and this loss is closely linked to changes in synaptic size⁶². Remarkably, Hs3st2 loss of function leads to activation of pathways related to cognition and memory and enhances synaptic density and connectivity. Altogether, our findings place the 3-*O*-sulphated heparan sulphates in the center of onset and evolution of tau pathology.

The exact aetiology of AD is not yet fully understood but is believed to be multifactorial. Genetic factors play an important role, particularly in Early-Onset Alzheimer's disease (EOAD) cases. EOAD is linked to mutations in the genes APP, PSEN1, and PSEN that lead to altered processing of amyloid precursor protein (APP) and overproduction or beta-amyloid peptide, resulting in the accumulation of amyloid plaques. On the other hand,

Late-Onset/sporadic Alzheimer's disease (LOAD) is the most common form of the disease. In this disease variant, the apolipoprotein E (APOE) gene has been identified as the strongest genetic risk factor. It is noteworthy that APP, PSEN1, PSEN2 and APP are all heparin binding proteins. The APOE gene has three major alleles: ϵ 2, ϵ 3, and ϵ 4 among which the ϵ 4 allele is associated with an increased risk and an earlier onset of AD. The ApoE isoforms exhibit different affinities for heparin, with ApoE4 having the highest affinity, followed by ApoE3, ApoE2, ApoE3cc. Furthermore, ApoE/heparan sulphates interactions and cellular binding/uptake are significantly enhanced by 3-O-sulphated heparan sulphates⁹. APOE ϵ 4 carriers have higher levels of amyloid plaques, and an increased risk of developing tau-related neurodegenerative diseases, leading to a higher risk of developing LOAD compared to non-carriers. Several other genetic risk factors have been identified through genome-wide association studies (GWAS). These include TREM2, CLU, PICALM, ABCA7, among others. These protein coding genes are membrane-associated proteins. For instance, TREM2 is a membrane protein capable of binding cell-surface proteoglycans. HSPG are a major component of the cell-surface ligand and specifically heparan sulphates displays a major component of the cell surface TREM2-L^{64,12}.

AD is characterised by the two main hallmarks: senile plaques (SP) principally made of the A β peptide (A β) and neurofibrillary tangles (NFT), principally made of abnormally phosphorylated forms of the microtubule associated protein tau (MAPT). A common hallmark for SP and NFT is the presence of heparan sulphates. Heparan sulphate proteoglycans promote A β or tau fibrillation and protects against their proteolytic breakdown¹⁹. Despite decades of research in AD, there is no effective treatment for AD. Noteworthy, most of the therapeutic agents in clinical trials target A β plaques⁴. However, cognitive decline does not correlate with the burden of A β plaques. Several studies have reported either absent or weak association between A β plaques and cognitive impairment in AD patients^{65,66}. Furthermore, the reduction of A β plaques in clinical trials has not proved cognitive benefit in AD patients⁶⁷. Several neuropathological studies have shown the correlation with the degree of cognitive impairment in AD and the burden of NFTs, but not of amyloid- β plaques, correlates with the degree of cognitive impairment in AD

patients and healthy individuals^{65, 68}. Moreover, advanced Braak stages are associated with cognitive impairment, explained by the fact that tau pathology is more intimately related to neuronal loss^{68, 69, 70}. Consequently, the first aim of this work consisted in establishing an *in vitro* model to study the implication of 3-O-sulphated heparan sulphates in tau pathology and cross talk with TGF- β signalling pathway.

PHN cell cultures provide a valuable tool for studying neurobiology. These cultures offer a relevant environment resembling *in vivo* conditions. PHN allows the observation of morphological changes, imaging of cellular structures, and genetic manipulation to study gene function. These cultures are particularly useful for investigating neuronal development, plasticity, responses to compounds and in dissecting physiopathology in neurodegenerative diseases, such as AD⁵³. Moreover, primary hippocampal neuron cultures reduce reliance on animal experiments, providing an ethical alternative for studying neuronal biology and disease processes following the 3R in animal research⁷¹. Three main types of neurons are observed in the hippocampus: granular cells and pyramidal cells which are excitatory neurons, and inhibitory interneurons. We dissected embryonic PHN at E16 and cultivated them with supplemented glial conditional medium for 20 days. Glial cells, like astrocytes, offer crucial support by providing nutrients, growth factors, and metabolic assistance that promote neuronal survival, development, and synaptic function. The supplementation of PHN with GCM enhances the formation of functional neuronal networks, maintains a stable microenvironment, and better mimics the physiological conditions of the brain⁷². We demonstrated by co-immunostaining using the pan neuronal markers NeuN and MAP2, and the Syn, marker of functional synapses, the long-term culture at a low cell density, enrichment of PHN, stable morphological pattern, and proper neuronal connectivity. We applied this technique for the establishment of an *in vitro* model to study tau pathology using the rTg4510 model. The rTg4510 mice model resembles specific pathological features observed in human AD. In the rTg4510 model, a mutated form of human tau containing the P301L mutation is overexpressed under the control of the tetracycline-regulated promoter system. The expression of the mutant tau protein leads to the formation of neurofibrillary tangles (NFTs) in the neurons

of the mice^{54,58}. Even though this model has been extensively characterized in vivo, to date there are no in vitro studies demonstrating the progression of the tau pathology. Here, following our established method for PHN in vitro cell culture, we dissected embryonic PHN at E16 from females FVB mice carrying the responder tetO-MAPT*P301L transgene crossed with males C57BL/6 mice expressing the tetracycline-controlled transactivator protein under control of the forebrain-specific calcium-calmodulin-dependent kinase II (CaMK2a) promoter. Our results showed an increased phosphorylation of the s202/205 with the clinical approved and commonly used to mark NFT pathology AT8 antibody, and s396/404 with PHF1 antibody staining paired helical filaments of tau. These two abnormally phosphorylated sites are located in the Microtubule assembly domain, which has been mainly involved in the process of tau aggregation⁶³. Furthermore, immunostaining with Syn demonstrated a decrease in synaptic density and function, resembling the changes previously reported in the in vivo rTg4510 model⁵⁴. Tau soluble oligomers are highly toxic to neurons, disrupting cellular functions and hindering synaptic activity. A growing number of studies have demonstrated that soluble oligomers of tau are critical players in the AD progression³². Here, analysis of tau soluble oligomers on the PHN revealed an increase of tau oligomerization overtime, with a peak at 15-DIV followed by a decrease in its oligomerization. This finding allowed us to establish our time window, at 15-DIV as the optimal time for the following experiments.

In AD the progression of tau deposition follows a hierarchical pattern, initially impacting regions receiving hippocampal input and projection zones, such as the entorhinal cortex and CA1^{73,74}. We recovered rTg4510 mice brains, Tg (+/+) and WT (-/-), at 4 months old and immunolabelled full brain slices with the AT8 antibody and counterstaining with Cresyl violet with the chromogen DAB, and co-staining AT8 with a human tau antibody, confirming the transgene mice model, and unveiling the presence of abnormally phosphorylated tau and NFT in the CA1 region. Changes in spatial memory and spatial navigation occur before the presence of NFT⁵⁴. In the rTg4510 we detected NFT lesions at 4 months in hippocampus CA1, and it has been reported up to 60% neuronal decrease in hippocampal CA1 neurons by about 5.5 months⁵⁸. Thus, we decided to study the

kinetics of tau oligomerization in the hippocampus at an early stage, 2 months old, and middle stage, 4 months. Remarkably, we found a peak of oligomerization at 2 months, followed by a decrease at 4 months. Concordantly with our previous results, we found an increase in the phosphorylation of tau in S396/404, phosphorylation sites commonly found in paired helical filaments of tau. Thus, our PHN model of tauopathy recapitulates the disease evolution of the source mouse and is suitable for studying the mechanisms involved in tau pathology onset and evolution.

In this work, our main hypothesis was that HSPG are crucial players in the development of tau pathology. HSPG are the most complex type of proteoglycans with a broad display of functions. Proteoglycans exhibit extensive functional diversity, defined by the identity of the core protein and the structure of the attached glycanic chain. This diversity has been shown in various diseases due to gene defects in their biosynthesis⁷⁵. While some genes are vital for normal development and tissue stability, others are not, suggesting that certain HSPG assume indispensable biological roles, contingent on the specific core protein and associated HS chains produced by the HSPG biosynthetic machinery within individual tissues or cells^{39,76}. HSPG has been detected in the intracellular compartment in non-tangle bearing neurons in AD brains, suggesting a possible intracellular accumulation before the NFT formation⁷⁷. Moreover, the specialized 3-O-sulphated heparan sulphates have been shown to act as molecular chaperones and interact with tau and promote its abnormal phosphorylation and aggregation, the two main molecular events characteristic of AD-related tau pathology^{27,43}. To depict the transcriptomic landscape of HSPG biosynthetic machinery genes in the rTg4510 mouse in relation with our related PHN model, we recovered brains and dissected the hippocampus of rTg4510 Tg (+/+) and WT (-/-) aged 2 and 4 months and isolated high-quality RNA to perform RNAseq. Differential gene expression analysis comparing Tg and WT at 2 and 4 months revealed a general upregulation in HSPG biosynthetic genes at 2 months, followed by a decrease at 4 months. Remarkably, the upregulation of HSPG biosynthetic genes correlates with the increase in tau oligomerization at 2 months, suggesting the involvement of the HSPG in the development of tau pathology. Altogether, these findings

support the hypothesis of heparan sulphates accumulate intraneuronal prior to the NFT formation. Yet, it has not been clearly deciphered how heparan sulphates interact with tau. However, it has been shown *in vitro*, that the 3-O-sulphated heparan sulphates bind to tau, but not to GSK3B, protein kinase A or protein phosphatase 2, inducing the tau abnormal phosphorylation likely through specific conformational states allowing kinases to access to previously inaccessible tau epitopes, ultimately leading to aggregation. However, it is not known the sequence or domain of 3-O-sulphated heparan sulphates interacting with tau. Therefore, we decided to elucidate the potential binding sites of 3-O-sulphated heparan sulphates with tau. We modelled the tau human protein in its native form with the 3-O-sulphated heparan sulphates disaccharide units. Docking simulations revealed a specific binding to the tau microtubule assembly domain, which has been mainly involved in the process of tau aggregation⁶³. Interacting sites included the residues S202, S205, S396 and S404. Noteworthy, these residues have been shown to be abnormally phosphorylated as shown by their recognition with the antibodies AT8 and PHF1. These results suggest a crucial role of the intracellular 3-O-sulphated heparan sulphates in the development of tau pathology. Previous work in the field demonstrated that 3-O-sulphated heparan sulphates produced by the enzyme Hs3st2 accumulates intracellularly and induces tau aggregation^{27,43}. Hs3st2 is one of the seven heparan sulphate 3-O-sulphotransferases and has been shown to be upregulated in the hippocampus of AD patients³⁷. Though, its transcriptional regulation neurons are unknown.

Gene expression is a tightly regulated process that allows cells to control which genes are expressed, thereby determining the production of its coding proteins⁷⁸. In AD, there is an abnormal gene expression influencing crucial roles in brain function, such as neural survival, and synaptic maintenance¹³. In a recent work, the comparison of gene expression between AD and old-matched patients showed a specific signature of significantly upregulated and downregulated genes⁴⁷. Further examination of the upregulated genes within the “regulation of transcription” GO term revealed the presence of several transcription factors, including SMAD4, effector of the TGFB1 pathway. TGF- β 1 is a pleiotropic cytokine upregulated in the brain of AD patients playing a role in the

development and progression of the disease by at least inducing APP synthesis and prompting A β formation^{50,79,51}. Remarkably, TGF- β 1 has been shown to regulate the expression of Hs3st3b1, a member of the group of the heparan sulfate D-glucosamine 3-O-sulphotransferase enzymes⁴⁵. Altogether, this data suggests an important role of TGF- β 1 in transcriptional regulation of AD related genes. Nonetheless, its implication in tau pathology has not been extensively studied. We decided to evaluate the activation of the TGF- β 1 pathway in AD through the phosphorylation of the R-SMADs, SMAD2/3, which forms a complex with SMAD4 and translocates to the nucleus to regulate gene expression. Co-immunostaining of the phosphorylated SMAD2/3 with AT8 from human CA1 hippocampal brain slices from AD patients compared with healthy controls showed an increase in the abnormal phosphorylation of tau (AT8) and in the phosphorylation of SMAD2/3 in AD brains. Furthermore, the localization of phosphorylated SMAD2/3 displays a specific nuclear localization, suggesting a crucial role of TGF- β 1 signaling pathway in gene transcriptional regulation⁴⁹. To investigate the role TGF- β 1 in our in vitro established model of tau pathology we dissected PHN from rTg4510 Tg (+/+) and WT (-/-). Consistently with our previous findings in the human brain, we found an increase in the phosphorylation of Smad2/3 in Tg PHN with a specific nuclear localization. Furthermore, immunoblotting corroborated the increase in Smad2/3 phosphorylation in Tg PHN. Our findings suggest a crucial role of TGF- β 1 signaling pathway through the phosphorylation of Smad2/3, in a complex with the transcriptional regulator Smad4 and therefore, regulating transcriptional regulation in AD.

Having deciphered the crucial role of TGF- β 1 signaling pathway in AD transcriptional regulation we decided to explore the possible regulation of the heparan sulphate 3-O-sulphotransferases in the mechanism leading to the pathologic tau accumulation. The transcriptional regulation of heparan sulphate 3-O-sulphotransferases has been extensively studied in the context of cancer. This gene expression regulation has been shown to occur through different mechanisms, such as DNA methylation and VEGF-dependent activation of transcriptional factors⁷⁵. Noteworthy, TGF- β 1 controls the expression of Hs3st3b1⁴⁵. The Smad MH1 domains has a remarkable conservation

enabling it to achieve high-affinity binding with multiple variants of the consensus sequence GGC(GC)|(CG)⁴⁸. We modelled the crystal structure of SMAD4 MH1 domain with the DNA promoter sequence of Hs3st2, and found several GGC(GC)|(CG) sequences along its promoter. This suggests that Hs3st2 expression can possibly be regulated through the TGF- β 1 signaling pathway, particularly through SMAD4. Indeed, a common regulation of Hs3st through the TGF- β pathway cannot be ruled-out, since heparan sulphate 3-O-sulphotransferases coding genes are paralogs, coming from a common ancestor and evolving in the 7 enzymes through gene duplication. These 7 coding genes share a high homology sequence. Thus, we hypothesized that most if not all heparan sulphate 3-O-sulphotransferases coding genes, including Hs3s3b1 and Hs3st2, can be regulated by TGF- β 1. Accordingly, we found that by blocking the activation of TGF- β 1 pathway with inhibitors of the TGF- β receptor I, there is a significant decrease in gene expression in the seven heparan sulphate 3-O-sulphotransferases in rTg4510 PHN, and contrarily, by activating the TGF- β 1 signaling pathway by treating cells with the recombinant protein TGF- β 1, we increased their expression. Overall, we found that heparan sulphate 3-O-sulphotransferases are under the control of TGF- β 1. Having demonstrated the regulation of the heparan sulphate 3-O-sulphotransferases by TGF- β 1, we decided to explore its role in tau pathology. The role of TGF- β 1 in AD pathophysiology is not unequivocal, and inconsistent results have been reported⁵⁹. Moreover, studies involving the TGF- β 1 in AD tau pathology have been observational⁸⁰, and none of them have shown the in vitro or in vivo effect of reducing the activation of TGF- β 1 signaling pathway. Thus, we decided to block the TGF- β receptor I of PHN from rTg4510 Tg (+/+) and WT (-/-). Immunoblotting with PHF1 antibody revealed a decrease in the tau phosphorylation at residues s396 and s404 in the PHN Tg (+/+) treated with the TGF- β receptor I inhibitor. Co-immunostaining with the antibody AT8 and anti-phospho-Smad2/3 confirmed the increased levels of phosphorylation of Smad2/3 in AT8-positive neurons, the specificity of the TGF- β receptor I in decreasing the phosphorylation of Smad2/3 and the reduction in the phosphorylation of tau at residues 202/205. Moreover, there was a reduction in the tau oligomerization in PHN Tg (+/+), as detected by immunofluorescence. Altogether, we propose a mechanism in which the inhibition of the TGF- β 1 signaling pathway leads to a decrease in tau abnormal phosphorylation and oligomerization

through the downregulation of the 3-O-sulphated heparan sulphates, synthesized by the heparan sulphate 3-O-sulphotransferases.

3-O-sulphated heparan sulphates can bind and prompt the aggregation of tau, highlighting their role in facilitating tau intracellular accumulation^{81,18}. Numerous studies have associated the specific role of individual heparan sulphate 3-O-sulphotransferases in AD. HS3ST1 was found to be upregulated in the frontal cortex in AD patients and the inhibition of its 3-O-sulphation domains in heparan sulphates inhibits tau fibrils internalization during their spreading⁸². Moreover, HS3ST2 and HS3ST4 expression have been reportedly upregulated in the hippocampus of AD patients³⁷, and the expression of Hs3st2 was shown to be critical for the abnormal hyperphosphorylation and internalization of tau²⁷. Recently, it was shown that HS3ST2 gain of function induces the cell autonomous aggregation of tau⁴³. However, to date their individual role in the production of 3-O-sulphated heparan sulphates leading to tau aggregation is unknown. To answer this question, we analyzed the expression of the seven 3-O-sulphated heparan sulphates in healthy hippocampus human brain using the publicly available GTeX repository and comparing this data with RNAseq data of PHN from rTg4510 Tg (+/+) and WT (-/-). We found that HS3ST1, HS3ST2 and HS3ST4 have a higher expression in the healthy human hippocampus and in rTg4510 PHN WT (-/-). Remarkably, Hs3st2 and Hs3st4 are the only two enzymes upregulated in rTg4510 PHN Tg (+/+). The upregulation of Hs3st2 and Hs3st4 is consistent with the previous reports²⁷. Noteworthy, Hs3st1 is downregulated in PHN Tg (+/+), contrarily with previous findings showing its increase in AD brains⁸². However, different brain regions have different gene signatures and vulnerability⁸³. HS3ST1 was found to be upregulated in the frontal cortex, an area not severely affected in AD⁵⁷. Thus, we decided to study the role of Hs3st2 and Hs3st4 in the AD related tau pathology. We designed shRNA sequences and packed them in lentiviral particles to transduce PHN and induced a LOF of Hs3st2 and Hs3st4. By using qPCR, we validated the transduction efficiency and specificity of the transduction and LOF of Hs3st2 and Hs3st4 in rTg4510 PHN Tg (+/+) by qPCR. We showed by immunoblotting that the LOF of Hs3st4 did not decrease the levels of tau abnormal phosphorylation at residues s396

and s404. However, the LOF of Hs3st2 alone or combined with Hs3st4 resulted in a highly significant decrease of the abnormal phosphorylation of tau. Furthermore, the Hs3st2 LOF leads to a reduction of tau oligomerization. Immunofluorescence confirmed the increased levels of Hs3st2 in AT8 positive PHN. Strikingly, the LOF of Hs3st2 in rTg4510 PHN led to a specific decrease in the 3-O-sulphated heparan sulphates, confirming the specificity and relevance of Hs3st2 in 3-O-sulphated heparan sulphates biosynthesis in hippocampal neurons, one of the first and most affected areas in AD⁵⁷. Hs3st2 is a tissue restricted heparan sulfate biosynthetic gene and its LOF has not been shown to be deleterious nor affected tissue homeostasis³⁹. Accordingly, immunostaining with the MAP2 neuronal marker of PHN after Hs3st2 LOF ruled out a negative effect in neuronal structure²⁶. Altogether, this data shows for the first time the specificity of the Hs3st2 enzyme in the reduction of 3-O-sulphated heparan sulphates, with non-effect of Hs3st4, leading to a decrease in the tau abnormal phosphorylation and oligomerization in neurons in AD related tau pathology.

Tau pathology is characterized by the tau abnormal phosphorylation, leading to its detachment from microtubules⁸⁴. This altered tau forms toxic oligomers and insoluble fibrils⁸⁵. The presence of these pathological forms of tau at synapses correlates with synaptic impairment and cognitive decline in AD⁶². Tau aggregates disrupt synaptic vesicle trafficking, impair neurotransmitter release, and disrupt synaptic plasticity leading to the loss of dendritic spines²⁶. If the Hs3st2 LOF leads to a decrease in tau pathology, we hypothesize that by decreasing the levels 3-O-sulphated heparan sulphates we will have a synapse recovery. RNAseq differential expression analysis from rTg4510 PHN Tg (+/+) revealed a cluster of upregulated genes after Hs3st2 LOF. Gene Ontology revealed at the top of the “Biological process”, genes associated with cognition and learning or memory. Additionally, genes involved in the term “Cellular component” are associated with healthy synapses, such as, neuron to neuron synapse, postsynaptic specialization and postsynaptic density. We confirmed this data by immunofluorescence labeling synaptophysin in which we found synaptic recovery, translated as an increase in synaptic number and size after the Hs3st2 LOF. Moreover, co-staining with the presynaptic marker VGLUT-1 and postsynaptic marker PSD95 revealed a significant increase and recovery

in synaptic density, as well as colocalization between both markers, indicating formed synapses. Taken together, this data shows that the LOF of Hs3st2 enhances synaptic density and connectivity leading to a recovery in cognition and memory.

Together, our results show that the TGF- β signalling pathway induce the expression of Hs3sts, that Hs3st2 and Hs3st4 are the main heparan sulphate 3-O-sulphotransferase paralogues in cultured hippocampal neurons, and that Hs3st2, and not Hs3st4, is involved in the production of 3-O-sulphated heparan sulphates that during disease, and that these 3-O-sulphated heparan sulphates are internalized in neurons. We show that 3-O-sulphated heparan sulphates can interact with tau and that this interaction is a key event for the induction of the abnormal phosphorylation and aggregation of tau. Together, our results position intracellular 3-O-sulphated heparan sulphates, and the heparan sulphate 3-O-sulphotransferase, HS3ST2, as a key modulators of tau pathology, opening a wide area of research with therapeutic potential for AD and other tauopathies.

9. Conclusion

AD is the most common cause of dementia, and its prevalence is expected to triple by 2050. AD is characterised by the accumulation of senile plaques principally and NFTs leading to a cognitive decline. To date there is no effective treatment for AD. Research has focused on therapeutic agents that target A β peptides. However, numerous studies have shown no correlation with the degree of cognitive impairment in AD with the presence of senile plaques. Remarkably, NFTs correlate better with the degree of cognitive impairment in AD patients. NFTs are the result of tau aggregation. NFTs are not alone in the brain, they co-localize with heparan sulphates and it has been shown that heparin, a highly sulphated heparan sulphate carrying rare 3-O-sulphation, induces tau aggregation. Heparan sulphates also modulate inflammatory responses, potentially influencing the chronic neuroinflammation observed in AD. Furthermore, in a cellular model it was shown that 3-O-sulphated heparan sulphates accumulates intracellularly and induce tau aggregation. 3-O-sulphated heparan sulphates are the product of heparan sulphate 3-O-sulphotransferases. However, the specificity and the specific role of heparan sulphate proteoglycans biosynthetic machinery genes in AD it has not been studied. With this aim, here we used the rTg4510 *in vivo* model of tau pathology and established an *in vitro* model. We have identified the specific binding sites of 3-O-sulphated heparan sulphates to tau protein and correlated the upregulation in the expression of heparan sulphate proteoglycan biosynthetic related genes with the increased of tau oligomerization in early stages of the disease, supporting the hypothesis of intracellular heparan sulphate accumulation prior to NFT formation. HS3ST1, HS3ST2 and HS3ST4 expression is upregulated in AD brains, however its transcriptional regulation remains unknown. In this context, we found that the TGF- β signalling pathway is upregulated in the AD brain and modulates gene expression through its transcriptional factor SMAD4. SMAD4 binds to specific DNA sequences at the promoter of its targets. Remarkably, we found that all heparan sulphate 3-O-sulphotransferases are under the transcriptional control of TGF- β signalling pathway, which inhibition leads to reduction in tau pathology probably through the decrease of 3-O-sulphated heparan sulphates levels in cells. We investigated the expression of heparan sulphate 3-O-sulphotransferases in

AD and our model of *in vitro* tau pathology, revealing an upregulation of HS3ST2 and HS3ST4, according to previous findings. Hs3st2 loss of function and not Hs3st4, decrease in the production of 3-O-sulphated heparan sulphates and leads to a decrease of tau abnormal phosphorylation and oligomerization. These data shows that 3-O-sulphated heparan sulphates produced specifically by Hs3st2 are crucial for the abnormal phosphorylation and oligomerization of tau, which accumulation if which leads to synaptic loss. Cognitive impairment is the result of synaptic loss, The presence of pathological tau at synapses results in synaptic impairment, translated as cognitive decline in AD patients. Gene ontology from transcriptomic analysis revealed that Hs3st2 loss of function leads to the upregulation in genes related to cognition and learning or memory. Furthermore, its loss of function recovers synaptic density and connectivity. Altogether, we show the crucial role of Hs3st2 in tau pathology, and propose Hs3st2 as a potential therapeutic target in AD.

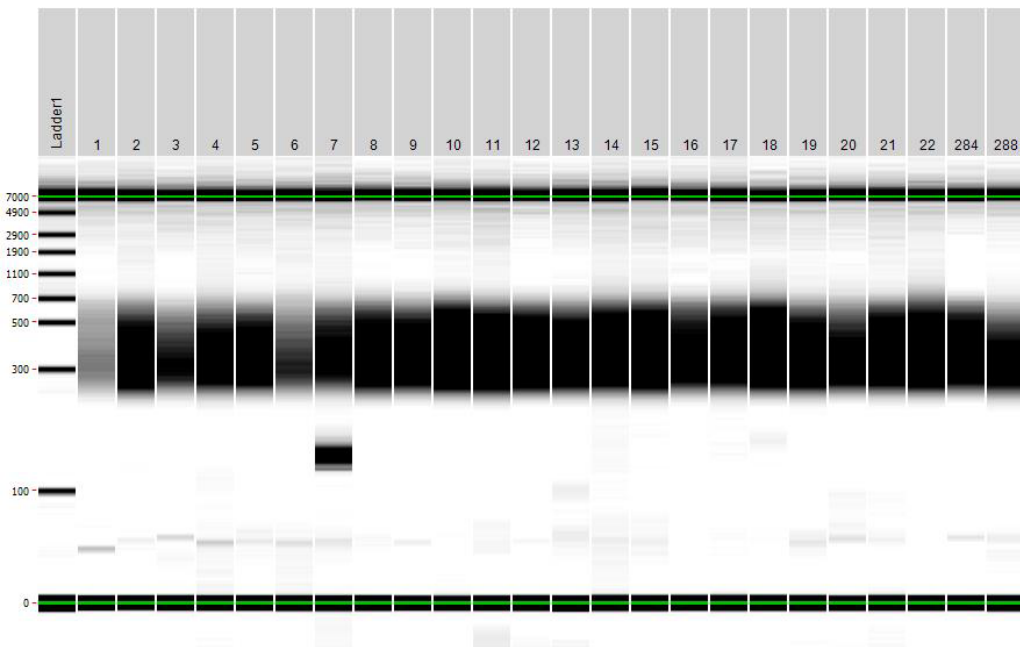
10. Annex

10.1. Context of the research

This work was a collaborative effort with the Glycobiology - Croissance cellulaire, Réparation, et Régénération Tissulaire (GLY-CRRET) Research unit under the direction of Prof. Dulce Papy-García at the Université Paris-Est Créteil, France. The lab rotation was partially funded by the project ArrestAD (Stop Alzheimer's Disease) - Programme Européen pour la Recherche et l'Innovation « FET-OPEN Horizon 2020 Technologies Futures et Emergentes » (FET OPEN RIA 737390), Glycanix, and the Giessen Graduate Centre of Life Sciences (GGL). Experiments carried out at the Gly-CRRET were under the supervision of Dr. Mohand Ou Idir Ouidja and Dr. Minh Bao Huynh. Experiments done at the Gly-CRRET included the breeding of the rTg4510 mice model, dissection and cell culture of primary hippocampal neurons and further biochemical and histological analysis. Sequencing data used in this thesis comes from the ArrestAD generated database.

10.2. RNAseq quality controls

Sample Name	Quantity (ng)	Index	P7 Index sequence	P5 Index sequence (Novaseq v1.5)	Number cycles PCR	Concentration Qubit HS (ng/μL)	Volume (μl)
1WT NT	200	UDP0098	CACTCAATTC	CACAACCTAA	12	35.205	1.4
1WT HS3ST2	200	UDP0099	TCTCACACGC	TCACGTCCG	12	13.887	3.6
2WT NT	200	UDP0102	ATGGCGCCTG	AGGCCGTGGA	12	12.219	4.1
2WT HS3ST2	200	UDP0103	TCCGTTATGT	TACACTACAA	12	18.936	2.6
3WT NT	200	UDP0122	GATATTGTGT	ACCGTGTGGT	12	47.48	1.1
3WT HS3ST2	200	UDP0123	CGTACAGGAA	AGAGAACCTA	12	40.934	1.2
1Tg NT	200	UDP0126	AGGAGGTATC	TGCCAACTGG	12	28.222	1.8
1Tg HS3ST2	200	UDP0127	GCTGACGTTG	AATGCGAACA	12	36.784	1.4
2Tg NT	200	UDP0110	TAATTAGCGT	TTCTTAACCA	12	25.213	2.0
2Tg HS3ST2	200	UDP0133	AACGAGGCCG	ATCCAGGTAT	12	31.405	1.6
3Tg NT	200	UDP0147	ACGTTCCCTA	CACAGCGGTC	12	21.946	2.3
3Tg HS3ST2	200	UDP0134	TGGTGTATG	TAGAATTGGA	12	28.894	1.7
WT-Tg 4M 284	200	UDP0135	TGGCCTCTGT	CGCTGTCTCA	12	28.534	1.8
WT-Tg 4M 288	200	UDP0165	TTAACCTTCG	TGTCTGGCCT	12	20.791	2.4
WT-Tg 4M 300	200	UDP0137	CCGGTTCCTA	CTCGAATATA	12	26.995	1.9
WT-Tg 2M 352	200	UDP0138	GGCCAATATT	TATCGGACCG	12	21.342	2.3
rTg4510 4M 356	200	UDP0139	GAATACCTAT	ACTTATTGT	12	15.233	3.3
rTg4510 4M 357	200	UDP0140	TACGTGAAGG	CTAATAACCG	12	18.121	2.8
rTg4510 4M 358	200	UDP0141	CTTATTGGCC	ACTTGTATC	12	21.34	2.3
WT-Tg 2M 360	200	UDP0142	ACAACACTG	TGTGATAACT	12	19.302	2.6
WT-Tg 2M 365	200	UDP0143	GTTGGATGAA	TTACCTGGAA	12	10.423	4.8
rTg4510 2M 405	200	UDP0144	AATCCAATTG	CCTTACATG	12	15.619	3.2
rTg4510 2M 409	200	UDP0145	TATGATGGCC	TATGACAATC	12	25.551	2.0
rTg4510 2M 410	200	UDP0146	CGCAGCAATT	ATAGCGGAAT	12	25.754	1.9

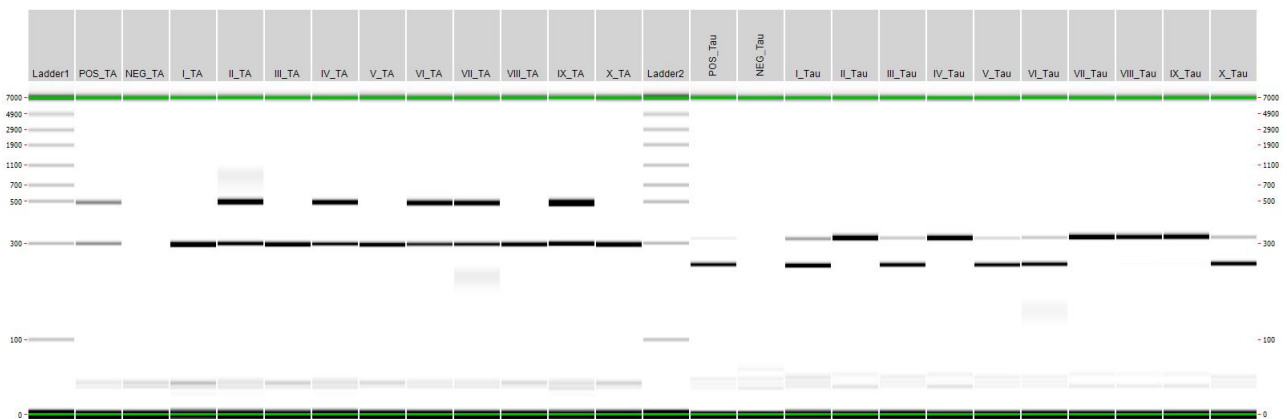


10.3. Percentage of mapped reads by Salmon

Sample Name	Salmon quantification
1WT NT	"percent_mapped": 90.74038877419413,
1WT HS3ST2	"percent_mapped": 90.82707755997397,
2WT NT	"percent_mapped": 90.76128674488352,
2WT HS3ST2	"percent_mapped": 91.29346668437077,
3WT NT	"percent_mapped": 89.90928311656782,
3WT HS3ST2	"percent_mapped": 91.4811664055564,
1Tg NT	"percent_mapped": 90.14843615214875,
1Tg HS3ST2	"percent_mapped": 89.64311768152791,
2Tg NT	"percent_mapped": 90.4647491443235,
2Tg HS3ST2	"percent_mapped: 90.68050275999652,
3Tg NT	"percent_mapped": 90.18112296884368,
3Tg HS3ST2	"percent_mapped: 90.58202750841727,

10.4. rTg4510 genotypage confirmation

Samples	Line	Tau			TA		
		Mutant (240 pb)	CI (320 pb)	Genotype	Mutant (500 pb)	CI (300 pb)	Genotype
I	rTg4510	1	1	Muté	0	1	WT
II	rTg4510	0	1	WT	1	1	Muté
III	rTg4510	1	1	Muté	0	1	WT
IV	rTg4510	0	1	WT	1	1	Muté
V	rTg4510	1	1	Muté	0	1	WT
VI	rTg4510	1	1	Muté	1	1	Muté
VII	rTg4510	0	1	WT	1	1	Muté
VIII	rTg4510	0	1	WT	0	1	WT
IX	rTg4510	0	1	WT	1	1	Muté
X	rTg4510	1	1	Muté	0	1	WT



10.5. Glial cell culture from P5 rats

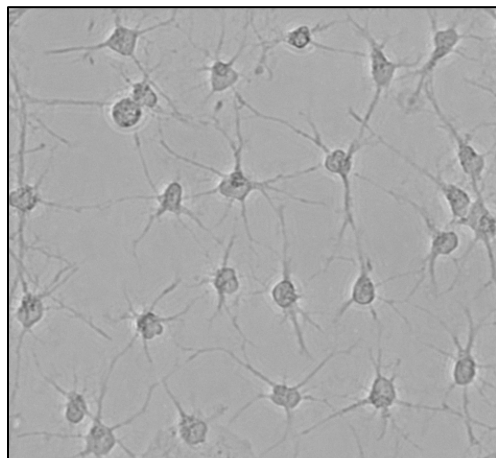
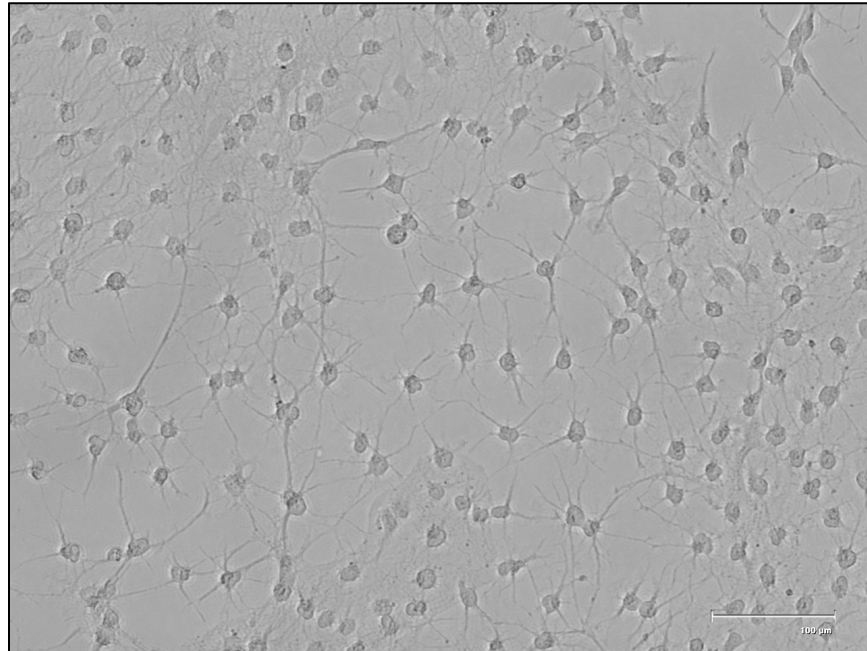


Figure 1 Annex. Glial cell culture from P5 rats. Brightfield image of glial cells at 10 days in vitro. Representative images (n=3). Scale bars represent 100 μm.

11. Declaration

I declare that I have completed this dissertation single-handedly without the unauthorized help of a second party and only with the assistance acknowledged therein. I have appropriately acknowledged and referenced all text passages that are derived literally from or are based on the content of published or unpublished work of others, and all information that relates to verbal communications. I have abided by the principles of good scientific conduct laid down in the charter of the Justus Liebig University of Giessen in carrying out the investigations described in the dissertation.

12. References

1. Livingston, G. *et al.* Dementia prevention, intervention, and care: 2020 report of the Lancet Commission. *The Lancet* **396**, 413–446 (2020).
2. Breijyeh, Z. & Karaman, R. Comprehensive Review on Alzheimer's Disease: Causes and Treatment. *Molecules* **25**, 5789 (2020).
3. Launer, L. J. Statistics on the burden of dementia: need for stronger data. *Lancet Neurol.* **18**, 25–27 (2019).
4. Cummings, J. *et al.* Alzheimer's disease drug development pipeline: 2022. *Alzheimers Dement. Transl. Res. Clin. Interv.* **8**, (2022).
5. Lane, C. A., Hardy, J. & Schott, J. M. Alzheimer's disease. *Eur. J. Neurol.* **25**, 59–70 (2018).
6. Bellenguez, C. New insights into the genetic etiology of Alzheimer's disease and related dementias. *Nat. Genet.* **54**, (2022).
7. Cacace, R., Sleegers, K. & Van Broeckhoven, C. Molecular genetics of early-onset Alzheimer's disease revisited. *Alzheimers Dement.* **12**, 733–748 (2016).
8. Rabinovici, G. D. Late-onset Alzheimer Disease. (2019).
9. Mah, D. *et al.* Apolipoprotein E Recognizes Alzheimer's Disease Associated 3- O Sulfation of Heparan Sulfate. *Angew. Chem. Int. Ed.* **62**, e202212636 (2023).
10. Lumsden, A. L., Mulugeta, A., Zhou, A. & Hyppönen, E. Apolipoprotein E (APOE) genotype-associated disease risks: a phenome-wide, registry-based, case-control study utilising the UK Biobank. *eBioMedicine* **59**, 102954 (2020).

11. Alzheimer's Disease Neuroimaging Initiative *et al.* ApoE4 markedly exacerbates tau-mediated neurodegeneration in a mouse model of tauopathy. *Nature* **549**, 523–527 (2017).
12. Kober, D. L. *et al.* Neurodegenerative disease mutations in TREM2 reveal a functional surface and distinct loss-of-function mechanisms. *eLife* **5**, e20391 (2016).
13. Chen, X.-F., Zhang, Y., Xu, H. & Bu, G. Transcriptional regulation and its misregulation in Alzheimer's disease. *Mol. Brain* **6**, 44 (2013).
14. Busche, M. A. & Hyman, B. T. Synergy between amyloid- β and tau in Alzheimer's disease. *Nat. Neurosci.* **23**, 1183–1193 (2020).
15. Snow, A. D., Cummings, J. A. & Lake, T. The Unifying Hypothesis of Alzheimer's Disease: Heparan Sulfate Proteoglycans/Glycosaminoglycans Are Key as First Hypothesized Over 30 Years Ago. *Front. Aging Neurosci.* **13**, 710683 (2021).
16. Cras, P. *et al.* Senile plaque neurites in Alzheimer disease accumulate amyloid precursor protein. *Proc. Natl. Acad. Sci.* **88**, 7552–7556 (1991).
17. Selkoe, D. J. & Hardy, J. The amyloid hypothesis of Alzheimer's disease at 25 years. *EMBO Mol. Med.* **8**, 595–608 (2016).
18. Maïza, A. *et al.* The role of heparan sulfates in protein aggregation and their potential impact on neurodegeneration. *FEBS Lett.* **592**, 3806–3818 (2018).
19. Liu, C.-C. *et al.* Neuronal heparan sulfates promote amyloid pathology by modulating brain amyloid- β clearance and aggregation in Alzheimer's disease. *Sci. Transl. Med.* **8**, (2016).
20. Sandwall, E. *et al.* Heparan sulfate mediates amyloid-beta internalization and cytotoxicity. *Glycobiology* **20**, 533–541 (2010).

21. Karisetty, B. C. *et al.* Amyloid- β Peptide Impact on Synaptic Function and Neuroepigenetic Gene Control Reveal New Therapeutic Strategies for Alzheimer's Disease. *Front. Mol. Neurosci.* **13**, 577622 (2020).
22. Lee, C. Y. D. & Landreth, G. E. The role of microglia in amyloid clearance from the AD brain. *J. Neural Transm.* **117**, 949–960 (2010).
23. Alexander, G. C., Emerson, S. & Kesselheim, A. S. Evaluation of Aducanumab for Alzheimer Disease: Scientific Evidence and Regulatory Review Involving Efficacy, Safety, and Futility. *JAMA* (2021) doi:10.1001/jama.2021.3854.
24. Wang, Y. & Mandelkow, E. Tau in physiology and pathology. *Nat. Rev. Neurosci.* **17**, 22–35 (2016).
25. Robbins, M., Clayton, E. & Kaminski Schierle, G. S. Synaptic tau: A pathological or physiological phenomenon? *Acta Neuropathol. Commun.* **9**, 149 (2021).
26. Iqbal, K. *et al.* Tau pathology in Alzheimer disease and other tauopathies. *Biochim. Biophys. Acta BBA - Mol. Basis Dis.* **1739**, 198–210 (2005).
27. Sepulveda-Diaz, J. E. *et al.* HS3ST2 expression is critical for the abnormal phosphorylation of tau in Alzheimer's disease-related tau pathology. *Brain* **138**, 1339–1354 (2015).
28. Hasegawa, M., Crowther, R. A., Jakes, R. & Goedert, M. Alzheimer-like Changes in Microtubule-associated Protein Tau Induced by Sulfated Glycosaminoglycans. *J. Biol. Chem.* **272**, 33118–33124 (1997).
29. Wolfe, M. S. Tau Mutations in Neurodegenerative Diseases. *J. Biol. Chem.* **284**, 6021–6025 (2009).

30. Griffin, W. S. T. Neuroinflammatory Cytokine Signaling and Alzheimer's Disease. *N. Engl. J. Med.* **368**, 770–771 (2013).
31. Giovannini, J. *et al.* Tau protein aggregation: Key features to improve drug discovery screening. *Drug Discov. Today* **27**, 1284–1297 (2022).
32. Niewiadomska, G., Niewiadomski, W., Steczkowska, M. & Gasiorowska, A. Tau Oligomers Neurotoxicity. *Life* **11**, 28 (2021).
33. Simon Davis, D. A. & Parish, C. R. Heparan Sulfate: A Ubiquitous Glycosaminoglycan with Multiple Roles in Immunity. *Front. Immunol.* **4**, (2013).
34. Zhang, P. *et al.* Heparan Sulfate Organizes Neuronal Synapses through Neurexin Partnerships. *Cell* **174**, 1450-1464.e23 (2018).
35. Fu, Y. *et al.* Apolipoprotein E lipoprotein particles inhibit amyloid- β uptake through cell surface heparan sulphate proteoglycan. *Mol. Neurodegener.* **11**, 37 (2016).
36. Südhof, T. C. Towards an Understanding of Synapse Formation. *Neuron* **100**, 276–293 (2018).
37. Huynh, M. B. *et al.* Glycosaminoglycans from Alzheimer's disease hippocampus have altered capacities to bind and regulate growth factors activities and to bind tau. *PLOS ONE* **14**, e0209573 (2019).
38. Sahu, B., Sharma, D. D., Jayakumar, G. C., Madhan, B. & Zameer, F. A review on an imperative by-product: Glycosaminoglycans- A holistic approach. *Carbohydr. Polym. Technol. Appl.* **5**, 100275 (2023).
39. Ouidja, M. O. *et al.* Variability in proteoglycan biosynthetic genes reveals new facets of heparan sulfates diversity. A systematic review and analysis.

<http://medrxiv.org/lookup/doi/10.1101/2022.04.18.22273971> (2022)

doi:10.1101/2022.04.18.22273971.

40. Kreuger, J. & Kjellén, L. Heparan Sulfate Biosynthesis: Regulation and Variability. *J. Histochem. Cytochem.* **60**, 898–907 (2012).
41. Nagarajan, A., Malvi, P. & Wajapeyee, N. Heparan Sulfate and Heparan Sulfate Proteoglycans in Cancer Initiation and Progression. *Front. Endocrinol.* **9**, 483 (2018).
42. Maïza, A. *et al.* OPEN 3-O-sulfated heparan sulfate interactors target synaptic. *Sci. Rep.* **14**.
43. Huynh, M. B. *et al.* HS3ST2 expression induces the cell autonomous aggregation of tau. *Sci. Rep.* **12**, 10850 (2022).
44. Dankov□, Z. *et al.* Methylation status of KLF4 and HS3ST2 genes as predictors of endometrial cancer and hyperplastic endometrial lesions. *Int. J. Mol. Med.* (2018) doi:10.3892/ijmm.2018.3872.
45. Zhang, Z., Jiang, H., Wang, Y. & Shi, M. Heparan sulfate D-glucosamine 3-O-sulfotransferase 3B1 is a novel regulator of transforming growth factor-beta-mediated epithelial-to-mesenchymal transition and regulated by miR-218 in nonsmall cell lung cancer. *J. Cancer Res. Ther.* **14**, 24–29 (2018).
46. Vijaya Kumar, A. *et al.* HS3ST2 modulates breast cancer cell invasiveness via MAP kinase- and Tcf4 (Tcf7l2)-dependent regulation of protease and cadherin expression: Involvement of HS3ST2 in Breast Cancer Cell Invasion and Chemosensitivity. *Int. J. Cancer* **135**, 2579–2592 (2014).
47. Nativio, R. *et al.* An integrated multi-omics approach identifies epigenetic alterations associated with Alzheimer’s disease. *Nat. Genet.* **52**, 1024–1035 (2020).

48. Martin-Malpartida, P. *et al.* Structural basis for genome wide recognition of 5-bp GC motifs by SMAD transcription factors. *Nat. Commun.* **8**, 2070 (2017).
49. Lesné, S. *et al.* Transforming Growth Factor- β 1—Modulated Cerebral Gene Expression. *J. Cereb. Blood Flow Metab.* **22**, 1114–1123 (2002).
50. Burton, T., Liang, B., Dibrov, A. & Amara, F. Transforming growth factor- β -induced transcription of the Alzheimer β -amyloid precursor protein gene involves interaction between the CTCF-complex and Smads. *Biochem. Biophys. Res. Commun.* **11** (2002).
51. Lee, M.-H. *et al.* TGF- β induces TIAF1 self-aggregation via type II receptor-independent signaling that leads to generation of amyloid β plaques in Alzheimer's disease. *Cell Death Dis.* **1**, e110–e110 (2010).
52. Town, T. *et al.* Blocking TGF- β –Smad2/3 innate immune signaling mitigates Alzheimer-like pathology. *Nat. Med.* **14**, 681–687 (2008).
53. Fath, T., Ke, Y. D., Gunning, P., Götz, J. & Ittner, L. M. Primary support cultures of hippocampal and substantia nigra neurons. *Nat. Protoc.* **4**, 78–85 (2009).
54. SantaCruz, K. *et al.* Tau Suppression in a Neurodegenerative Mouse Model Improves Memory Function. *Science* **309**, 476–481 (2005).
55. Nieznanska, H. *et al.* Neurotoxicity of oligomers of phosphorylated Tau protein carrying tauopathy-associated mutation is inhibited by prion protein. *Biochim. Biophys. Acta BBA - Mol. Basis Dis.* **1867**, 166209 (2021).
56. Gyparaki, M. T. *et al.* Tau forms oligomeric complexes on microtubules that are distinct from tau aggregates. *Proc. Natl. Acad. Sci.* **118**, e2021461118 (2021).

57. Braak, H., Alafuzoff, I., Arzberger, T., Kretschmar, H. & Del Tredici, K. Staging of Alzheimer disease-associated neurofibrillary pathology using paraffin sections and immunocytochemistry. *Acta Neuropathol. (Berl.)* **112**, 389–404 (2006).
58. Ramsden, M. *et al.* Age-Dependent Neurofibrillary Tangle Formation, Neuron Loss, and Memory Impairment in a Mouse Model of Human Tauopathy (P301L). *J. Neurosci.* **25**, 10637–10647 (2005).
59. Caraci, F. *et al.* TGF- β 1 Pathway as a New Target for Neuroprotection in Alzheimer's Disease: Neuroprotective Role of TGF- β 1 in AD. *CNS Neurosci. Ther.* **17**, 237–249 (2011).
60. Baig, S., Helmond, Z. V. & Love, S. TAU HYPERPHOSPHORYLATION AFFECTS Smad 2/3 TRANSLOCATION. **10** (2009).
61. Gummy, L. F. *et al.* MAP2 Defines a Pre-axonal Filtering Zone to Regulate KIF1- versus KIF5-Dependent Cargo Transport in Sensory Neurons. *Neuron* **94**, 347-362.e7 (2017).
62. Chen, Y., Fu, A. K. Y. & Ip, N. Y. Synaptic dysfunction in Alzheimer's disease: Mechanisms and therapeutic strategies. *Pharmacol. Ther.* **195**, 186–198 (2019).
63. Wegmann, S., Biernat, J. & Mandelkow, E. A current view on Tau protein phosphorylation in Alzheimer's disease. *Curr. Opin. Neurobiol.* **69**, 131–138 (2021).
64. Kober, D. L. & Brett, T. J. TREM2-Ligand Interactions in Health and Disease. *J. Mol. Biol.* **429**, 1607–1629 (2017).
65. Arriagada, P. V., Growdon, J. H., Hedley-Whyte, E. T. & Hyman, B. T. Neurofibrillary tangles but not senile plaques parallel duration and severity of Alzheimer's disease.

66. Guillozet, A. L., Weintraub, S., Mash, D. C. & Mesulam, M. M. Neurofibrillary Tangles, Amyloid, and Memory in Aging and Mild Cognitive Impairment. *Arch. Neurol.* **60**, 729 (2003).
67. Salloway, S. *et al.* Two Phase 3 Trials of Bapineuzumab in Mild-to-Moderate Alzheimer's Disease. *N. Engl. J. Med.* **370**, 322–333 (2014).
68. Schöll, M. *et al.* PET Imaging of Tau Deposition in the Aging Human Brain. *Neuron* **89**, 971–982 (2016).
69. Cho, H. *et al.* In vivo cortical spreading pattern of tau and amyloid in the Alzheimer disease spectrum: Tau and Amyloid in AD. *Ann. Neurol.* **80**, 247–258 (2016).
70. Giannakopoulos, P. *et al.* Tangle and neuron numbers, but not amyloid load, predict cognitive status in Alzheimer's disease. *Neurology* **60**, 1495–1500 (2003).
71. Tannenbaum, J. & Bennett, B. T. Russell and Burch's 3Rs Then and Now: The Need for Clarity in Definition and Purpose. *J. Am. Assoc. Lab. Anim. Sci.* **54**, (2015).
72. Guerril, B. C., Porta, E. S., Schlamilch, M. A., González, F. C. & Calatayud, V. Effects of glia-conditioned medium on primary cultures of central neurons.
73. Lace, G. *et al.* Hippocampal tau pathology is related to neuroanatomical connections: an ageing population-based study. *Brain* **132**, 1324–1334 (2009).
74. De Flores, R., La Joie, R. & Chételat, G. Structural imaging of hippocampal subfields in healthy aging and Alzheimer's disease. *Neuroscience* **309**, 29–50 (2015).
75. Denys, A. & Allain, F. The Emerging Roles of Heparan Sulfate 3-O-Sulfotransferases in Cancer. *Front. Oncol.* **9**, 507 (2019).

76. Lorente-Gea, L. *et al.* Heparan Sulfate Proteoglycans Undergo Differential Expression Alterations in Alzheimer Disease Brains. *J. Neuropathol. Exp. Neurol.* **79**, 474–483 (2020).
77. Hasegawa, M., Crowther, R. A., Jakes, R. & Goedert, M. Alzheimer-like Changes in Microtubule-associated Protein Tau Induced by Sulfated Glycosaminoglycans. *J. Biol. Chem.* **272**, 33118–33124 (1997).
78. Coulon, A., Chow, C. C., Singer, R. H. & Larson, D. R. Eukaryotic transcriptional dynamics: from single molecules to cell populations. *Nat. Rev. Genet.* **14**, 572–584 (2013).
79. Docagne, F. *et al.* Sp1 and Smad transcription factors co-operate to mediate TGF- β -dependent activation of amyloid- β precursor protein gene transcription. *Biochem. J.* **383**, 393–399 (2004).
80. Ueberham, U., Ueberham, E., Gruschka, H. & Arendt, T. Altered subcellular location of phosphorylated Smads in Alzheimer's disease. *Eur. J. Neurosci.* **24**, 2327–2334 (2006).
81. Van Horssen, J., Wesseling, P., Van Den Heuvel, L. P., De Waal, R. M. & Verbeek, M. M. Heparan sulphate proteoglycans in Alzheimer's disease and amyloid-related disorders. *Lancet Neurol.* **2**, 482–492 (2003).
82. Wang, Z. *et al.* Increased 3- O -sulfated heparan sulfate in Alzheimer's disease brain is associated with genetic risk gene *HS3ST1*. *Sci. Adv.* **9**, eadf6232 (2023).
83. Negi, S. K. & Guda, C. Global gene expression profiling of healthy human brain and its application in studying neurological disorders. *Sci. Rep.* **7**, 897 (2017).

84. Neddens, J. *et al.* Phosphorylation of different tau sites during progression of Alzheimer's disease. *Acta Neuropathol. Commun.* **6**, 52 (2018).
85. Martin, L. *et al.* Tau protein kinases: Involvement in Alzheimer's disease. *Ageing Res. Rev.* **12**, 289–309 (2013).

13. Acknowledgements

First, I want to acknowledge the Glycobiology - Croissance cellulaire, Réparation, et Régénération Tissulaire (GLY-CRRET) Research unit at the Université Paris-Est Créteil for their warm welcome and support during this collaborative project.

Additionally, I want to thank all the institutions and grants who funded my PhD project. Consejo Nacional de Ciencia y Tecnología - Deutscher Akademischer Austauschdienst (CONACyT-DAAD), Programme Européen pour la Recherche et l'Innovation « FET-OPEN Horizon 2020 Technologies Futures et Emergentes » (FET OPEN RIA 737390), and Giessen Graduate Centre of Life Sciences.

It would be impossible to acknowledge and to thank everyone who helped and supported me through all these times. Each one of you listed here already know or will know my thoughts and gratitude personally. For sure I forgot some names, and for this I sincerely apologize, I just want to thank you all for being there.

Sería imposible agradecer a cada persona que me ha ayudado durante todo este tiempo. Cada una de las personas enlistadas aquí ya lo saben o sabrán mis pensamientos y agradecimiento personalmente. Seguramente olvidé algunos nombres, lo siento de verdad, solo quiero agradecer a todos por estar ahí.

My parents (mis papás). Agatha Ribeiro Da Silva. Ajitha Thuraisamy. Alvaro Rendón. Angelica Zepeda. Anne Repellin. Dulce Papy-Garcia. Elena Bittner. Francoise Lucas. Gael Le Douaron. Héloïse Merrick. Ivan Ramos Martinez. Martin Diener. Minh Bao Huynh. Mohand Ou Idir Ouidja. Ombeline Girard. Oulfa Ben Abdelouhab. Peter Jedlicka. Selva Raj Sethupathi. Shegnang Zhao. Wilton Gomez Henao. Xavier Laffray.